APPLICATION OF 5-OH POLYMETHOXYFLAVONES AND SAFE MITOCHONDRIAL UNCOUPLERS IN PREVENTING AND TREATING TYPE 2 DIABETES AND FATTY LIVER DISEASES

BY

JINGJING GUO

A dissertation submitted to the

School of Graduate Studies

Rutgers, The State University of New Jersey

In partial fulfillment of the requirements

For the degree of

Doctor of Philosophy

Graduate Program in Food Science

Written under the direction of

[Dr. Qingrong Huang and Dr. Shengkan Jin]

And approved by

_____

_____

_____

_____

New Brunswick, New Jersey

January, 2019

ABSTRACT OF THE DISSERTATION

APPLICATION OF 5-OH POLYMETHOXYFLAVONES AND SAFE MITOCHONDRIAL UNCOUPLERS IN PREVENTING AND TREATING TYPE 2 DIABETES AND FATTY LIVER DISEASES

BY JINGJING GUO

Dissertation Directors:

Dr. Qingrong Huang and Dr. Shengkan Jin

In modern society, obesity-related metabolic diseases have become a serious public health concern globally. The increasing prevalence, disease progression, diverse complications and subsequent morbidity and mortality impose great medical challenges and socioeconomic burden. Type 2 diabetes (T2D) and nonalcoholic fatty liver diseases (NAFLD) are the two representative metabolic diseases. Current anti-diabetic medications only ameliorate diabetic symptoms but not effective in correcting the underlying causes of insulin resistance. Patients have to keep the medications for the rest of their lifetime. Nonalcoholic steatohepatitis (NASH) is an active form of NAFLD with no FDA-approved pharmacotherapy. Patients with NASH have higher risk of developing end-stage liver diseases including liver cirrhosis and hepatocellular carcinoma, and await liver transplantation to save life. The significant unmet medical needs of T2D and NAFLD call for therapeutics with novel working mechanisms. Excessive lipid accumulation is attributed to the underlying cause of multiple metabolic diseases, in particular T2D and NAFLD. At the same time, abnormal lipid deposition, particularly hepatic lipid accumulation, plays a fundamental role in the pathogenesis of some liver-based genetic disease

such as lysosomal acid lipase deficiency (LAL-D), a genetic disease with profound lipid accumulation in liver.

The objective of my PhD research work is to identify novel nutraceuticals and pharmaceuticals that target lipid accumulation for treatment of T2D, NASH and LAL-D. My strategy is to target cellular metabolism to reduce intracellular lipid load. Depletion of fat accumulation corrected the causal factors of T2D and NASH as well as reduced the driving force of LAL-D disease progression. Our work on nutraceuticals focused on a group of 5-OH PMFs which presented promising therapeutic potential for the treatment of T2D and NAFL by targeting lipogenesis of adipogenesis. Our work on pharmaceuticals focused on a group of mitochondrial uncouplers which demonstrated strong therapeutic potential for the treatment of T2D, NASH and LAL-D by targeting hepatic lipid accumulation.

The first part of the work on nutraceuticals focused on the application of aged citrus peel (*chenpi*) extract as a novel nutraceutical for preventing obesity and T2D. *Chenpi* has long been used as an herbal medication and dietary supplement with excellent safety profile. Moreover, *chenpi* extract is uniquely enriched with 5-OH polymethoxyflavones (5-OH PMFs) compared to the fresh citrus peel extract. The chemical profile of *chenpi* extracts were quantitatively characterized. The therapeutic potential and underlying molecular mechanism of *chenpi* extract were systematically examined in relevant in vitro and in vivo models. The results demonstrated that 5-OH PMFs-enriched *chenpi* extract is effective to prevent high-fat diet induced obesity, insulin resistance, hyperglycemia, hypercholesterolemia and fatty liver in mice. And the beneficial effects of *chenpi* extract is attributed to the direct impact on lipid metabolism in adipocyte through activating AMPK pathway. A 5-OH PMFs content-dependent lipid-lowering efficacy of *chenpi* extract was also revealed.

Encouraged by the striking efficacy of 5-OH PMFs-enriched *chenpi* extract, the effect of casticin, a 5-OH PMF derivative, on lipid metabolism was investigated in differentiating adipocyte model. Casticin bears one extra hydroxyl group at 3' position compared to its 5-OH PMF counterpart, 5-OH nobiletin. The results showed that casticin reduces intracellular lipid accumulation in differentiated adipocytes, which arises from the direct inhibition on cell proliferation and lipogenesis of adipogenesis. Moreover, casticin presents higher lipid-reducing efficacy and a different working mechanism compared to that of 5-OH nobiletin, which reveals a structure-activity relationship of 5-OH PMFs on suppressing adipogenesis.

Mitochondrial uncoupling is a biological process that efficiently stimulates lipid oxidation independent of ATP synthesis. Small chemicals that are capable of inducing mitochondrial uncoupling have emerged as a novel therapeutic approach to treat a myriad of diseases. However, how to improve the safety profile of the chemical uncouplers becomes the key obstacle of clinical translation of mitochondrial uncouplers strategy. In current work, we identified a group of safe mitochondrial uncouplers which induce mild mitochondrial uncoupling and specifically function in liver. Niclosamide ethanolamine (NEN) and niclosamide piperazine (NPP) are the two representative safe mitochondrial uncouplers exploited in current work. NEN and NPP, the salt forms of the FDA-approved drug, niclosamide, are bioavailable and have excellent safety profiles documented in mammals. When orally administrated, NEN and NPP distribute primarily to liver where they uncouple mitochondria of liver cells, which elevates lipid oxidation and reduces hepatic lipid load. We investigated the effect of NEN and NPP on treating obesity, T2D, NAFLD and LAL-D in relevant *in vitro* and *in vivo* models.

For treating obesity and T2D, oral administration of NPP effectively reduce the body weight gain and T2D symptoms through depletion of hepatic fat accumulation in HFD-induced obese/diabetic mouse model. For treating NAFLD and NASH, oral administration of NEN significantly reduces the hepatic steatosis, inflammation and fibrosis and improves the general

metabolic profile in western diet-induced NASH mouse model. In addition, oral NEN treatment prevents and reverses CCl_4 induced fibrosis in mice by directly inhibiting hepatic stellate cell activation. Overall, NEN-induced mitochondrial uncoupling targets hepatic steatosis and hepatic stellate cells activation, which accounts for its therapeutic potential of treating NASH. For treating LAL-D, oral NEN treatment significantly reduces hepatosplenomegaly, liver damage and dramatically prolongs the life span of *lal-/-* mice, suggesting the therapeutic potential of mitochondrial uncoupler for treating hepatic accumulation caused by gene mutations.

In summary, I developed chenpi extract and casticin as novel nutraceuticals and repurposed NEN and NPP as novel pharmacotherapies for treating T2D and NAFLD by targeting lipid metabolism. My work provided strong evidence that 5-OH PMFs-based nutraceuticals and safe mitochondrial uncouplers are promising therapeutic approaches for the treatment of T2D and fatty liver diseases.

Acknowledgement

When I look back over my PhD study, I feel like it is an enjoyable and fruitful journey that helps me become a responsible, independent and confident individual. It provides me with not only research capabilities but also life philosophy, like how to face and resolve the mistakes, how to balance life and work, as well as how to be faithful to my dream life. I am so grateful to learn these lessons from many great people and many memorable moments happened in my PhD journey.

First of all, I would like to express my deepest gratitude to my two PhD advisors, Dr. Qingrong Huang and Dr. Shengkan Jin, for their mentoring, encouragement, support and patience throughout my PhD study. I feel so fortunate to receive the guidance from two advisors who provide me with an excellent opportunity to learn and work in the multidisciplinary fields. They are not only my research supervisors but also the mentors of my self-development. They are always open to my concerns, mitigating my frustration, offering me constructive advice and encouraging me to move forwards.

My sincere appreciation is extended to my committee members, Dr. Chi-tang Ho and Dr. Qingli Wu. I would like to thank Dr. Ho for his constant support and valuable suggestions to my research. Dr. Ho is very nice to introduce his connections and provide strong support letters that significantly help my career development. I also want to thank Dr. Wu for his excellent advices and input to facilitate the completion of my PhD study. Dr. Wu is always helpful and supportive to provide me with the knowledge from his expertise.

I wish to convey my gratitude to Dr. Hanlin Tao, who is a co-worker and mentor of my PhD study. Hanlin is always generous to share his working experience and technical skills with me, which helps me a lot to resolve the technical problems of my research. Moreover, I received tons of advice on my career development from him.

I would also like to thank all of my family and friends for their unconditional love and endless support. Your love and support are the invaluable assets of my PhD study.

Table of Contents

List of Tables

List of illustration

Chapter I. Introduction and Background Information

1. Overview of obesity, T2D, NAFLD and LAL-D: epidemic, pathogenesis, and current efforts on disease management

1.1 Obesity

Obesity is characterized by excessive body fat deposition, including abdominal adiposity and ectopic lipid accumulation in non-adipose tissues such as liver and muscle. The most widely accepted definition and categorization of obesity is based on body mass index (BMI), which is determined by the ratio of body weight (kilograms) over square of height (in meters) [1]. According to the WHO guidelines, overweight is defined with a BMI over or equivalent to 25 and obese state is defined with a BMI over 30 [2].

Obesity has become a global health problem. It is estimated over 300 million world population are affected by obesity and over 65% people in United States are overweight or obese. Moreover, obesity, in particular morbid obesity (BMI> 35 or 40), is casually associated with a wide array of diseases including type 2 diabetes (T2D), nonalcoholic fatty liver diseases (NAFLD), dyslipidemia, atherosclerosis, cardiovascular diseases and even cancer. In 2010, overweight and obesity were estimated to cause 3.4 million deaths, 4% of years of life lost, and 4% of disability-adjusted life-years globally. The global and domestic epidemics of obesity together with severe obesity-related complications imposes great socioeconomic burden to modern society.

1.2 Type 2 diabetes (T2D)

Overview of type 2 diabetes

Type 2 diabetes (T2D) is a metabolic disorder that is characterized by hyperglycemia (high blood sugar) in the context of insulin resistance and relative lack of insulin.[3] Insulin is a vital anabolic hormone secreted by pancreatic beta cells. Insulin promotes the storage of glucose and lipid in liver, muscle and adipose, whereas represses the degradation and release of these substrates or their metabolites,[4] thus regulating the metabolism of glucose and lipid. The revealed role of insulin in lipid metabolism bridges the relationship between abnormal lipid metabolism and T2D, which extends glucose-oriented T2D to a more comprehensive concept.[5]

T2D is a progressive disease starting with the insulin resistance. The insulin-mediated metabolic events are accomplished through a cascade of signal transductions[6] which are determined by both insulin availability and sensitivity to insulin signal. Although impaired beta cell function is ultimately responsible for the progression to hyperglycemia, insulin resistance predates and proceeds with the pathophysiology of T2D.[7] Resistance to insulin signal in insulin-responsive tissues leads to defects in insulin-mediated glucose regulation including decreased glucose uptake in liver, muscle and adipose, and increased hepatic glucose production. To compensate for insulin resistance, pancreatic beta cells increase the insulin secretary capacity along with beta cell mass. The normal blood glucose level is then maintained in the context of hyperinsulinemia. The compensatory response of beta cell in face of insulin resistance could last for long time until the exhaust of secretion and proliferation of beta cells. Eventually, beta cells die and produce no more insulin, resulting in the total loss of glycemic control.[8, 9] Furthermore, without wise control, diabetes will induce a series of severe or even fatal diabetic complications including skin problems, eye complications, retinopathy, neuropathy, high blood pressure, stroke, cardiovascular disease, etc.[10] Therefore, insulin resistance is attributed to the underlying cause of T2D.

Prevalence of T2D

Over the past three decades, the number of T2D cases has more than doubled worldwide, making T2D a globally epidemic problem.[11] World Health Organization (WHO) reports that in 2014 the global prevalence of diabetes was estimated to be 9% among adults over aged 18. And T2D accounts for 90%-95% of newly diagnosed diabetes cases. In 2012, an estimated 1.5 million deaths were directly caused by diabetes. WHO projects that diabetes will be the 7th leading cause of death in 2030. In United States, one of the most affected western countries by T2D, the facts on diabetes are even more challenging. According to the national diabetes statistics report, approximate 29.1 million people are on diabetes with 1.7 million newly diagnosed cases in 2012. The estimated economic cost of diabetes is up to 245 billion. Moreover, in addition to diabetic cases, 86 million Americans are on pre-diabetes. Without proper control, 15%-30% of people with prediabetes will develop diabetes within 5 years. Unfortunately, majority of the people with diabetes or prediabetes are undiagnosed.[12] Therefore both prevention and treatment are important and urgent to the management of T2D.

Pathogenesis of T2D

The positive correlation of obesity with development of insulin resistance and T2D has been recognized for years. Several mechanisms have been proposed to link this cause-and-effect relationship, mainly ectopic deposition of lipids, systemic chronic inflammation, and activation of "endoplasmic reticulum stress" (ER stress)[13].

Glucose and fatty acids are two basic molecules essential for the energy metabolism, including energy supply and energy storage. The chemical energy reserved in glucose and FAs are converted to ATP to supply the cell survival and various metabolic events. The excessive energy will be stored as back-up fuel primarily in adipose tissue in the form of triglycerides. In response to increased lipid accumulation, adipocytes undergo expansion and proliferation to increase their lipid depot capacity. However, in the context of persistent positive energy balance,

the capacity of adipocyte is overwhelmed, resulting in "inflamed adipose tissue" which increases the release of free fatty acids, various proinflammatory cytokines and adipokines. The excessive lipids could also be directed to non-adipose tissue, including liver and muscle, leading to insulin resistance and hepatic steatosis.

Ectopic lipid accumulation

The concept of lipid-induced insulin resistance was firstly described as the competition between fatty acids and glucose for oxidative metabolism in insulin-responsive cells. [14] More recently, it is proposed that the lipid overflow into insulin-responsive tissues (mainly skeletal muscle and liver) disrupts the insulin signaling, resulting in reduced glucose transport, decreased glycogen synthesis and increased gluconeogenesis, which is the basic idea of lipid-induced insulin resistance[15]. In human, Fabbrini found that hepatic insulin resistance is primarily related to intrahepatic lipid content.[16] Consistently, T2D patients who received calorie-restricted diet for up to 12 weeks manifest a remarkable decrease in hepatic fat content (~85%), accompanied with a normalization of hepatic insulin sensitivity, fasting glucose level, and hepatic glucose production [17]. Human experiments also demonstrated that intramyocellular lipid content is a stronger predictor of muscle insulin resistance[18], suggesting that intramyocellular lipids may cause muscle insulin resistance. All these data suggested that ectopic lipid deposition in liver and skeletal muscle could directly cause insulin resistance.

The molecular mechanism underlying the casual role of lipid moiety in the pathogenesis of insulin resistance is still not fully understood. It is generally believed that certain toxic lipid metabolites directly interrupt insulin signaling. Ceramides, a major lipid moiety found in cell membranes, impair insulin signaling by inhibiting Akt activation, which lead to upregulation of gluconeogenesis enzymes, decreased glucose uptake, and decreased glycogen synthesis [43]. In addition, insulin resistance is found to be associated with diacylglycerols (DAGs) accumulation

in liver and skeletal muscle in clinic [25, 44, 45]. It is reported that DAGs-mediated PKCs activation interfere with insulin receptor activation by phosphorylating inhibitory serine sites on IRS-1, which ultimately lead to reduced glucose transport, reduced glycogen synthesis and increased gluconeogenesis [54].

Inflammation mechanism

Systemic chronic inflammation has been proposed to play important role in the pathogenesis of insulin resistance and T2D. It has been shown that inflammatory biomarkers, such as tumor necrosis factor-α (TNFα), interleukin-6 (IL-6), and C-reactive protein (CRP), are present at high level in obese and insulin resistant individuals. And some classic anti-inflammatory drug, like aspirin, is effective to reduce diabetic symptoms and restore glucose tolerance[19]. The detrimental visceral fat, also known as abdominal adiposity, indicates the body fat deposited in abdominal cavity and surrounds a series of important internal organs like liver, pancreas, and intestine. The abdominal fat is attributed as one major origin of inflammatory insults through secreting various proinflammatory cytokines and recruitment of adipose tissue macrophages (ATMs). In liver, ectopic lipid accumulation also induces the activation of inflammatory pathways and recruitment of macrophages. Moreover, local inflammation will expand to systemic inflammatory response when all these inflammatory stimuli are delivered into portal vein.

The causative role of inflammation in insulin resistance is realized through crosstalk between intracellular inflammatory pathways and insulin signaling. The inflammatory cytokines serve as stimuli that activate inflammatory signaling pathways in adipocytes, hepatocytes, and macrophages, particularly the inhibitor of nuclear factor-κB (NF-κB) kinase-β (IKKβ) /NF-κB pathway and Jun kinase (JNK) pathway. Activation of JNK pathway will interfere with physiologically functional phosphorylation of insulin receptor substrate-1(IRS-1), leading to the

reduced response to insulin signal. IKKβ can impact insulin signaling both by directly phosphorylating IRS-1 on the inhibitory serine residues[20, 21] and by activating NF-κB, a transcription factor that stimulates production of multiple inflammatory mediators including TNFα and IL-6[22].

Endoplasmic reticulum stress

Endoplasmic reticulum stress is also termed as unfolded protein response (UPR). It is a cellular response that triggered by the accumulation of mis-folded or unfolded protein in endoplasmic reticulum. Accompanied with activation of UPR, a set of signaling transducers will be activated including Inositol requiring enzyme-1 (IRE1α), PKR-like ER kinase (PERK), and activating transcription factor-6 (ATF6), which works to reduce ER stress by increasing membrane biogenesis, halting protein translation and enhancing protein folding.[13] Chemical inducers of the UPR impaired insulin signaling,[23] while chemical enhancers of protein folding that reduce ER stress promote insulin sensitivity.[24] Activation of the ER stress was found in obese and diabetic ob/ob mouse model.[23] And markers of the UPR are decreased after surgical induced-weight loss,[25] suggesting that UPR induced signal pathways may be involved in the pathogenesis of insulin resistance in obese states in rodents as well as in humans. The exact molecular mechanism relative with ER stress or UPR is still not clear. Some data demonstrated the possible association with activation of JNK1 and subsequent impairment in insulin signaling.[26]

Other mechanisms

Besides the three broad themes of mechanisms described above, some other factors might also contribute to the pathogenesis of insulin resistance, such as endocrine factors, mitochondria dysfunctions, and oxidative stress.

Endocrine mechanism is associated with the dysfunction of adipose tissue.[27] Adipose tissue serves as both lipid storage depot and endocrine organ. On one hand, its lipid buffering capacity favors the clearance of circulation triglycerides and FAs and restricts the release of lipid metabolites, thus preventing the ectopic lipid deposition in liver, muscle and other peripheral tissues; on the other hand, adipose tissue could express and secrete a number of adipocyte hormones (adipokines) including leptin, adiponectin, resistin and some pro-inflammatory cytokines (IL-6 and TNF-α) which are highly implicated in the insulin signaling transactions.[28] In obesity, however, normal function of adipose tissue is disrupted. The lipid storage and mobilization in adipose tissue relatively decline, resulting in increased level of systematic FAs and lipid accumulation in non-adipose tissues.[29] Besides, increased adipose mass could lead to the pathogenic change in the profile of adipokines, which give rise to abnormal insulin signaling and downstream metabolic events .[29] For example, one of adipocyte-specific adipokines, adiponectin, is low in obesity, and administration of adiponectin increase the overall insulin sensitivity in animals.[30-32] As opposed to adiponectin, IL-6 and TNF- increase along with the increasing adiposity and insulin resistance in animals and humans.[33] Overall, various endocrine factors play vital role in the development of insulin resistance and they are usually thought to be related with dysfunctional abdominal adipose tissue.

Mitochondria works as cellular energy plant in which fuel molecules are oxidize to produce ATP. Since ATP is essential to various cellular processes, mitochondrial function plays important role in metabolic health. Mitochondrial dysfunction could be defined as different ways such as decreased mitochondrial content, diminished mitochondrial activity and substrate oxidation, and increased ROS production.[34] In elderly people, severe insulin resistance and significant rise in triglycerides are found in both liver and muscle, which is also accompanied with decreased mitochondrial oxidative activity and ATP synthesis. Later on, microarray studies carried out in T2D patients showed a decrease in peroxisome proliferator coactivator 1a (PGC1a), a master

regulator involved in mitochondrial metabolism, which provide direct evidence that mitochondrial biogenesis and oxidative phosphorylation were down-regulated in insulin-resistant stage.[35, 36] The mechanism by which mitochondrial dysfunction affects insulin sensitivity is related to the deleterious lipid signaling molecules, such as DAGs and ceramides.[34] The reduction in substrate oxidation, particularly fatty acid oxidation in mitochondria leads to the accumulation of lipid metabolites which disrupts the insulin signaling as described before.

Obesity-associated insulin resistance is a complex disorder and proceeds along the pathogenesis of T2D. Certain lipid metabolites arising from ectopic lipid accumulation in insulin responsive organs, such as liver and muscle, directly disrupt insulin signaling; or they serve as stimuli that activate inflammatory pathways or UPR which crosstalk with insulin signaling cascades. The dysfunctional visceral fat might also contribute to the insulin resistance through release of fatty acids and various adipokines. Overall, ectopic lipid accumulation together with dysfunctional abdominal adipose could be the primary driving force of insulin resistance (**Figure 1.1**). Accordingly, reduction of excessive body fat could be one potent strategy against insulin resistance and T2D.

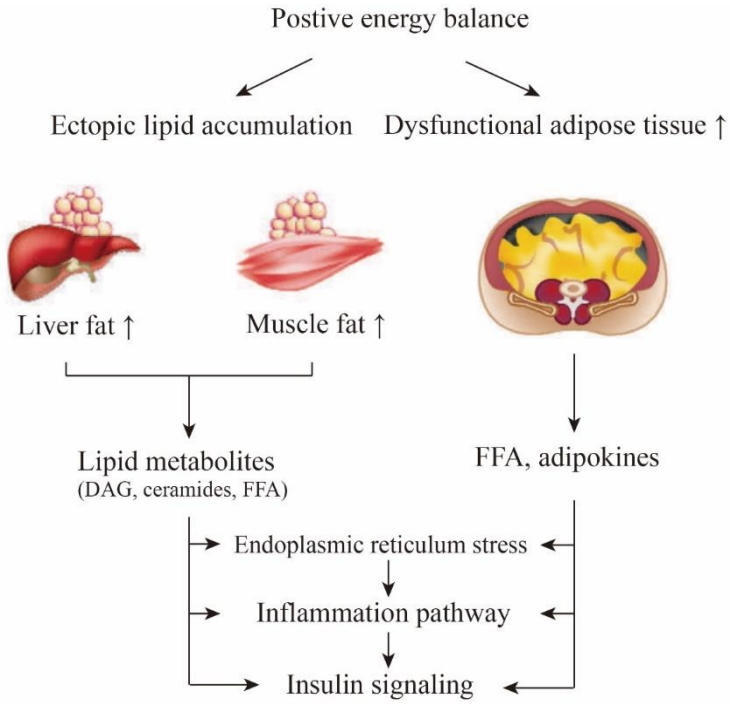

Figure 1. 1 Schematic diagram of pathogenesis of insulin resistance

Reduction of body fat improves insulin resistance

As the fat accumulation is attributed as the major cause of insulin resistance, reduction in body fat should make a great contribution to the improvement of insulin sensitivity and overall metabolic prolife. Given the energy imbalance in fat accumulation, decreasing calorie input and increasing energy output represent two mainstays of therapy for obesity and T2D.

Proper diet modification leading to weight loss reduces the risk of diabetes in subjects with impaired glucose tolerance (IGT). Similarly, in obese T2D patients, a 7-week very-low-fat diet therapy resulted in a significant loss of body weight as well as the plasma concentrations of high-density lipoprotein, low-density lipoprotein and triglycerides. In addition, obese people who accepted bariatric surgery lose weight and have improvements in glycemic control and they have lower incidences of diabetes.

Besides reducing calorie intake, increasing energy expenditure is an even more robust strategy to burn body fat. Exercise training directly increases muscle oxidative capacity which results in a decrease in skeletal lipid content, and an increase in rate of whole-body fat oxidation.[37] Due to the benefits in energy homeostasis, exercise training has been included in lots of preventive trials against T2D. It was shown that exercise training improves glucose tolerance and insulin action in healthy individuals [38, 39], persons with obesity [40, 41] and insulin resistance[42-44], and also in patients with type 2 diabetes[45-48]. Additionally, short-term aerobic exercise is found to improve hepatic steatosis and glucose tolerance in patients with NAFLD,[49] suggesting its beneficial role in regulating hepatic lipid synthesis.[50]

Therefore, it is convincible that reduction of body fat accumulation through regulating energy metabolism is a potent strategy to prevent or treat the insulin resistance and T2D. Therapeutic interventions that are capable of decreasing the fat accumulation are appealing in the development of anti-diabetic drugs or nutraceuticals.

Current efforts on T2D management

Based on the stage of disease progression, management of T2D usually progresses from lifestyle intervention (diet modification, physical activity) to mono-pharmacotherapy (use of one anti-diabetic drug) to multi-pharmacotherapies (use of combination of anti-diabetic drugs), and finally to combination of anti-diabetic agents with insulin.[51] A number of classes of oral medications for T2D patients are now available, including metformin (first-class pharmacotherapy), sulfonylureas, meglitinides, thiazolidinediones, glucagon-like peptide receptor-1 agonist, α-glucosidase inhibitors, dipeptidyl peptidase-4 inhibitors, SGLT2 inhibitors and others.[52] However, most agents focus on increasing insulin secretion or reducing glucose production, but failed to correct the underlying cause of insulin resistance and bring about some side effects like hypoglycemia, weight gain, stomach problems, etc.[52] As a result, most

diabetic patients have to rely on the oral medications over the life. Therefore, therapies that target the origin of insulin resistance are preferable for T2D treatment.

1.3 Nonalcoholic fatty liver disease (NAFLD)

Overview of NAFLD

By definition, nonalcoholic fatty liver disease (NAFLD) is characterized by excessive lipid deposition in liver in patients without excessive alcohol consumption. NAFLD is categorized as the hepatic manifestation of metabolic diseases. NAFLD comprehends a liver disease spectrum progressing from noninflammatory hepatic steatosis, defined by the presence of lipid droplets in > 5% of hepatocytes, to inflamed fatty liver disease which is defined as nonalcoholic steatohepatitis (NASH) [53]. NASH is an aggressive form of NAFLD, with the presence of hepatic steatosis, lobular inflammation, hepatocyte ballooning as well as various degrees of fibrosis. NASH patients have higher risk of developing liver cirrhosis or even hepatocellular carcinoma (HCC), at which late stages liver transplantation is the only therapy to save the life [54, 55].

Prevalence of NAFLD and NASH

In line with the epidemic of obesity and T2D, NAFLD has become the most common chronic liver disease in the western countries [56]. NASH is currently the second leading cause of liver cirrhosis for liver transplantation in United States and is projected to be the first leading etiology of end-stage liver diseases required for liver transplantation in the near future [57]. Globally, it is estimated that over 24% world adult population are affected by NAFLD and 70% NAFLD patients with NASH [58]. In the United States, the prevalence rate of NAFLD and NASH is estimated to be around 25% and 3-8%, respectively [58].

Pathogenesis of NASH

NASH is a complex disease and the pathogenesis of NASH is still not fully understood yet. It is now believed that multiple factors, including genetic and environmental hits, work synergistically in a genetically predisposed individual to induce NASH [59]. Among these contribution factors, it is generally believed that ectopic lipid accumulation plays the fundamental role in the pathogenesis of NASH, which might explain why most NASH patients were diagnosed with simple NAFLD at early time point [60]. Hepatic lipid accumulation provides the pool of free fatty acids which could further generate various lipotoxic intermediates such as ceramides, diacylglycerols, lysophosphatidyl choline and other potential mediators [61]. These lipotoxic lipid metabolites will trigger oxidative stress, inflammation and apoptosis, resulting in lipotoxic liver injury and development of steatohepatisis and fibrosis [62].

Current efforts on NASH treatment

Despite of great global and domestic prevalence of NASH, there is no FDA-approved pharmacotherapies for NASH treatment. The current drug development of NASH therapies focuses on targeting different aspects of NASH pathogenesis, including targeting steatosis, inflammation, cell death, and fibrosis [63, 64].

Targeting hepatic steatosis

It is generally believed that NASH is casually related to excessive lipid accumulation in liver. Inhibiting and resolving steatosis has been proved to be an effective approach for NASH treatment. There are several drugs candidates with a primary metabolic target that has demonstrated promising therapeutic efficacy on ameliorating NASH symptoms. The representative medications in current group include PPAR agonists (stimulate lipid oxidation, improve insulin sensitivity) [65], FXR agonists (inhibit bile acid synthesis, reduce lipogenesis and steatosis) [66], ACC inhibitors (increase fatty acid oxidation, inhibit lipogenesis) [67], SCD-1 inhibitors (inhibit lipogenesis) [68], incretins and DPP-4 inhibitors (stimulate insulin secretion,

improve insulin sensitivity) [69, 70], FGF-21 analog (improve insulin sensitivity, reduce lipogenesis) [71], recombinant FGF-19 (decrease bile acid synthesis and decrease gluconeogenesis) [72] and MicroRNA-based treatment (target specific gene to modulate insulin sensitivity) [73].

Targeting inflammation

NASH represents inflamed fatty liver disease which is manifested by activation and infiltration of inflammatory cells, and production of proinflammatory cytokines and chemokines. Accordingly, there are some agents targeting inflammation that have exhibited benefits to improve NASH symptoms. The representative medications include antioxidants (reduce oxidative stress) [74], Immune modulators (reduces inflammatory cells activation and migration into liver) [75],

Targeting apoptosis

Hepatocyte injury and death is an important contribution factor of NASH pathogenesis, which is usually manifested by apoptosis. Accordingly, some caspase inhibitors have shown efficacy to improve liver damage and inflammation in preclinical and preliminary human studies[76].

Targeting fibrogenesis

How to reduce and resolve fibrosis is the key determinate of NASH treatment. Fibrosis is characterized by excessive deposition of extracellular matrix of which major composition is collagen I. In addition to the medications targeting early events of NASH pathogenesis, some anti-fibrotic agents directly inhibit or reduce fibrosis for NASH treatment [77, 78].

1.4 Lysosomal acid lipase deficiency (LAL-D)

Overview of LAL-D

Lysosomal acid lipase (LAL) is an essential enzyme responsible for hydrolysis of cholesterol ester(CE) and triglycerides (TG) in the lysosome in to free fatty acids (FFA)and free cholesterol (FC). The FA and FC are then released from lysosome back to cytosol to maintain the cytosolic fatty acids and cholesterol homeostasis [79]. LAL is encoded by *LIPA* gene and is abundantly expressed in liver, intestine and spleen. *LIPA* gene mutations causes absolute or partial loss of LAL activity in LAL-D patients, resulting in the lysosomal sequestration of CE and TG in liver, spleen and intestine [80].

There are basically two types of LAL-D: the life-threatening early-onset Wolman Disease and late-onset milder Cholesterol Ester Storage Disease (CESD). Wolman Disease is characterized by absence of LAL activity and consequent liver failure, adrenal calcification, nutrient malabsorption and mortality, which is usually present in infants. The affected infants typically present the symptoms on the first week after birth and die within 6 to 12 months [81]. Comparatively, the severity and symptoms of CESD vary across individuals depending on the residue of LAL activity [82]. The typical clinical presentation of CESD include hepatospenomegaly, liver damage and elevated plasma cholesterol level [82].

Prevalence of LAL-D

LAL-D is a rare disease. The prevalence of LAL-D is estimated as 1/13000 [83], which has a great discrepancy with the reported LAL-D cases, indicating the disease is substantially under-recognized [84]. LAL-D has profound clinical presentation in liver and plasma lipid profile, which increases the risk of misdiagnosis as nonalcoholic fatty liver diseases or other types of hypercholesterolemia [80].

Pathogenesis of LAL-D

LAL-D is an autosomal recessive disease resulting from *LIPA* gene mutations. The most common *LIPA* mutation is the exon 8 splice site mutation by introducing an alternative acceptor site, resulting in skipping or partial deletion of exon 8 in mature LAL mRNA [85].

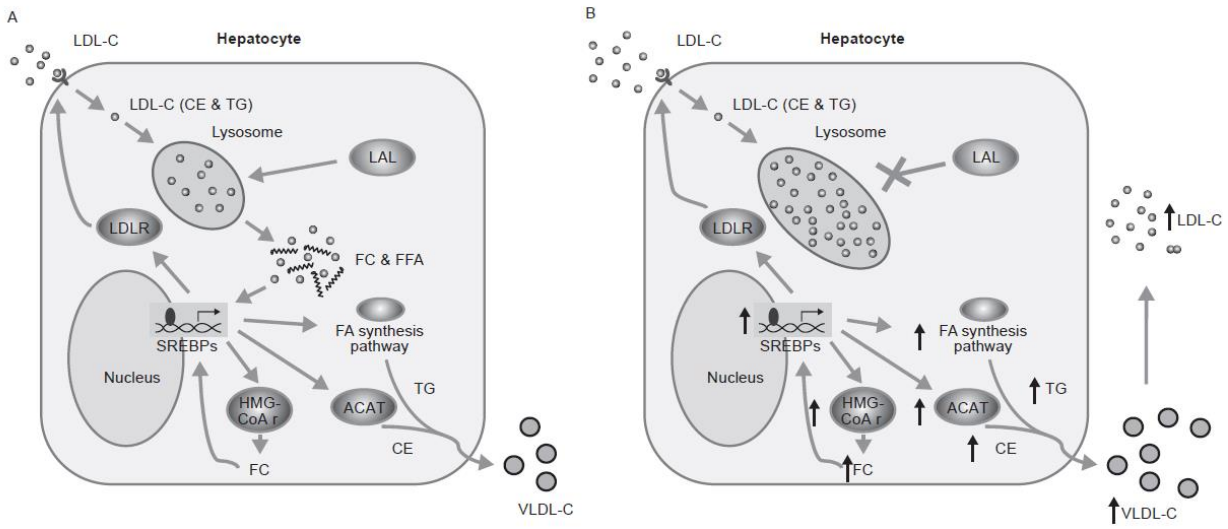

Figure 1. 2 Schematic view of cholesterol homeostasis and lipid metabolism in hepatocytes under (A) physiological condition and (B) LAL-D. Picture is cited from reference 84.

LAL plays vital role in the cholesterol and fatty acid metabolism. Low density lipoprotein (LDL) particles loaded with CE and TG are taken up by hepatocytes via LDL receptor, which eventually traffic to lysosomes. Loss of LAL function causes the failure of hydrolysis of CE and TG, resulting in massive lysosomal lipids accumulation and the scarcity of FC and FA released back to cytosol pool. The lack of cytosolic FC results in reduced suppression of SREBP-2 mediated cholesterol biosynthesis. The lack of cytosolic FA results in upregulation of SREBP-1c mediated lipogenesis [86]. The increased de novo synthesis of cholesterol and fatty acids expand the hepatocellular CE and TG pool, which exaggerates the hepatic accumulation of lipids and the development of hepatomegaly. The progressive lipid accumulation will further initiates liver damage, inflammation, which ultimately causes liver failure and death. Moreover, the increased

biosynthesis of CE and TG leads to overproduction of very low density lipoprotein (VLDL) particles and elevated plasma VLDL- and LDL-cholesterol levels, which correspond to the hypercholesterolemia symptom in LAL-D [87, 88].

Current efforts on LAL-D treatment

Sebelipase alfa, an innovative enzyme replacement therapy is the only FDA-approved treatment for LAL-D treatment. Sebelipase alfa is a recombinant human LAL (rhLAL) attached with the mannose-6-phosphate (M6P) moiety. M6P receptor expressed on the cell membranes of hepatocytes targets the enzymes to lysosomes. After intravenous infusion, Sebelipase alfa is taken up by hepatocytes via M6P receptor and then directed to lysosome where it compensates for the LAL function [89]. However, as protein-based therapeutic approach, Sebelipase alfa has the potential to induce immunogenicity. Actually, clinical reports have shown patients with Sebelipase alfa developed anti-drug antibodies or hypersensitivity reactions [90, 91]. Therefore, development of novel therapies as alternative or complementary treatment is important for LAL-D patients. Lipid-lowering medications (statins) are currently prescribed in clinics. However, their efficacy for LAL-D treatment is controversial because progressive liver damage or even liver failure were reported [82, 92]. Therefore, therapies with novel mechanism is warranted to improve LAL-D treatment.

In LAL-D, the abnormal hepatic lipid accumulation plays a fundamental role of the disease progression, driving the development of liver enlargement, liver damage as well as overproduction of VLDL and LDL-cholesterol. Therefore, targeting hepatic lipid accumulation becomes a reasonable and feasible strategy for LAL-D treatment.

2. Polymethoxyflavones (PMFs) and 5-OH PMFs as promising nutraceuticals for preventing the development of obesity and T2D

2.1 Citrus peel extract and PMFs

Citrus peel extract has been shown to exhibit various bioactivities, including anti-inflammation, anti-tumor, anti-obesity, anti-atherosclerosis, and etc[93]. In recent years, numerous studies have focused on the beneficial effects of citrus peel extract on obesity related metabolic disorders. The lipid-lowering effects of citrus peel extract can be traced to the very former study performed in Sprague-Dawley rats fed high cholesterol diet (HCD). Compare with the control group fed HCD diet alone, rats fed HCD supplemented with tangerine peel extract (16.7 g/100 g diet) exhibited significantly lower levels of hepatic triglycerides, hepatic cholesterol and plasma cholesterol. The beneficial effect of tangerine peel is related to the inhibition on two rate-limiting cholesterol synthesis enzymes in liver, HMG-CoA and acyl CoA: cholesterol O-acyltransferase (ACAT)[94]. More recently, in HFD-induced mouse, citrus sunki peel extract was found to reduce body weight gain, serum total cholesterol, serum triglycerides, adipose weight and hepatic steatosis by elevated beta oxidation and lipolysis in adipose tissue at dose of 150mg/kg/day[95]. Similarly, 1.5% citrus depressa hayata peel extract protected the mice from HFD-induced obesity and dyslipidemia by down-regulating lipogenic genes expression[96]. In consistency with the animal studies, nobiletin and tangeretin inhibited adipogenesis, regulated adipokines secretion[97], and stimulated glucose uptake[98] in 3T3-L1 differentiated mouse adipocytes, suggesting potential anti-obesity and anti-diabetes effects. Additionally, 0.1% and 0.3% nobiletin reduced VLDL production and atherosclerosis in western diet fed Ldlr-/- mouse.[99] The potential mechanism related to the anti-atherosclerosis effects of nobiletin involves reduced apoB secretion[99, 100], enhanced LDL-receptor expression[101] as well as acetylated LDL metabolism by mouse macrophages[102].

Polymethoxyflavones (PMFs) have been demonstrated as the active constituents of citrus peel extract. PMFs are a group of flavones bearing two or more methoxy groups on their basic benzo-γ-pyrone (15-carbon, C6–C3–C6) skeleton with a carbonyl group at the C4 position.

Among PMFs, nobiletin and tangeretin are the two dominating ones, containing 6 and 5 methoxy groups, respectively, found in citrus peel extract.

The water solubility of PMFs is very low (<100 μg/mL) due to their hydrophobic structure as indicated in multiple methoxy groups[93]. However, the lipophilic structure gives PMFs good membrane permeability to increase its oral absorption and bioavailability[93]. The distribution analysis of nobiletin suggested that nobiletin accumulate in a wide range of organs including the stomach, small and large intestines, liver and kidney during the 1–4 h period after a single dose[103]. Pharmacokinetic studies demonstrated that with identical dose of 50mg/kg in corn oil, nobiletin (9.03μg/mL) has 10 folds higher oral absorption in rats than tangeretin (0.38μg/mL)[104]. The metabolic pathway of PMFs is considered to be identical across the species. The 3'- and 4'- positions on the B-ring of PMFs are the primary sites of biotransformation, which gives the metabolites of 3'- and/or 4'- demethylated PMFs [93].

2.2 5-OH PMFs

Recently, demethylated PMFs, especially 5-demethylated PMFs (5-OH PMFs) are becoming a new focus in scientific research[105]. 5-OH PMFs are analogy of PMFs with a hydroxyl group replacement on 5-position. Emerging studies suggested that 5-OH PMFs present comparable or even better bioactivities than PMFs as anti-cancer and anti-inflammation treatment[106-108]. Regarding the effects of 5-OH PMFs on metabolic diseases, one recent study showed that addition of 0.25% and 0.1% synthetic hydroxylated PMFs mixture attenuated the high fat diet (HFD) induced body weight gain and hepatic steatosis in mice[109]. Moreover, in vitro studies revealed that a 5-OH PMF, 5-OH nobiletin, enhances the LDL receptor gene expression and decreased acyl CoA:diacylglycerol acyltransferase 2 (DAGT2) expression in HepG2 cells; and 5-OH nobiletin is more potent in inhibiting monocyte-to-macrophage

differentiation and foam cell formation[110]. However, in vivo systematical study of the impact of 5-OH PMFs or 5-OH PMFs containing nutraceuticals on metabolic disorders is still limited.

2.3 Aged citrus peel (chenpi)

History of chenpi

Aged citrus peel, or *chenpi*, is made from the dry peel of the fruit of Citrus reticulate Blanco or other cultivated varieties, such as Citrus reticulata ' Chachi', Citrus reticulata ' Dahongpao ', Citrus reticulata'Unshiu', and Citrus reticulata'Tangerina '. The fresh peels from certain ripe citrus species were dried under sun or low temperature and then stored under temperature/moisture controlled environment for aging processing[111]. The most famous and valuable type of *chenpi* is named Xinhui *Chenpi* from Guangzhou province in China.

Chenpi has long been used as an herb in traditional medicine for treating digestive, mucous and inflammation problems.[111] Due to its medicinal value and pungent flavor, people also use *chenpi* as dietary supplements or cuisine seasoning in cooking, which makes *chenpi* a medicinal food. There is a general belief that the longer of aging processing, the greater potency of *chenpi* will possess. However, despite of the general belief of the medicinal value of *chenpi*, the scientific study of this Chinese herb is still insufficient, most likely due to the short of knowledge in its constituent profile of *chenpi* extract.

Chemical pattern of chenpi

By using Continuous Phase Transition (CPT) extraction method and HPLC analysis, we profiled the chemical pattern of extract from 1-year and 5-year Xinhui *chenpi* and compared them to the extract from freshly prepared dry citrus peel. It turned out that nobiletin and tangeretin universally exist in regular dry citrus peel and one or five year *chenpi* extract. However, compared to regular ones, *chenpi* extract contains higher amount of 5-OH PMFs, including 5-OH

nobiletin and 5-OH tangeretin. And the amount of 5-OH PMFs increases with the aging year (**Figure 6**), which coincides with the general observation that the more aged *chenpi* is more valuable in medicine and commercial market.

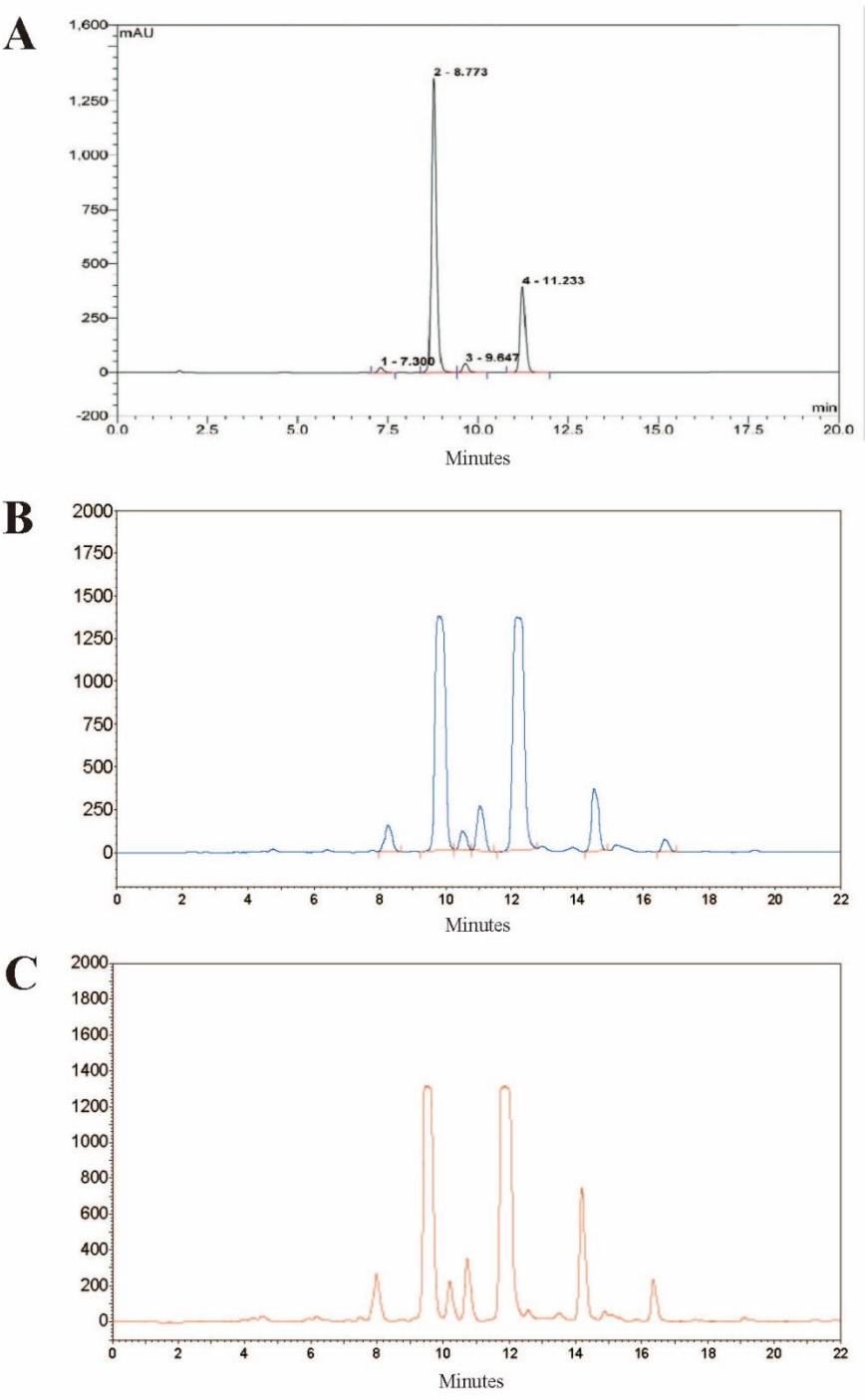

Figure 1. 3 HPLC chromatograph of (A) fresh dry citrus peel extract, (B) 1-year-old chenpi extract, and (C) 5-year-old chenpi extract.

2.4 Casticin

Casticin(3',5-dihydroxy-3,4',6,7-tetramethoxyflavone) is a major flavonoid of the active constituents of Viticis Fructus (Manjingzi in Chinese).[111] Viticis Fructus is the dry fruit of shrub chaste tree, which has been used anciently for treatment of inflammation and pain-relief.[111]

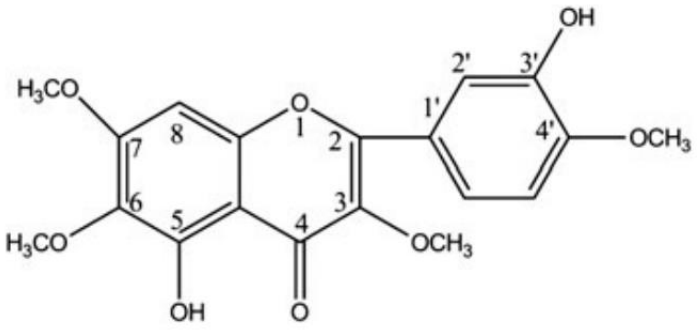

Figure 1. 4 Chemical structure of casticin (3',5-dihydroxy-3,4',6,7-tetramethoxyflavone).

In rats, oral administration of 400mg/kg casticin in saline gives a mean C_{max} value of 287.06 ± 40.68 ng/ml with an elimination half-life ($t_{1/2}$) of 36min, indicating a poor absorption of casticin in aqueous system. Intravenous injection of 50mg/kg casticin produces a mean C_{max} value of 12.74± 0.72 μg/mL and a $t_{1/2}$ of 20.86 ± 2.02 min, suggesting rapid distribution and elimination of casticin in rats.[112] After oral administration of casticin to rats, there are 25 metabolites in addition to the parent compound were identified in rat plasma, urine, and six selected tissues[113]. Demethylation, methylation, glucuronidation and sulfation were demonstrated as major biotransformation pathways of casticin in vivo. Liver, kidney, and lung are the major distribution organs of casticin in rats[113].

It has been shown that casticin exerts a wide array of bioactivities, such as anti-inflammation, anticancer, and immunoregulatory. Regarding its anti-inflammation property, one recent mouse study showed that casticin strongly inhibited the smoke-induced lung inflammatory responses with a daily dose of 10mg/kg via i.p. injection during 2-weeks treatment.[114] The

striking anticancer activities of casticin has been proved in a broad array of human cell lines with various proposed mechanisms, including induction of apoptosis via ROS-mediated mitochondrial dysfunction[115]or ROS-mediated JNKs activation[116], inhibition of angiogenesis,[117] and remaining sensitivity to drug-resistant cancer cell lines.[118]

So far, there is no study regarding the effect of casticin on metabolic regulation has been reported. Casticin can be structurally recognized as 5-OH PMF derivative with one extra hydroxyl group on 3'-postions. Based on the previous studies, 5-OH PMFs present therapeutic potential to prevent and treat metabolic diseases. It is thus interesting and important to determine the effect of casticin on glucose and lipid metabolism, in particular compare its effect with 5-OH PMF counterpart.

3. Safe mitochondrial uncoupler as novel pharmacotherapy for treating metabolic diseases

3.1 Coupled mitochondrial respiration

Mitochondria is the center of cellular metabolism with the principle function of generating ATP through mitochondrial respiration. Nutrient molecules, such as the metabolites of glucose and fatty acids are directed to mitochondria to get completely oxidized. The extracted chemical energy is then temporally stored in high-energy electron carriers, nicotinamide adenine dinucleotide (NADH) and flavin adenine dinucleotide ($FADH_2$). NADH and $FADH_2$ undergo redox reactions across the electron transport chain (ETC) located at the mitochondrial inner membrane, resulting in the final reduction of oxygen into water. At the same time, the electron flow across ETC releases the energy that drives the proton efflux from mitochondrial matrix to intermembrane space, thus establishing the proton gradient across mitochondrial inner membrane. The proton motive force stored in the proton gradient is used for phosphorylation of ADP to ATP when protons reenter mitochondrial matrix through ATP synthase [119]. By coupling

mitochondrial oxidation with ATP generation, the chemical energy from nutrients are eventually transformed to ATP .

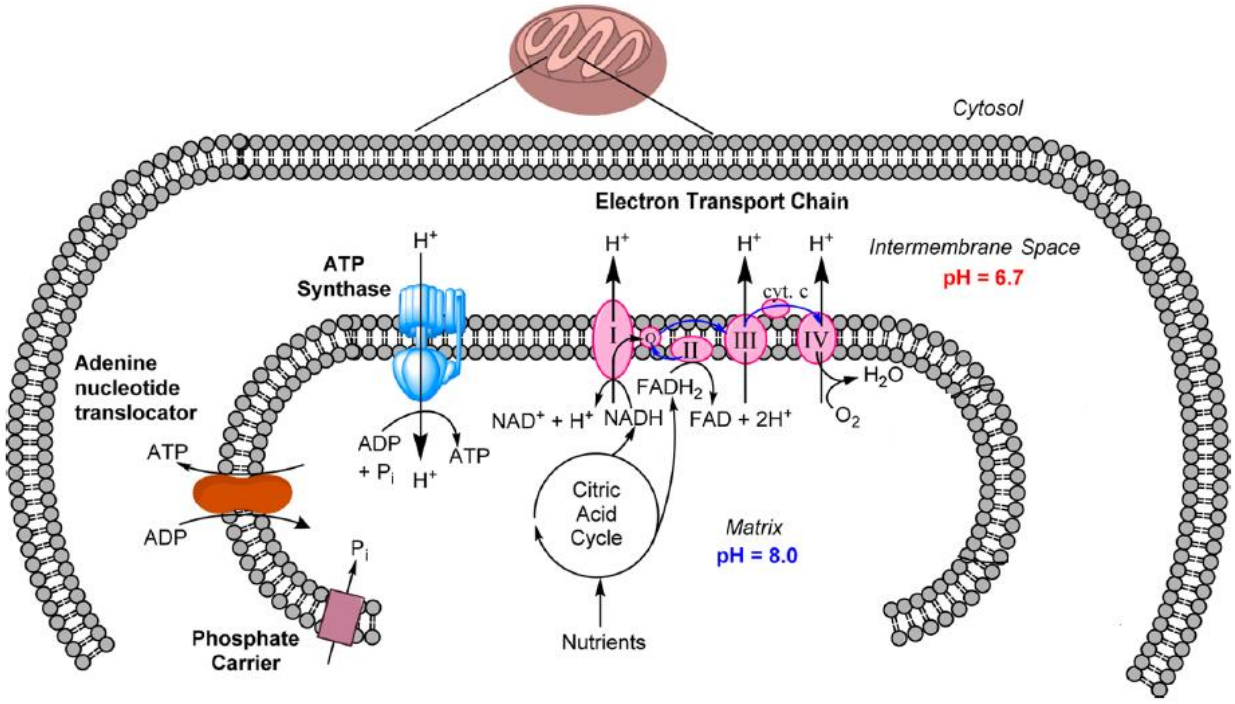

Figure 1. 5 Schematic view of mitochondrial oxidative phosphorylation event. Image is cited from reference 121.

3.2 Mitochondrial uncoupling

Overview of mitochondrial uncoupling

Mitochondrial uncoupling describes the process that decouples nutrient oxidation and ATP generation. The process is usually caused by proton leaking across mitochondrial inner membrane, which can be mediated by either endogenous proton ion transport protein (uncoupling proteins, UCPs) or some chemical molecules (mitochondrial uncouplers) [120]. Unlike ATP synthase-mediated proton transport, the proton shuttling event mediated by mitochondrial uncoupling does not generate ATP, but dissipates the proton motive force energy as heat. As a result, mitochondrial uncoupling reduces proton gradient and ATP synthesis, which creates a

futile cycle of nutrient oxidation. At the same time, mitochondrial uncoupling up-regulates the nutrient consumption and electron transfer across ETC to compensate for the ATP generation inefficiency [121]. Consequently, the biological function of mitochondrial uncoupling contributes to the elevation of energy expenditure and reduction in reactive oxidative species production.

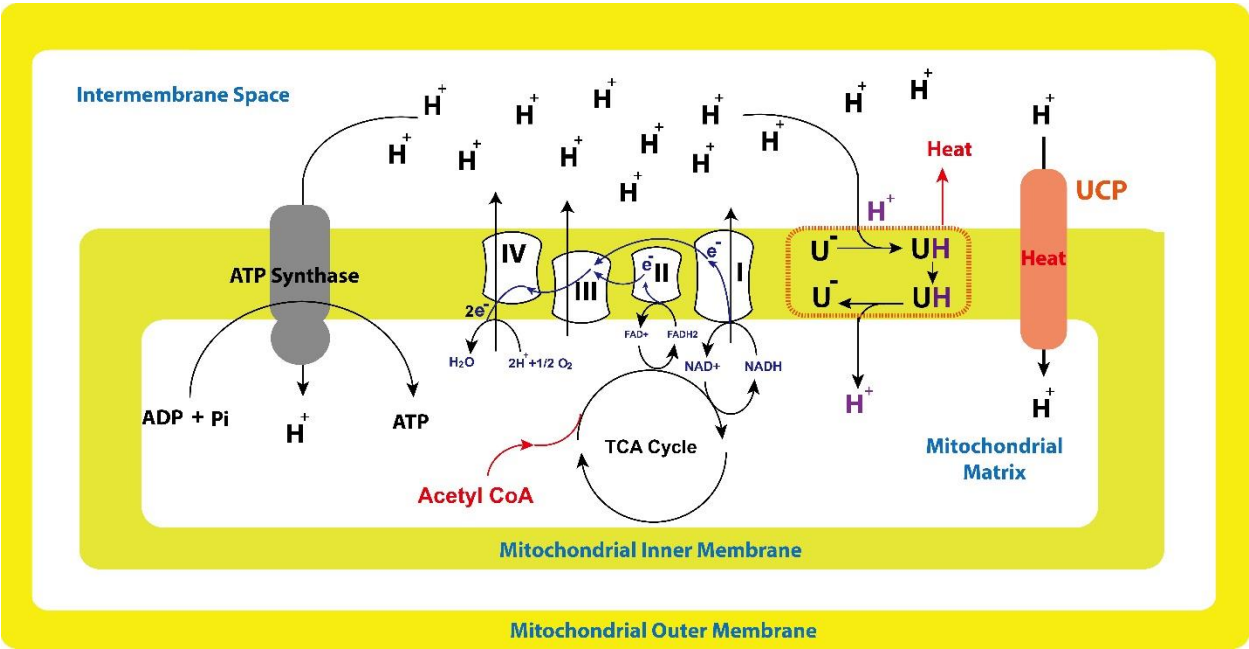

Figure 1. 6 Schematic view of mitochondrial uncoupling induced by uncoupling protein (UCP) and small molecule uncoupler

Uncoupling proteins (UCPs)

UCPs is a group of mitochondrial anion transporter proteins located at mitochondrial inner membrane. UCP-1 is the first and one of the most well-studied uncoupling proteins. UCP-1 is pre-dominantly expressed in brown adipose tissue (BAT) where UCP-1 induced mitochondrial uncoupling accounts for the thermogenic role of BAT in response to cold temperature exposure [122].

Chemical uncouplers

Some small molecules induce mitochondrial uncoupling by directly transporting proton across mitochondrial inner membrane and dissipate the energy as heat [121]. These chemicals are referred to mitochondrial uncouplers. The most representative group of mitochondrial uncouplers are some lipophilic weak acids with electron-withdrawing group inside their chemical structures [123, 124]. The hydrophobicity and electron-withdrawing property allow the molecules staying on the mitochondrial inner membrane; and the acidic dissociable group is the functional group of these mitochondrial uncouplers which allows themselves protonating at the outer side and deprotonating at inner side, thus catalyzing the proton influx back to mitochondrial matrix [124].

The small molecule 2,4- dinitrophenol (DNP) is the most well-known mitochondrial uncoupler. DNP had gained popularity in inducing weight loss in 1930s but was withdrawn from the market due to severe side effects and death reports [121]. In addition to DNP, some FDA-approved drugs are also well-documented mitochondrial uncouplers such as bupivacaine (local anesthetic drug), niclosamide (anthelmintic drug), and aspirin (nonsteroidal anti-inflammatory drug) [125, 126]. Moreover, some natural products are able to present uncoupling activities by favoring the proton translocation from intermembrane space back to mitochondrial matrix [127], such as quercetin [128] , curcumin [129], xanthohumol [130] and usnic acid [131].

Therapeutic potential of mitochondrial uncoupling

Mitochondrial uncoupling stimulates the mitochondrial respiration independent of ATP demand, which elevates the consumption of glucose and fatty acids and accelerates the electron transfer across ETC. The increased nutrient oxidation directly promotes energy expenditure, which underscores the therapeutic role of mitochondrial uncoupling in treating diseases that causally related to excessive lipid accumulation, in particular multiple obesity-related metabolic diseases [132, 133]. In addition, ETC is the major site of ROS production, resulting from the interaction of single electron with molecular oxygen at the redox centers of ETC. The faster

electron transport shortens the dwelling time of single electron in ETC and thereby reduces the risk of mitochondrial superoxide production [134], which underlines the therapeutic potential of mitochondrial uncoupling for treating diseases causally associated with ROS production and inflammation, such as NASH [133], aging [135], neurodegenerative diseases [136] and cancer [137].

The therapeutic roles of mitochondrial uncoupling have been revealed in multiple proof of concept animal studies in which UCPs are genetically knocked out or introduced in specific tissues. For example, mice with transgenic expression of UCP-1 in white adipose tissue display a lean phenotype [138]. Consistently, overexpression of UCP-1 in muscle increases lipid metabolism and overall energy expenditure and prevents diet-induced obesity and diabetic symptoms in mice [139].

Small molecule uncouplers allow the application of mitochondrial uncoupling strategy as a practical therapeutic approach. Accumulating evidences in rodent animals demonstrate that small molecule uncouplers present beneficial effects on glucose homeostasis, lipid metabolism, insulin sensitivity, aging, neurodegenerative diseases, and prolonging lifespan [121]. However, how to improve the therapeutic index of mitochondrial uncoupler is the key hurdle of translating bench work studies to clinical applications. An ideal mitochondrial uncoupler is expected to present a) selectivity on mitochondria and specific tissue to avoid off-target toxicity, b) relatively high window between efficacious dose and toxic dose, as well as c) moderate uncoupling activity to balance the mitochondrial depolarization extent [121].

Specifically, for treating liver-based diseases (e.g. T2D, NAFLD) with mitochondrial uncoupling strategy, it is important to identify the safe mitochondrial uncouplers that selectively function in liver with moderate uncoupling activity and wide therapeutic window.

3.3 Niclosamide ethanolamine and Niclosamide piperazine

Niclosamide is an FDA-approved drug for treating intestinal tapeworm infection with the working mechanism of uncoupling mitochondria of parasitic worms. Niclosamide ethanolamine (NEN) and niclosamide piperazine (NPP) are the salt forms of niclosamide, which process better water solubility and similar safety profiles in mammals compared to niclosamide free base. The chemical structures of niclosamide, NEN and NPP are demonstrated in **Figure 1.8**.

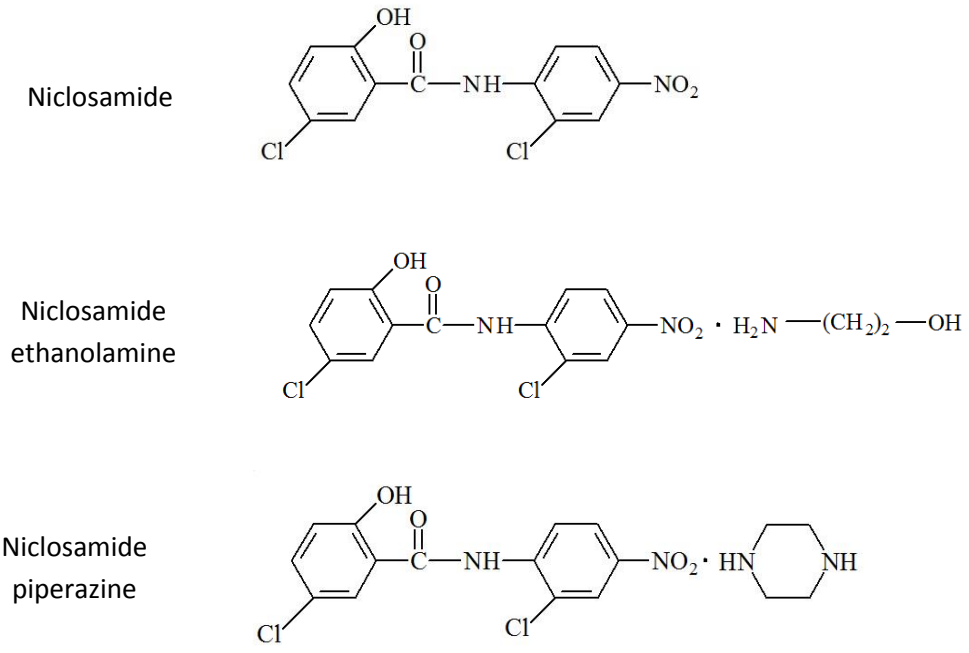

Figure 1. 7 Chemical structures of niclosamide, niclosamide ethanolamine (NEN) and niclosamide piperazine (NPP)

Niclosamide ethanolamine (NEN)

As a salt form of niclosamide, NEN presents mild mitochondrial uncoupling activity in mammalian cells and in mice, with an EC_{50} around 0.5μM. Consistent with its uncoupling activity, NEN promotes the overall energy expenditure in mice, which mostly attributes to the elevation in lipid oxidation. Pharmacokinetic studies showed that with an oral dose of 40mg/kg body weight, NEN presents half-life time of 1.25 hour and peak plasma concentration of 1.0-2.5 μM, suggesting that NEN is bioavailable. Tissue distribution studies demonstrated that when

orally administrated, NEN is primarily distributed to liver with an exposure of 300~500 ng/mg tissue weight. Low to negligible level of NEN was identified in brain, muscle, adipose, lung, and heart. The safety profile of NEN is well documented in mammals [140]. Oral LD_{50} of NEN is around 10,000 mg/kg body weight in rat and no adverse effect was found in rat fed 25,000 ppm NEN for over one year [141]. Previous study demonstrated that at the safe dose of 150 mg/kg body weight, NEN is effective to prevent and reverse high-fat diet induced obesity, insulin resistance and hepatic steatosis in mice. NEN also improved the diabetic symptoms and liver lipid accumulation in db/db diabetic mice. Mechanistically, the beneficial effects of NEN on treating obesity, T2D and hepatic steatosis are attributed to its mitochondrial uncoupling activity [140]. The data collectively indicate that NEN is a liver-targeting mitochondrial uncoupler with mild uncoupling activity and excellent safety profile (therapeutic window >50).

The therapeutic features of NEN provide the rationale of apply NEN as a safe mitochondrial uncoupler for treating other liver-based diseases caused by ectopic lipid accumulation, such as NAFLD/NASH and LAL-D.

Niclosamide piperazine

As another salt form of niclosamide, the water solubility of NPP is between niclosamide and NEN. The safety profile of NPP is comparable to niclosamide and NEN with oral LD_{50} of 5000 mg/kg body weight in rat [141]. The striking efficacy of NEN suggests the therapeutic potential of niclosamide-based drugs for treating obesity, T2D and fatty liver diseases.

For the drug development purpose, it is important to perform in-house study to determine the anti-obese and anti-diabetic effect of NPP in relevant animal models so as to compare its therapeutic potential to NEN.

Chapter II. Determine the anti-obese and anti-diabetic effects of 5-OH PMF-enriched *chenpi* extract in mice

The work of Chapter II was published in the title of 'Prevention of obesity and type 2 diabetes with aged citrus peel (Chenpi) extract' on Journal of Agriculture and Food Chemistry, 2016. 64(10): p. 2053-61.

Prevention of obesity and type 2 diabetes with aged citrus peel (Chenpi) extract

Jingjing Guo[1,2], Hanlin Tao[2], Yong Cao[3], Chi-Tang Ho[1], Shengkang Jin[2]* and Qingrong Huang[1,]*

[1] Department of Food Science, Rutgers University, 65 Dudley Road, New Brunswick, New Jersey 08901, USA

[2] Department of Pharmacology, Rutgers University-Robert Wood Johnson Medical School, Piscataway, New Jersey 08854, USA

[3] College of Food Science, South China Agricultural University, Guangzhou 510642, P. R. China

Abstract

Chenpi is the dry peel of the plant *Citrus reticulata Blanco* after aging processing. It has been used as an anti-digestive and anti-inflammatory traditional medicine, as well as culinary seasoning and dietary supplements in China. But its efficacy and underlying scientific mechanism have not been sufficiently investigated. *Chenpi* is uniquely enriched with high content of 5-demethylated polymethoxyflavones (5-OH PMFs). The effect of *chenpi* extract on improving metabolic features was examined using high fat diet (HFD) induced obesity/diabetes mouse model. Oral administration of 0.25% and 0.5% *chenpi* extract in food over 15 weeks markedly prevented HFD-induced obesity, hepatic steatosis, and diabetic symptoms. The beneficial effect is associated

with 5'-adenosine monophosphate-activated protein kinase (AMPK) activation in adipose tissue. Our results indicate that 5-OH PMFs enriched *chenpi* extract is effective in preventing obesity and type 2 diabetes and its effect might be related to improvement in lipid metabolism associated with activation of AMPK pathway.

1. Introduction

Type 2 diabetes (T2D) has reached epidemic proportions worldwide.[142] It is characterized by insulin resistance and altered glucose and lipid metabolism.[5] Insulin resistance is also linked to a wide array of metabolic syndromes including non-alcoholic fatty liver diseases, dyslipidemia, and cardiovascular disease.[143] The increased prevalence of T2D and other metabolic diseases is becoming a major medical challenge globally. Most medications available failed to correct the underlying causes of insulin resistance and have their own inherent limitations.[144, 145] Pharmacotherapy targeting the origin of insulin resistance is preferable to improve T2D treatment.

Morbid obesity is linked to the development of T2D and insulin resistance.[143, 146] Although it is not fully understood how excessive lipid contributes to the impaired insulin function at molecular level, reversal of insulin resistance is highly correlated with reduction of triglyceride content in liver.[17] Consistently, lifestyle interventions, including diet modification, weight control, and regular exercise, which significantly reduce hepatic lipid load, increase insulin sensitivity.[147, 148] Thus, pharmacological therapies that reduce hepatic steatosis are potentially effective strategies for correcting an underlying cause of insulin resistance.[140, 149]

Polymethoxyflavones (PMFs)-rich citrus peel extracts have been demonstrated as promising therapeutic agent for metabolic disorders.[96, 150-152] Previous studies have shown that 5-demethylated polymethoxflavones (5-OH PMFs) appear to have better bioactivities than PMFs for anti-cancer and anti-inflammation.[93] One recent study showed that the synthetic

hydroxylated PMF mixture attenuated the high fat diet (HFD) induced adiposity and hepatic steatosis in mice. [109] Moreover, in vitro studies revealed that a 5-OH PMF, 5-OH nobiletin, enhances the low density lipoprotein (LDL) receptor gene expression in HepG2 cells.[110] However, in vivo systematical study of the impact of 5-OH PMFs or 5-OH PMFs containing nutraceuticals on metabolic disorders is limited.

Aged citrus peel, also called *chenpi* in China, is usually made from dry peel of the plant *Citrus reticulata Blanco* either by sun-dry or low-temperature dryer, followed by storing under temperature/moisture controlled conditions for aging process.[153] It has long been used in traditional medicine for treatment of digestive and mucous disorders as well as skin inflammation.[153] However, it has not been clearly explored scientifically due to the lack of knowledge of its chemical constituents. In addition, *chenpi* also serves as culinary seasoning and dietary supplements in China, with an excellent safety profile. Compared to regular PMFs-rich citrus peel, we found that *chenpi* contains higher percentage of 5-OH PMFs including 5-OH nobiletin and 5-OH tangeretin in its active constituents. Interestingly, the contents of 5-OH PMFs increase with aging time, which coincides with a general observation that more aged *chenpi* seems to have better medicinal efficacy.

For treating metabolic disorders, until now, studies are limited to anti-obesity effects of PMFs from fresh citrus peels or synthetic hydroxylated PMFs. No animal studies related to the hypoglycemic, hypolipidemic and insulin-sensitizing effects of 5-OH PMFs or 5-OH PMFs containing nutraceuticals were reported. *Chenpi* extract is naturally enriched with 5-OH PMFs and have excellent safety profile. Also the study of *chenpi* will substantiate our understanding of its traditional health-promoting benefits, and provide evidence for the development of *chenpi* nutraceuticals. The overall objective of current study is to determine the effectiveness of a *chenpi* extract in preventing the development of obesity, T2D and related diabetic complications in a mouse model.

2. Material and Methods

2.1 Sample preparation and characterization

Chenpi extract was prepared by using Continuous Phase Transition extraction method (CPT) with n-butane as the solvent (0.5 MPa extraction pressure, 50 ºC extraction temperature and 60 min extraction time). The oil-like *chenpi* extract was further subjected to silica gel column chromatography by using n-hexane as the mobile phase to remove essential oils and waxes. The eluate was then evaporated by rotary evaporator followed by vacuumed dried. The pale-yellow power obtained was analyzed by HPLC, and the constituent profile of *chenpi* extract was thereafter determined. As shown in **Fig. 2.1A**, nobiletin (**Fig. 2.1B**), tangeretin (**Fig. 2.1C**), and 5-OH nobiletin (**Fig. 2.1D**) were identified as three dominating PMFs in *chenpi extract*, with mass ratio of 6.24:4.8:1 (**Fig. 2.1E**).

A

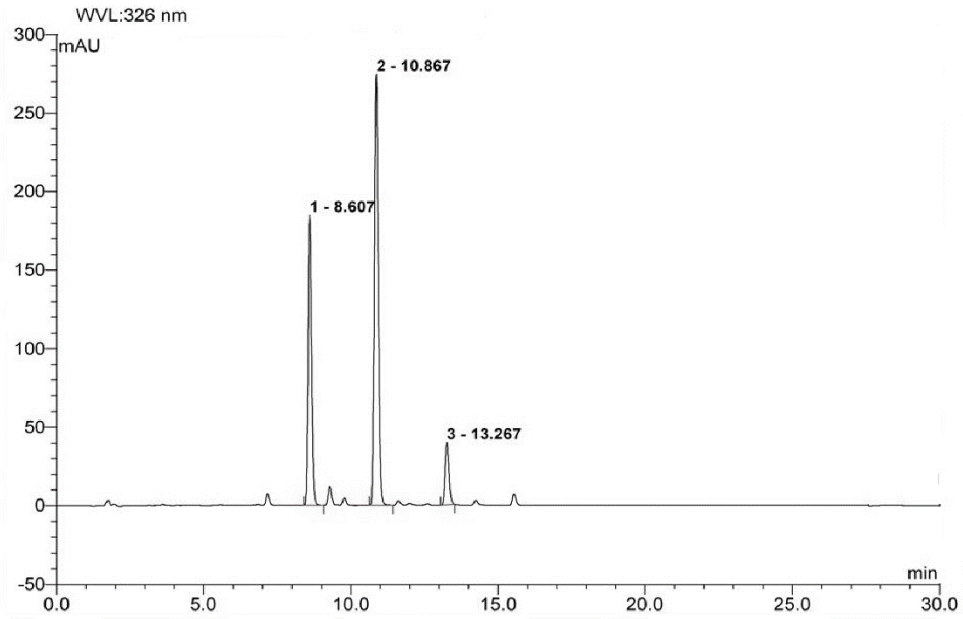

B

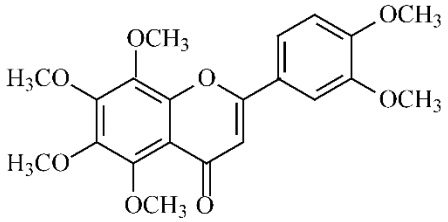

C

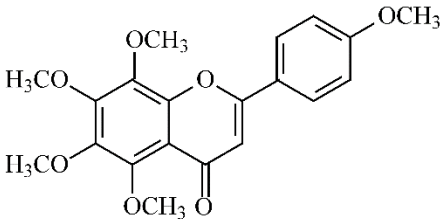

D

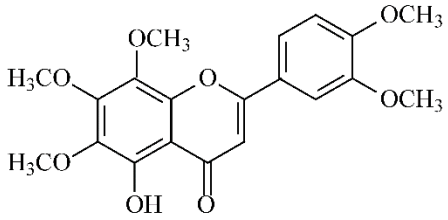

E

Peak	Compound	Percentage
1	Nobiletin	31.28%
2	Tangeretin	22.82%
3	5-OH Nobiletin	9.22%

Figure 2. 1 Major constituents of chenpi extract. (A) HPLC chromatogram of polymethoxyflavones from chenpi extract, peak 1 as nobiletin, peak 2 as tangeretin, peak 3 as 5-OH nobiletin, (B) structure of nobiletin (hexamethoxyflavone), (C) structure of tangeretin (pentamethoxyflavone), (D) structure of 5-OH nobiletin (5-demethoxylated nobiletin), (E) relative content of major polymethoxyflavones.

2.2 Animals and treatment

Four-week old male C57BL/6J mice were purchased from Jackson Laboratory (Harbor, ME), and housed in a vivarium of Rutgers-RWJMS following the Vivarium and Institutional Regulations. All experimental protocols were approved by the Institutional Animal Care and Use Committee. Mice were housed 2 per cage and maintained in temperature/humidity controlled room with 12 h light/dark cycle. Starting at age of 5 week, mice were randomly divided into the following three groups (n=10), which were fed HFD (60% fat calorie, Research Diet, New Brunswick, NJ), or HFD supplemented with 0.25% *chenpi* extract (LD) or HFD supplemented with 0.5% *chenpi* extract (HD) for 15 weeks. Mice were allowed free access to water and food throughout the experiment. Body weight was recorded weekly, while food intake and feces excretion were monitored daily. At the end of study, mice were anesthetized with ketamine and xylazine for cardiac blood draw, followed by tissue collection. Heparin plasma samples were obtained by centrifugation at 1000 g for 15 min at 4 ^{o}C, and stored at -80 ^{o}C for plasma biochemical tests. Tissue samples were stored in liquid nitrogen for further analysis.

Table 2. 1 Ingredients of high fat diet from Research diet.

Ingredient	**gm**	**kcal**
Casein, 30 Mesh	200	800
L-Cystine	3	12
Corn Starch	0	0
Maltodextrin 10	125	500
Sucrose	68.8	275.2
Cellulose, BW200	50	0
Soybean Oil	25	225
Lard	245	2205
Mineral Mix S10026	10	0
DiCalcium Phosphate	13	0

Calcium Carbonate	5.5	0
Potassium Citrate, 1 H2O	16.5	0
Vitamin Mix V10001	10	40
Choline Bitartrate	0.05	0

2.3 Blood glucose and plasma insulin measurement

Blood glucose level was determined by tail bleed from 16-hr pre-fasted mice with a glucometer (OneTouch UltraSmart blood glucose monitoring system, Lifescan, Milpitas, CA). For plasma insulin measurement, mice were fasted 5 hr before experiment. Blood samples were then collected and subjected to ultra-sensitive mouse insulin ELISA kit (Crystal Chem Inc., Downers Grove, IL).

2.4 Plasma biochemical analysis

Plasma samples collected from 5hr-fasted mice were sent to the US National Mouse Metabolic Phenotyping Center (MMPC) at University of California, Davis (UC Davis), for the measurement of plasma triglycerides (TG), total cholesterol (TC), and non-esterified fatty acid (NEFA), alanine transaminase (ALT), and aspartate transaminase (AST).

2.5 Glucose tolerance assay and insulin sensitivity assay

Mice were fasted for 16 hr before glucose tolerance test. Glucose load was given by intraperitoneal injection with 20% D-glucose at dosage of 2 g/kg body weight. Blood glucose levels were measured initially and at defined time points after injection (15min, 30min, 60min, 90min, and 120min). For insulin sensitivity study, 5-hr fasted mice were intraperitoneally injected with recombinant human insulin (Eli Lilly, Indianapolis, IN) at a dosage of 0.75 U/kg body weight.

Blood glucose concentrations were measured thereafter at the same time points as indicated in glucose tolerance test.

2.6 Hepatic and fecal triglyceride determination

For the measurement of triglyceride content in liver and feces, samples were first homogenized in saline solution. Total lipids were then extracted by Folch's method with modification described before.[140] Briefly, chloroform and methanol (v/v, 2:1) were added to the homogenates, followed by shaking, filtration and evaporation. Final triglyceride content was determined by triglyceride determination kit (Sigma, St. Louis, MO), and normalized against sample weight.

2.7 Protein extraction and immunoblotting analysis

Collected tissues were homogenized with lysis buffer containing 10 mM TRIS-HCl (pH 7.9), 10% glycerol, 0.1 mM EDTA, 100 mM KCl, 0.2% NP-40, 0.5 mM PMSF, 1 mM DTT, mini-complete protease inhibitor cocktail (Roche Diagnostics, Indianapolis, IN) and phosphatase inhibitor cocktail (Roche Diagnostics, Indianapolis, IN). Nuclei and insoluble debris were pelleted in an Eppendorf micro-centrifuge at 12,000 rpm for 15 min at 4 °C. Supernatant was then stored at -20 °C or immediately subjected to SDS-PAGE. The proteins were then transferred to polyvinylidene difluoride (PVDF) membranes (Millipore, Belgium) overnight. Following probing with antibodies against AMPK-α, Phospho-AMPK-α (Thr172), ApoB, or RAs-related Nuclear protein (RAN) proteins, chemiluminescent detection was completed with ECL western blotting reagents (Amersham, Buckinghamshire, UK).

2.8 Histology of liver and adipose tissue

Liver and abdominal adipose tissues (epididymal white adipose tissue, epididymal WAT) were fixed with 10% neutral buffered formalin (Surgipath Medical Industries, Inc., Richmond, IL)

and embedded in paraffin. Tissue sections were then prepared and stained with hematoxylin and eosin (H&E). Histological images were captured by Nikon Eclipse Ni-U imaging system. The quantification of adipocyte size were performed by ImageJ based Adiposoft program as described before.[154]

2.9 Statistics

Data are presented as the means ± s.d.. One-way ANOVA was used for all the statistical comparison among groups. Statistical significance is denoted as *P < 0.05, **P < 0.01 and ***P < 0.001, vs HFD.

3. Results

3.1 *Chenpi* extract reduced diet-induced body weight gain

To determine the potential effect of the *chenpi* extract on management of metabolic status, we used HFD-induced obese/diabetic mouse in which adiposity, hyperglycemia, insulin resistance, dyslipidemia and hepatic steatosis develop after long-term high calorie challenge.[155] As shown in **Fig. 2.2A**, the control mice fed HFD alone developed dramatic body weight after initiation of HFD regime. In contrast, age-matched mice with treatment of *chenpi* extract showed significantly smaller body weight gains throughout the study even with HFD feeding. By the end of 12 weeks, mice treated with 0.25% and 0.5% *chenpi* extract in food exhibited a reduction of 21 and 34%, in body weight, respectively, compared to those control mice fed HFD alone. There were no apparent differences in food intake among the three different diet groups (**Fig. 2.2B**). Additionally, as shown in **Fig. 2.2C and D**, feces excretion and fecal triglyceride contents were comparable among the three groups. The results indicate that the rates of nutrient absorption were similar in these mice, and lower body weight gain was not due to malnutrition.

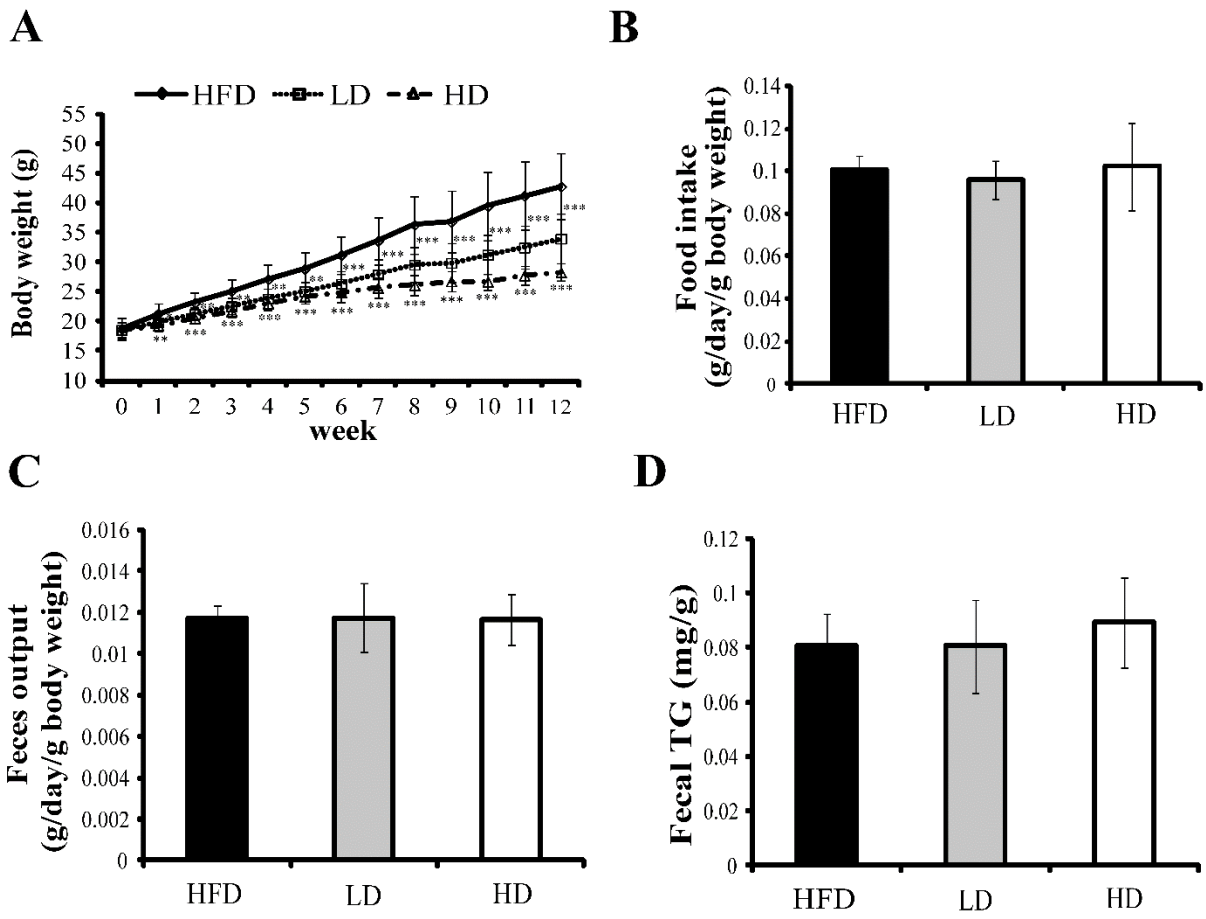

Figure 2. 2 Chronic oral treatment of chenpi extract reduced HFD-induced body weight gain in mice. (A) Body weights, (B) daily food intake, (C) daily feces output, and (D) fecal triglyceride contents of C57BL/6J male mice which were fed HFD, HFD plus 0.25% chenpi chenpi extract (LD), or HFD plus 0.5% chenpi extract (HD) for 15 weeks. Data are presented as mean value ± s.d. (n=10). *P<0.05, **P<0.01, *** P<0.001 vs HFD. All error bars, s.d.

3.2 *Chenpi* extract improved glycemic control and insulin resistance

The slower rate of body weight gain with treatment of *chenpi* extract prompted us to determine the effect of *chenpi* extract on glycemic control and insulin sensitivity. First we tested whether oral *chenpi* extract was efficacious in preventing the development of hyperglycemia and hyperinsulinemia. Compared to HFD-fed alone mice, treatment with *chenpi* extract significantly

reduced blood glucose level (**Fig. 2.3A**) (106±16mg/dL in LD, 104±18mg/dL in HD vs 139±16mg/dL in HFD) though the value did not reach the normal level observed in chow diet- fed mice (82±3mg/dL) [156]. *chenpi* extract treatment can dramatically reduce plasma insulin levels (**Fig. 2.3B**) (0.48±0.08ng/mL in LD, 0.30±0.04ng/mL in HD vs 1.9±1.6ng/mL), which is within the normal range of mice fed chow diet (0.26±0.1ng/mL) [156]. To further investigate the effects on insulin sensitivity, we performed glucose tolerance assay and insulin tolerance assay. In glucose tolerance test, significant higher glucose tolerance was found in mice treated with 0.5% *chenpi* compared to those fed HFD alone (**Fig. 2.3C**). In insulin tolerance test, mice in both *chenpi* extract-treated groups exhibited better insulin sensitivity in response to insulin load as shown in **Fig. 2.3D**.

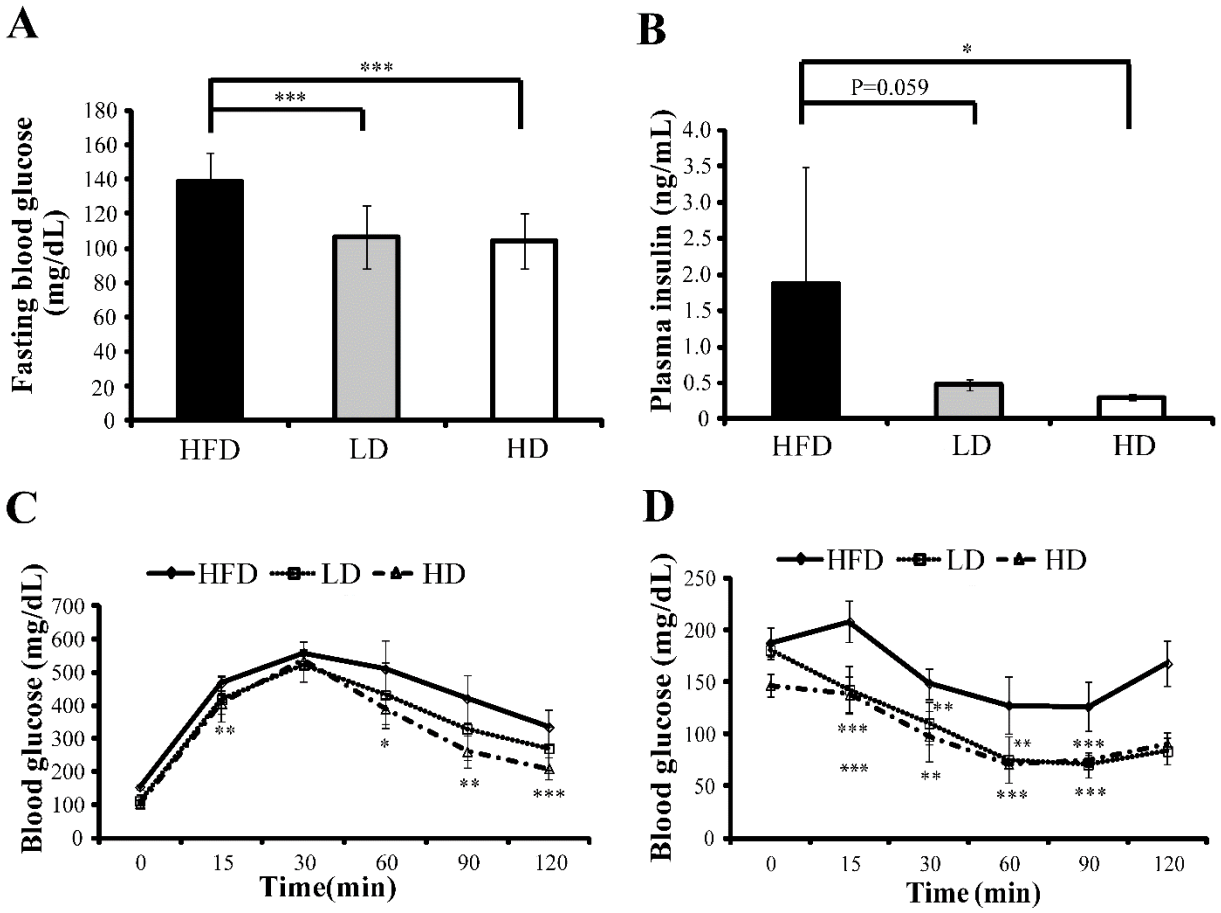

Figure 2. 3 Chronic oral treatment of chenpi extract improved glycemic control and insulin sensitivity in mice. (A) Fasting blood glucose levels of C57BL/6J male mice fed HFD, HFD plus

0.25% chenpi extract (LD), or HFD plus 0.5% chenpi extract (HD) measured at week 15. (C) Glucose tolerance assay and (D) insulin sensitivity assay were performed as described above on week 13 and week 14, respectively. Data are presented as mean value ± s.d. (n=10). *P<0.05, **P<0.01, *** P<0.001 vs HFD. All error bars, s.d..

3.3 *Chenpi* extract prevented diet-induced hepatic steatosis

First, we examined the gross appearance of mouse liver in control and *chenpi* treated groups. By the end of 15-week treatment, control mice fed HFD alone developed fatty liver represented by enlarged size and pale color (**Fig. 2.4A**). In contrast, mice fed HFD containing either dose of *chenpi* extract showed regular size and normal appearance of livers (**Fig. 2.4A**). Histological analysis of liver samples showed the reduction of hepatic intracellular lipid load under treatment of *chenpi* extract. As shown in **Fig. 2.4C**, the hepatocytes of HFD-fed mice had significant vacuolation, resulting from the massive intracellular lipid droplets. In contrast, few lipid droplets were observed in mice fed HFD plus *chenpi* extract. Moreover, we identified significantly lower liver weights (**Fig. 2.4A**), and lower liver triglyceride contents (**Fig. 2.4B**) in both 0.25% and 0.5% *chenpi* groups, which confirmed the amelioration of hepatic steatosis. Consistent with the observation on liver histology, 0.25% *chenpi* extract significantly reduced plasma ALT (**Fig. 2.4D**). 0.5% *chenpi* extract does not affect plasma ALT and AST significantly when compared to HFD alone group (**Fig. 2.4D and E**).

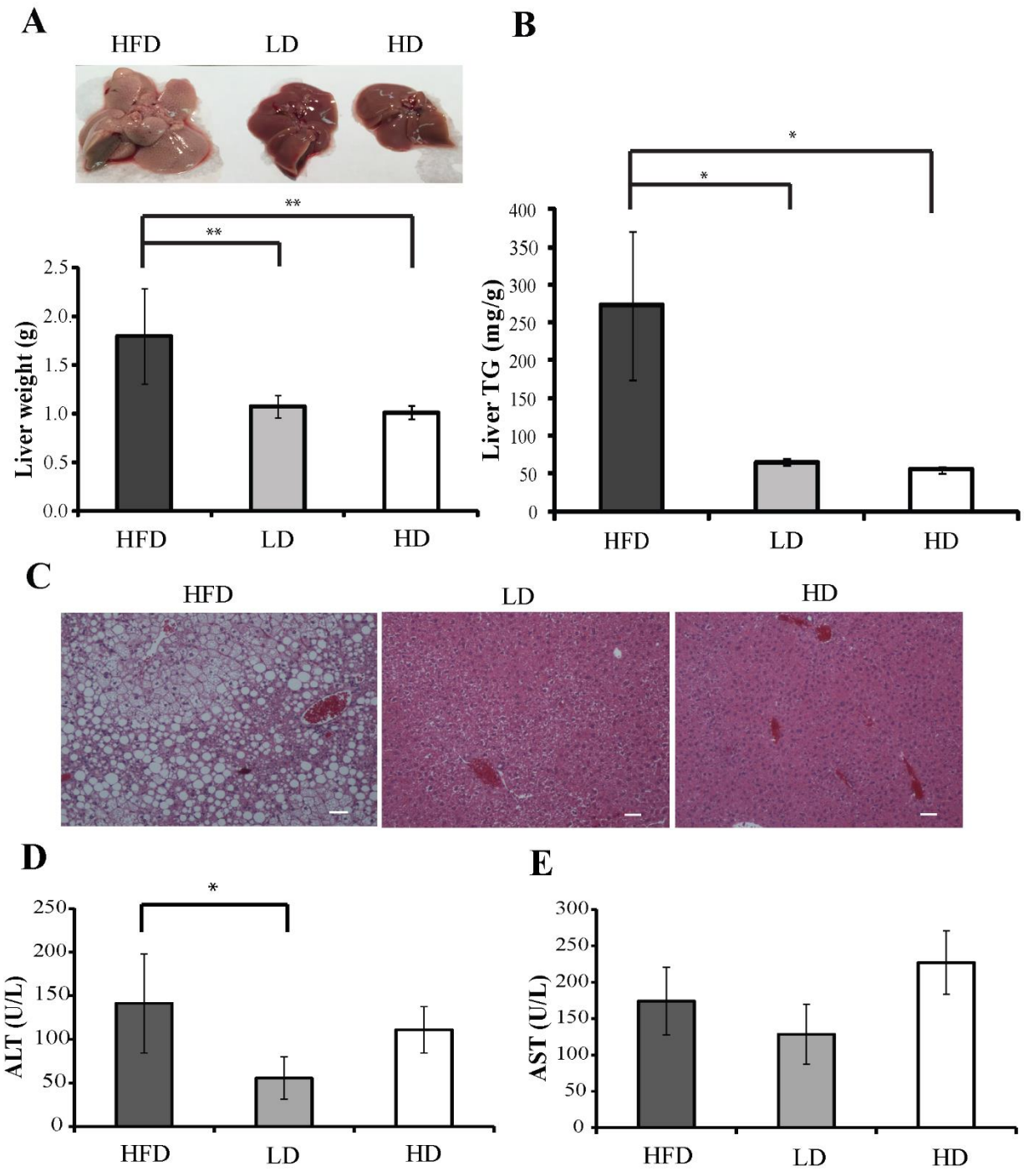

Figure 2. 4 Chronic oral treatment of chenpi extract prevented HFD-induced hepatic steatosis in mice. (A) Liver weight, (B) hepatic triglyceride content, and (C) representative pictures of H&E stained liver tissues from mice fed HFD, HFD plus 0.25% chenpi extract (LD), or HFD plus 0.5% chenpi extract (HD) for 15 weeks. The white areas in hepatocytes are intracellular lipid droplets.

Scale bars indicated 50μm. (D) Plasma ALT and (E) plasma AST were measured by the end of the week 15. Data are presented as mean value ± s.d. (n=10). *P<0.05, **P<0.01, *** P<0.001 vs HFD. All error bars, s.d..

3.4 *Chenpi* extract reduced adipose tissue mass and adipocyte size

Correlated with lower body weight and improvement of hepatic steatosis, we found that at the end of 15-week treatment, oral *chenpi* extract reduced the epididymal fat mass by 34% and 60% in 0.25 and 0.5% *chenpi* group, respectively (**Fig. 2.5B**). Histological analysis of epididymal fat pad (**Fig. 2.5A**) and quantification of adipocyte size (**Fig. 2.5C**) revealed that the mean values of adipocyte size from both treated groups are significantly smaller than those from HFD alone group. Treatment with *chenpi* extract shifted the distribution of adipocyte size to a more condensed range (**Fig. 2.5C**).

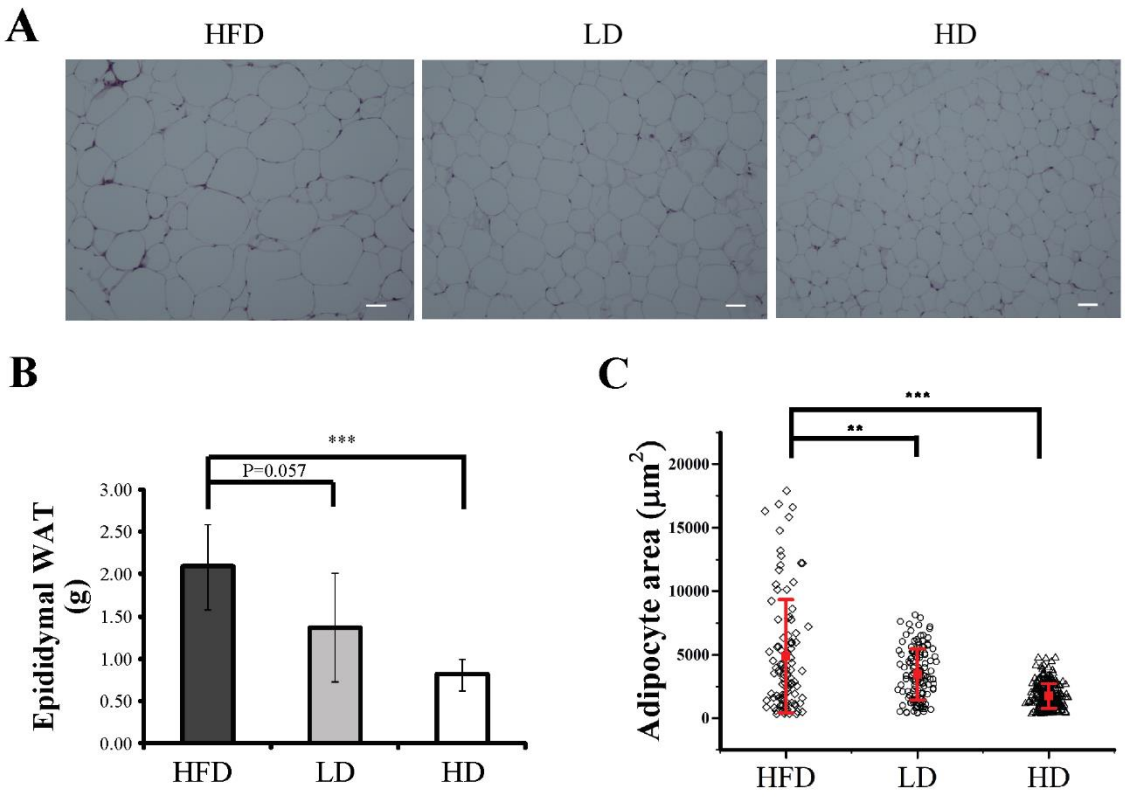

Figure 2. 5 Chronic oral treatment of chenpi extract decreased HFD-induced white adipose tissue mass (WAT) and adipocyte size in mice. (A) Representative pictures of H&E stained epididymal WAT from mice fed HFD, HFD plus 0.25% chenpi extract (LD), or HFD plus 0.5% chenpi extract (HD) for 15 weeks. Scale bars indicated 50μm. (B) Epididymal WAT mass measured at week 15. All groups, n=10. (C) Size of adipocytes from epididymal WAT were presented as mean value (red dot) and distribution of section area of each individual adipocyte from H & E stained histological picture. Diamond, HFD; circle, LD; triangle, HD. Data were analyzed using Adiposoft program. Data are presented as mean value ± s.d.. *P<0.05, **P<0.01, *** P<0.001 vs HFD. All error bars, s.d..

3.5 *Chenpi* extract improved diet-induced dyslipidemia symptoms

Dyslipidemia is one of the common insulin-resistant complications of metabolic syndrome. It is characterized by elevated atherogenic lipid and lipoprotein profile, especially

hepatic very low density lipoprotein (VLDL) overproduction. Elevated hepatic VLDL secretion leads to increased plasma apolipoprotein B100 (apoB-100)-containing lipoprotein. Mice fed HFD supplemented with either 0.25 or 0.5% *chenpi* extract exhibited significantly lower plasma total cholesterol (TC, 26% and 46 % of the levels found in the control mice, respectively) (**Fig. 2.6A**), Moreover, *chenpi* extract supplementation decreased the level of plasma apoB-100 (**Fig. 2.6B**) in a dose-dependent way, suggesting *chenpi* extract reduced the production of VLDL/LDL. No difference in plasma TG (**Fig. 2.6C**) or NEFA (**Fig. 2.6D**) levels were observed.

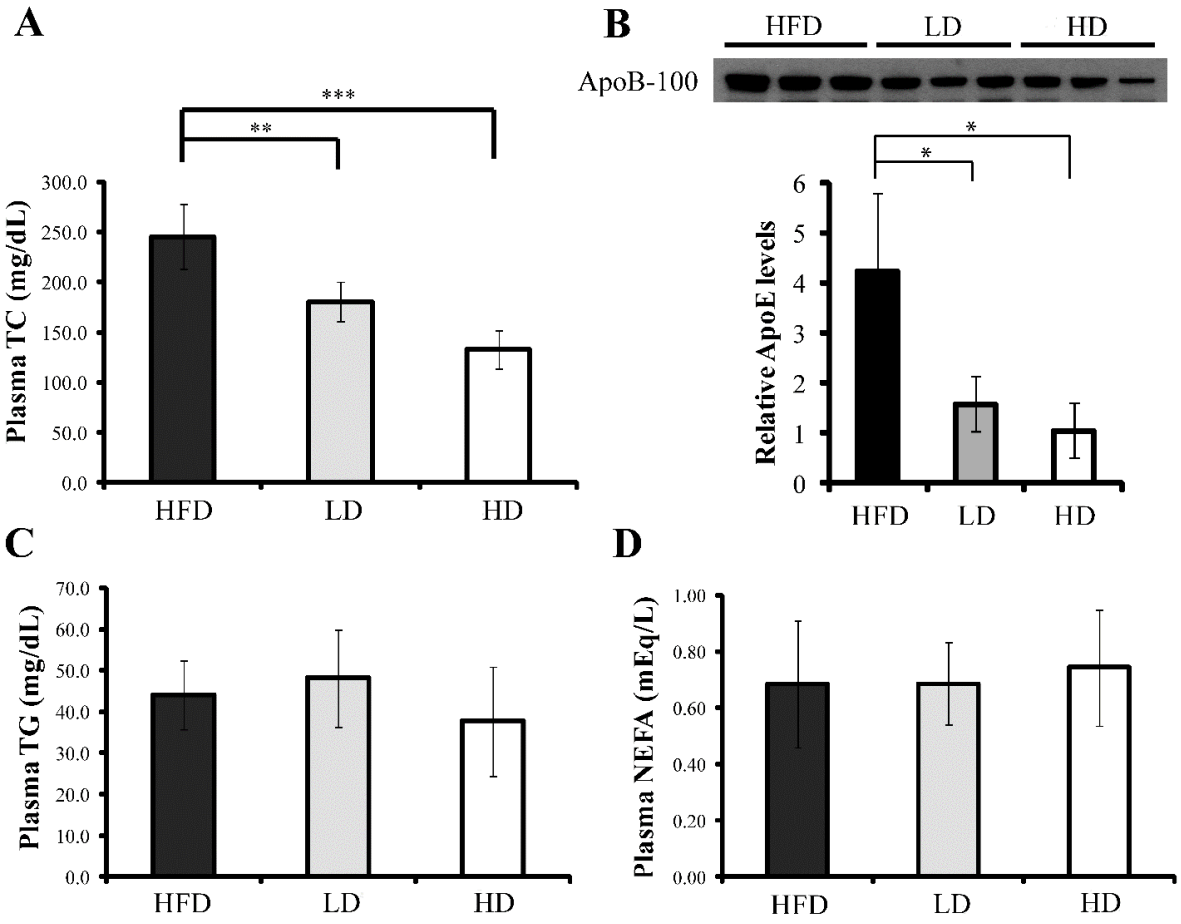

Figure 2. 6 Chronic oral treatment of chenpi extract decreased plasma total cholesterol and reduced VLDL production in mice. (A) Plasma total cholesterol (TC), (B) plasma apoB-100, (C) plasma triglycerides (TG), and (D) plasma non-esterified fatty acids (NEFA) levels of mice fed HFD, HFD plus 0.25% chenpi extract (LD), or HFD plus 0.5% chenpi extract (HD), as indicated,

for 15 weeks. Data are presented as mean value ± s.d. (n=10). *P<0.05, **P<0.01, *** P<0.001 vs HFD. All error bars, s.d..

3.6 *Chenpi* extract activated AMPK signaling pathway

The reduced lipid accumulation in liver and adipose implied changes in cellular metabolism induced by supplementation of *chenpi* extracts. 5'-adenosine monophosphate-activated protein kinase (AMPK) is a pivotal cellular and systematic energy homeostasis sensor. Previous studies showed that hydroxylated PMFs could activate AMPK in cultured cells.[109] We investigated the effect of *chenpi* extract on AMPK activity in vivo. Immunobloting analysis showed that *chenpi* treatment elevated the phosphorylated AMPK level in a dose-dependent manner in adipose tissue (**Fig. 2.7**) but not in liver (data not shown), indicating enhanced AMPK activity in adipose tissue.

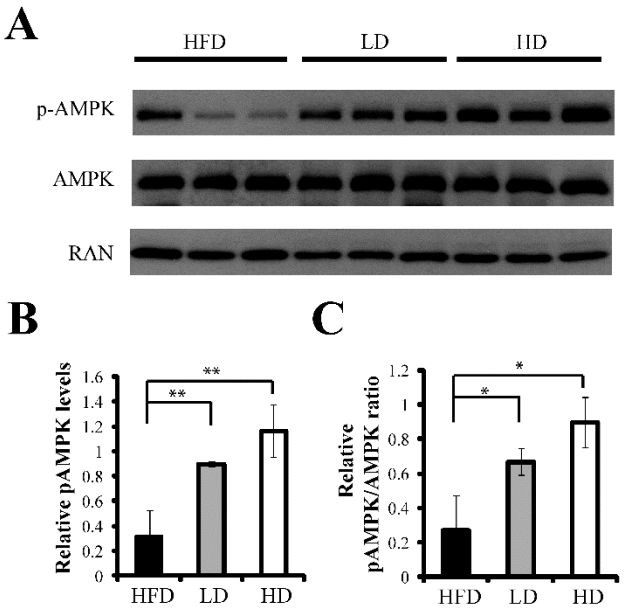

Figure 2. 7 Immunoblot analyses (A) and quantification (B, C) of the expression and phosphorylation of AMPK in epididymal white adipose tissue (WAT) samples from mice fed HFD, HFD plus 0.25% chenpi extract or HFD plus 0.5% chenpi extract, as indicated, for 15

weeks. pAMPK, AMPK phosphorylated at Thr172. RAN protein used as loading control. The immunoblot data are representative results from three independent experiments. Data are presented as mean value ± s.d.. All error bars, s.d..

4. Discussion

In current study, we documented the effects of 5-OH PMFs-enriched *chenpi* extract on prevention of obesity and type 2 diabetes in a mouse model. The first notable observation is the suppressed body weight gains and lower abdominal fat mass in *chenpi* treated groups, which are not caused by reduction of food intake or nutrient absorption. Consistently, 0.25% and 0.5% *chenpi* extract prevent diverse metabolic symptoms induced by HFD, including fatty liver, hyperglycemia, hyperinsulinemia and dyslipidemia.

Adipose tissue serves as the principal lipid storage organ as well as a critical regulatory organ for whole body metabolism.[157] Our data indicate that *chenpi* extract significantly increases AMPK activity in adipose tissue (but not in liver). Activation of AMPK in adipose tissue limits the release of fatty acid from adipocytes and favors local fatty acid oxidation, [158] which correlates with our observation that adipocyte size and adipose mass were significantly reduced in *chenpi* extract treated groups. The results support the idea that adipose tissue might be an important target organ for the action of *chenpi* extract. Moreover, *chenpi* extract significantly improved diet-induced hepatic steatosis. Reduction of lipid accumulation in adipose and liver would in turn favorably improve insulin sensitivity and glycemic control.[159-161] Meanwhile, improvement in hepatic insulin sensitivity and decrease of hepatic lipid pool promote apoB degradation and thereby reduce VLDL production,[162] leading to reduction of plasma total cholesterol. A working model to summarize the action of *chenpi* extract is proposed in **Fig. 2.8**.

One of the striking features of *chenpi* treated groups was the remarkable reduction of adiposity and hepatic steatosis, which correlate with their better glucose tolerance and insulin

sensitivity. Obesity induced ectopic lipid accumulation in insulin-responsive organs, like liver, is attributed as an underlying cause of insulin resistance.[163] Our results support the idea that *chenpi* extract could target the fundamental cause of insulin resistance and thereby contribute to the overall improvement of metabolic features in animal.

Accompanied with the improvement of hepatic steatosis and insulin resistance, we found that low dose of *chenpi* extract elicits protective effects against the HFD-induced liver damage, supported by significant lower plasma ALT level. High dose of *chenpi* extract did not affect plasma ALT and AST levels significantly in current study. These data suggested that *chenpi* extract within the current dose range does not cause hepatic toxicity.

In summary, we demonstrated that *chenpi* extract markedly reduced HFD-induced obesity and hepatic steatosis in mice. Metabolic parameters including glucose homeostasis, lipid metabolism and insulin sensitivity were improved over 15 weeks of *chenpi* extract treatment. The results from animal study provide strong evidence that 5-OH PMFs enriched *chenpi* extract could be effective in preventing the progression of metabolic syndromes. The study offers valuable information in understanding the beneficial effect of *chenpi* and for the future development of *chenpi*-enriched functional food and dietary supplements.

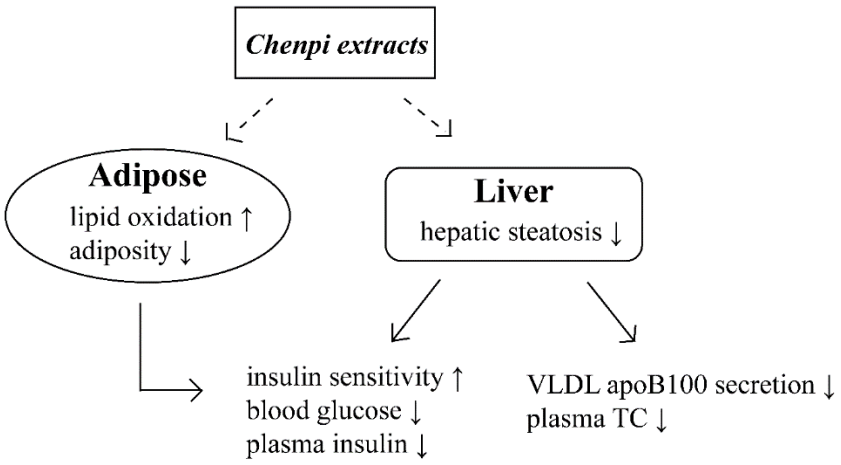

Figure 2. 8 Schematics of proposed working model of chenpi extract in HFD-induced obese/diabetic mice. Chenpi extract may directly affect adipose tissue or liver, leading to reduction in adipose tissue mass as well as improvement in hepatic steatosis. The reduction of lipid accumulation in the two important insulin-responsive organs in turn improves glycemic control and insulin sensitivity. The reduced hepatic steatosis together with increased hepatic insulin sensitivity promotes the apoB protein degradation, thereby contributing to the lower secretion of VLDL particle and lower circulating cholesterol level.

CHAPTER III. EVALUATE THE EFFECTS OF CHENPI EXTRACT ON LIPID METABOLISM IN DIFFERENTIATING MOUSE ADIPOCYTES

The work of Chapter III has been published in the title of 'Aged citrus peel (chenpi) extract reduces lipogenesis in differentiating 3T3-L1 adipocytes' on Journal of Functional Foods, 2017. 34: p. 297-303.

Aged citrus peel (chenpi) extract reduces lipogenesis in differentiating 3T3-L1 adipocytes

Jingjing Guo[1,2], Yong Cao[3], Chi-Tang Ho[1], Shengkan Jin[2], and Qingrong Huang[1]

[1] Department of Food Science, Rutgers University, 65 Dudley Road, New Brunswick, New Jersey 08901, USA

[2] Department of Pharmacology, Rutgers University-Robert Wood Johnson Medical School, Piscataway, New Jersey 08854, USA

[3]College of Food Science, South China Agricultural University, Guangzhou 510642, P. R. China

Abstract

Aged citrus peel (chenpi) is made from the dry peel of the fruit of *Citrus reticulate Blanco* or other cultivated varieties after aging process. It has long been used as a food ingredient, a dietary supplement, and for medicinal purpose. Compared to fresh citrus peel extract, chenpi extract uniquely presents aging- dependent enrichment of 5-demethylated polymethoxyflavones (5-OH PMFs). To investigate a potential direct role of chenpi extract on adipose tissue, we examined the effect of chenpi extract on differentiating 3T3-L1 cells. We showed that two types of chenpi extract samples varying in 5-OH PMF are effective in inhibiting intracellular lipid accumulation without significantly affecting cell viability and proliferation. The reduction in lipid accumulation is correlated with AMP-activated protein kinase (AMPK) activation and down-regulation of

adipogenic transcription factors as well as lipogenic genes. The results indicate that chenpi extract may directly affect lipogenesis in adipose tissue and the content of 5-OH PMFs likely affects the anti-lipogenic activity of chenpi extract.

1. Introduction

Obesity is a chronic condition characterized by excessive body fat accumulation that presents high health risks [164]. It has been recognized as a major risk factor for type 2 diabetes, dyslipidemia, fatty liver disease, and cardiovascular diseases [143]. The resultant morbidity and premature mortality associated with obesity [165] in combination with its worldwide epidemic [166] poses therapeutic challenge in modern society.

Obesity arises from the chronic positive energy balance resulting in an increase in both lipid deposition in individual adipocyte and total number of adipocytes [167]. Preadipocytes undergo consecutive stages to differentiate into mature adipocytes. Given the essential role of adipose tissue in lipid storage and energy homeostasis, adipocytes differentiation (adipogenesis) becomes an important target to control the development of obesity and obesity-related metabolic disorders [168, 169].

3T3-L1 mouse preadipocytes cell line is one of the most extensively studied *in vitro* models for adipogenesis [170]. Preadipocytes undergo growth arrest after reaching confluence. Treatment of post-confluent preadipocytes with differentiation inducers initiates mitotic clonal expansion followed by terminal differentiation. During differentiation process, various adipogenic genes express and give rise to adipocyte phenotypes including formation of lipid droplets and other metabolic features of adipocytes [171]. Adipogenesis is well regulated by a transcriptional cascade involving two master regulators, peroxisome proliferator-activated receptor γ (PPARγ) and CCAAT-enhancer binding protein α (C/EBPα) [172]. PPARγ and C/EBPα further regulate a couple of downstream adipogenic and lipogenic genes expression, such as adipocyte protein 2, lipoprotein

lipase, fatty acid transporter, and others [173]. AMP-activated protein kinase (AMPK) is an integrator of energy regulation signals [174]. Activation of AMPK in adipocyte favors lipid oxidation while shuts down biosynthesis of lipids, which makes AMPK a popular therapeutic target for obesity and obesity-related metabolic diseases [158, 174, 175].

Aged citrus peel, or chenpi, is made from the dry peel of the fruit of *Citrus reticulate Blanco* or other cultivated varieties after aging process [176]. Chenpi has long been used in traditional medicine for treating digestive, mucous and inflammation problems as well as used as dietary supplements and food ingredient [176]. Compared to fresh citrus peel extract which is rich in polymethoxyflavones (PMFs), chenpi extract contains higher percent of 5-demethylated PMFs (5-OH PMFs), including 5-OH nobiletin and 5-OH tangeretin [177]. The amount of 5-OH PMFs increases with aging time, and it is generally observed that the extract from longer aged chenpi has better medicinal efficacy. Our previous work demonstrated that chenpi extract reduces high-fat diet-induced obesity, hyperglycemia, insulin resistance and hepatic steatosis in mice. The beneficial effect is correlated with reduction in adipocyte hypertrophy and AMPK activation in adipose tissue. However, the underlying mechanism is not fully understood. In particular, it is not clear whether chenpi extract could directly affect adipose tissues. In the current study, we investigated the effect of chenpi extract on lipid accumulation in differentiating adipocytes using 3T3-L1 cells as a model system. To address the contribution of 5-OH PMF, we compared the effect of two types of chenpi extract varying in 5-OH PMF content.

2. Material and Methods

2.1 Reagents

Following reagents were used: antibodies including AMPK-α mAb, and Phospho-AMPKα (p-AMPKα) (Thr172) mAb, Acetyl-CoA Carboxylase (ACC) mAb, and fatty acid synthase mAb were from Cell Signaling Technology (Danvers, MA), all diluted 1: 1,000 for immunoblotting

analyses. RAs-related Nuclear protein (Ran) pAb, PPARγ mAb, and C/EBPα pAb were from Santa Cruz Biotechnology (Dallas, TX), diluted 1: 1,000 for immunoblotting analyses. 3-Isobutyl-1-methylxanthine (IBMX), insulin and dexamethasone were from Sigma (St. Louis, MO).

2.2 Sample preparation and characterization

Commercialized chenpi from two different vendors were purchased from Xinhui, China. For sample preparation, chenpi extract was prepared by using Continuous Phase Transition (CPT) extraction method with n-butane as the solvent (0.5 MPa extraction pressure, 50 ºC extraction temperature and 60 min extraction time). The oil-like chenpi extract was further subjected to silica gel column chromatography by using n-hexane as the mobile phase to remove essential oils and waxes. The eluate was then evaporated by rotary evaporator followed by vacuumed drying. The pale-yellow power obtained was analyzed by the UltiMate 3000 HPLC system (Dionex, CA, USA) using a Supelco's RP-Amide column, 15 cm x 64.6 mm id, 3 μm, (Bellefonte, PA, USA) connected to a variable wavelength detector. A linear gradient elution program composed of water (solvent A) and acetonitrile (solvent B) was carried out as follows: 0min, 40% B; 10min, 55% B; 15min, 70% B; 20min, 80% B; 21min, 100% B, 25min, 100% B; 26min, 40% B; 30min, 40% B. The flow rate was kept at 1ml/min and injection volume was 10μL. Multiple UV detection wavelengths were applied including 214 nm and 326 nm.

2.3 Differentiation of 3T3-L1 preadipocytes to adipocytes

3T3-L1 murine preadipocytes were seeded on 6-well plate at density of 3.0×10^6 cells/well, and maintained in complete cell culture medium, which is Dulbecco's modified Eagle's medium (Invitrogen, Carlsbad, CA) containing 10% (vol/vol) fetal bovine serum (Atlanta Biologicals, Flowery Branch, GA), 100U/ml of penicillin (Invitrogen, Carlsbad, CA), 100 μg/mL of streptomycin (Invitrogen, Carlsbad, CA) and 0.29 mg/ml of L-glutamine(Invitrogen, Carlsbad, CA), at 37 °C and 5% CO_2 for 24 hours, at 37 °C and 5% CO_2 until confluence. Two days after

confluence, designated as day 0, cells were switched to differentiation medium (DM) containing 10 μg/mL insulin, 0.5 mM IBMX, and 1 μM dexamethasone in complete culture medium for another 3 days. Cells were then maintained in complete culture medium plus 10 μg/mL which was changed every two days thereafter till day 8. For treatment, chenpi extract were first dissolved in dimethyl sulphoxide (DMSO) to make stock solution, and then were added directly to the culture medium to designated concentrations by 1:1000 dilutions.

2.4 MTS cell proliferation assay

For measuring post-confluent cell proliferation during first three days of differentiation, 3T3-L1 cells were seeded on 96-well plate at density of 1×10^4 cells/well. Two days after confluence, cells were switched to differentiation medium containing DMSO or chenpi extract for 72 hours. For measuring pre-confluent cell proliferation, 3T3-L1 cells were seeded on 96-well plate at density of 1×10^4 cells/well and incubated with DMSO or chenpi extracts for 24 or 48 hours. At the end of each treatment, cells were subjected to CellTiter 96 AQueous nonradioactive cell proliferation assay (Promega, Madison, WI). The cell viability was interpreted as average readout of cells treated with chenpi extract normalized by cells treated with DMSO. Six repeats were performed for each concentration to minimize variance.

2.5 Oil red O staining

On day 8, cells were first washed with phosphate-buffered saline (PBS) and fixed in 10% neutral buffered formalin (Surgipath Medical Industries Inc., Richmond, IL) for 15 min. After fixation and washed with PBS again, cells were subjected to oil red O staining for 30 min, followed by immediate rinse in water. The intracellular lipid droplets were observed under optical microscope, and imaged by Nikon Eclipse Ni-U imaging system. Intracellular lipid content was determined by oil red O elution in 4% NP-40/isopropanol. The absorbance was read under 520 nm. Intracellular lipid accumulation in differentiated mouse adipocytes was interpreted as: the average

readout of each group treated with certain dose of chenpi extract normalized by average of cells treated with DMSO vehicle.

2.6 Protein extraction and immunoblotting analysis

Cells were homogenized with lysis buffer containing 10 mM TRIS-HCl (pH 7.9), 10% glycerol, 0.1 mM ethylenediaminetetraacetic acid (EDTA), 100 mM KCl, 0.2% NP-40, 0.5mM PMSF, 1 mM DTT and mini-complete protease inhibitor cocktail (Roche Diagnostics, Indianapolis, IN) and phosphatase inhibitor cocktail (Roche Diagnostics, Indianapolis, IN). Lysates were syringed with 26 gauge ½ inch needles on ice. Nuclei and insoluble debris were pelleted in an Eppendorf micro-centrifuge at 12,000 rpm for 15 min at 4 ℃. Cell lysates were then stored at -20 ℃ or immediately subjected to sodium dodecyl sulfate polyacrylamide gel electrophoresis (SDS-PAGE). For the SDS-PAGE, cell lysates were mixed with loading buffer and heated at 95 ℃ for 5 min prior to electrophoresis. 12% tris-glycine mini gels (Life Technologies, Carlsbad, CA) were used for analysis of AMPK, p-AMPK, RAN, PPARγ and C/EBPα. 3-8% tris-acetate mini gel (Life Technologies, Carlsbad, CA) was used for ACC. 10% tris-glycine mini gel (Life Technologies, Carlsbad, CA) was for analysis of FAS. For immunoblotting, proteins were transferred to polyvinylidene difluoride membranes (Millipore, Belgium) for overnight. Following probing with antibodies, chemiluminescent detection was completed with ECL western blotting reagents (Amersham, Buckinghamshire, UK). Quantification was performed by measuring band intensity using ImageJ software and calculating the ratio of protein of interesting to internal loading control.

2.7 Statistics

Data are presented as the means ± SD. One-way ANOVA was used for all the statistical comparison among groups.

3. Results

3.1 Extraction and Characterization of chenpi extract

The constituent profiles of two different chenpi extract samples were analyzed and compared quantitatively by HPLC chromatograph. As shown in **Figure 3.1**, nobiletin and tangeretin were identified as the major PMFs, and 5-OH nobiletin as the major demethylated PMF. Their relative contents were presented in **Table 3.1**. The total PMFs (nobiletin and tangeretin) were 54.1% and 72.6%, respectively in two samples and the relative ratio between nobiletin and tangeretin were ~ 1.3 in chenpi extract. As for the 5-OH PMF content, one sample (H-chenpi) contains 9.22% of 5-OH nobiletin, which is twice as high as the other one (L-chenpi, 4.17%). The chemical structures of the major constituents of chenpi extract are shown in **Figure 3.2**.

	Nobiletin	Tangeretin	5-OH Nobiletin
Peak number	1	3	4
Retention Time (min)	8.6	11.0	13.7
H-chenpi	31.28%	22.82%	9.22%
L-chenpi	41.48%	31.16%	4.17%

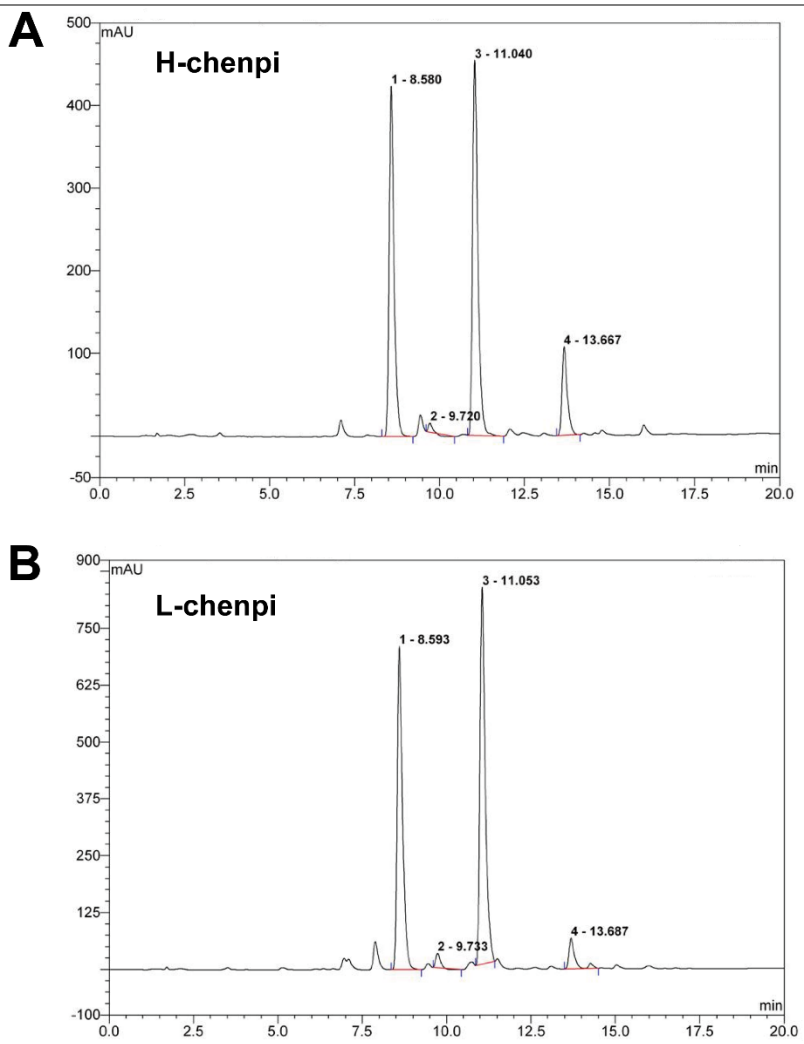

Figure 3. 1 HPLC chromatograph of two types of chenpi extract samples. (A) H-chenpi, (B) L-chenpi. Peak 1, nobiletin; peak2, tangeretin; peak3, 5-demethylated nobiletin (5-OH nobiletin).

Table 3. 1 Relative contents of major constituents of two types of chenpi extract samples. 5-OH nobiletin, 5-demethylated nobiletin.

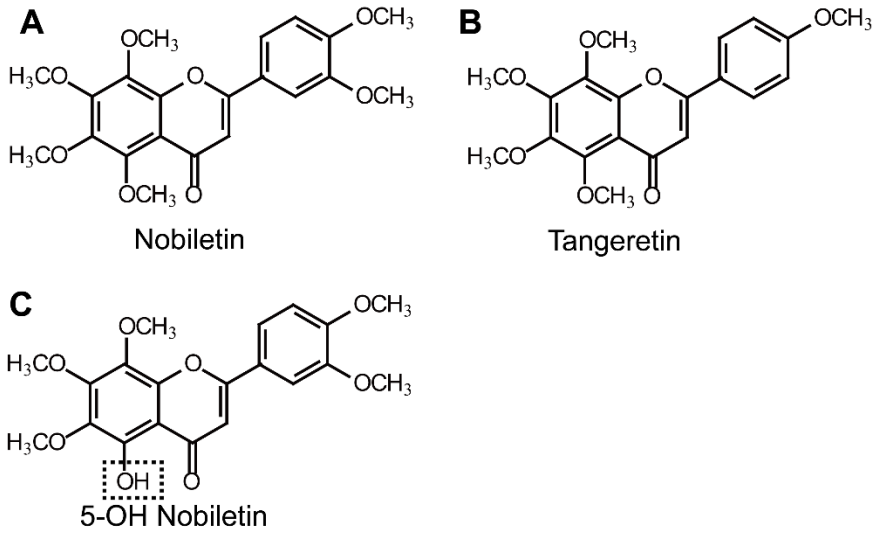

Figure 3. 2 Chemical structures of major components in chenpi extract. (A) Nobiletin, (B) Tangeretin, (C) 5-demethylated nobiletin (5-OH nobiletin).

3.2 Chenpi extract reduces lipid accumulation in differentiating mouse adipocytes

We examined the effect of chenpi extract on differentiating 3T3-L1 cells. Two-day post-confluent cells were switched to differentiation medium supplemented with or without series concentrations of chenpi extract. After 8 days, preadipocytes were successfully differentiated into mature adipocytes characterized by the formation of intracellular lipid droplets, as shown in **Figure 3.3A and B**. The lipid accumulation was quantified by Oil Red-O staining. At dosage between

3.125 to 12.5 µg/mL, both types of chenpi extract lower the levels of lipid accumulation of the differentiating adipocytes in a dose-dependent manner (**Figure 3.3 A-C**). Despite containing a lower level of PMFs, H-chenpi extract, which has a higher 5-OH nobiletin, nevertheless showed a comparable lipid reduction activity as compared to L-chenpi sample. At the concentration of 25 µg/mL, the reduction in lipid content is significantly higher in cells treated with H-chenpi extract as compared to L-chenpi extract (**Figure 3.3 C**).

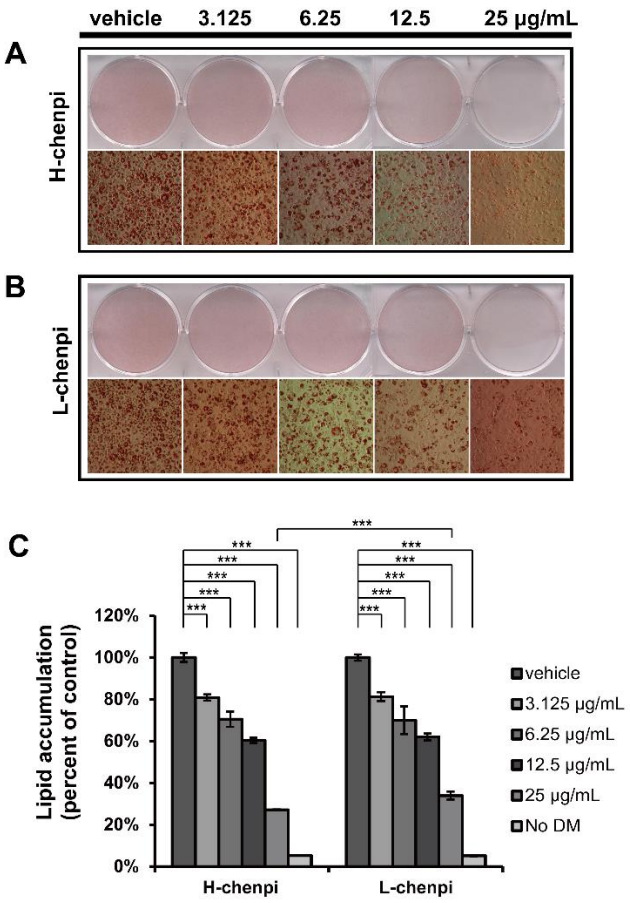

Figure 3. 3 Effect of chenpi extract on lipid accumulation in differentiating mouse adipocytes. 3T3-L1 cells were incubated in differentiation medium containing DMSO vehicle or chenpi extract. After 8 days of differentiation, cells were subjected to Oil Red O staining for microscope observation and quantification. Light microscopic images were shown as (A) H-chenpi and (B) L-chenpi. Oil Red O stain was then eluted with isoproponal containing 1% NP-40, and quantified

by measuring the absorbance under 520nm, which is interpreted as the relative lipid content in differentiated adipocytes. DM, differentiation medium. Data shown reflect the means ± SD of 3 experiments. (*) P<0.05, (**) P<0.01, and (***) P<0.001. All error bars, SD.

3.3 Effects of chenpi extract on post-confluent mitotic clonal expansion and pre-confluent preadipocyte proliferation

After addition of differentiation inducers, post-confluent preadipocytes undergo mitotic clonal expansion during the first 72 hours before expressing adipocyte-specific genes. To determine whether chenpi extract affects total cell number or lipid accumulation in each individual cells, we performed MTS assay on post-confluent cells. The activity of MTS assay reflects the total number of living cells. 2-day post-confluent cells were incubated with differentiation medium containing DMSO vehicle or chenpi extract for additional 72 hours. As shown in **Figure 3.4**, within the dose range between 3.125 and 12.5 μg/mL, chenpi extract did not significantly affect the number of living cells, indicating chenpi extract does not affect mitotic clonal expansion at this dose range. At the dose of 25 μg/mL, H-chenpi extract and L-chenpi extract reduced the cell proliferation by 13% and 21%, respectively.

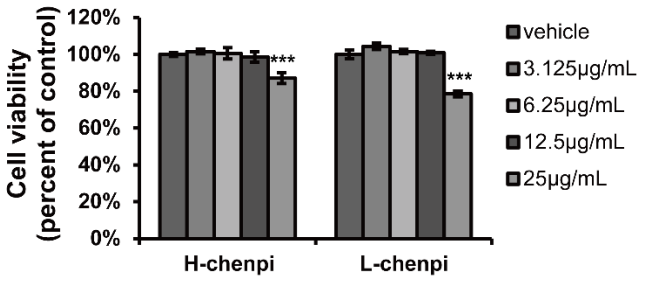

Figure 3. 4 Effect of chenpi extract on post-confluent preadipocyte proliferation. 2-day post-confluent 3T3-L1 cells were incubated in differentiation medium containing DMSO vehicle, H-chenpi extract or L-chenpi extract for 72 hours. Cell viability was then determined by

colorimetric proliferation assay. Data were interpreted as percent of control treated with DMSO vehicle. Data shown reflect the means ± SD of 6 experiments. (*) P<0.05, (**) P<0.01, and (***) P<0.001. All error bars, SD.

We then determined the potential effect of chenpi extract on the proliferation of pre-confluent preadipocytes. 3T3-L1 cells were incubated with chenpi extract for 24 or 48 hours after plating. As shown in **Figure 3.5**, chenpi extract had no effect on the proliferation of preadipocytes up to 12.5 µg/mL. At the concentration of 25 µg/mL, H-chenpi extract and L-chenpi reduced the cell proliferation by 2%, and 7%, respectively after 24 hours, and by 3.8%, and 14.5%, respectively after 48 hours.

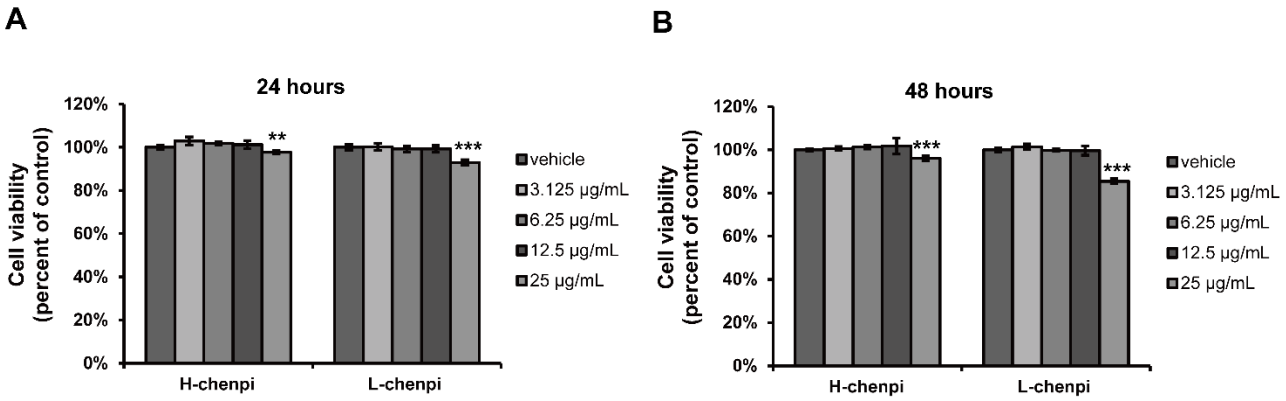

Figure 3. 5 Effect of chenpi extract on pre-confluent preadipocytes proliferation. 3T3-L1 cells were incubated with DMSO vehicle, H-chenpi extract or L-chenpi extract for (A) 24 or (B) 48 hours after plating. Cell viability was then determined by colorimetric proliferation assay. Data were interpreted as percent of control treated with DMSO vehicle. Data shown reflect the means ± SD of 6 experiments. (*) P<0.05, (**) P<0.01, and (***) P<0.001. All error bars, SD.

3.4 Chenpi extract reduces lipogenesis and down-regulate adipogenic transcription factors

To investigate the underlying mechanism, we further analyzed cells treated with H-chenpi extract on adipogenic transcription cascade and cellular metabolism regulators. PPARγ and C/EBPα are two key adipogenic transcription factors that work sequentially and cooperatively in stimulating fat cell differentiation. Chenpi extract reduced expression level of PPARγ and C/EBPα in a dose- dependent manner, as shown in **Figure 3.6A**. Moreover, the altered lipid metabolism in adipocytes was accompanied by the activation of AMPK (**Figure 3.6A**), which is consistent with previous mouse study in which 5-OH PMFs-enriched chenpi extract induced AMPK activation in adipose tissue [178]. In addition, the expression of ACC and FAS, which are two critical enzymes involved in fatty acid biosynthesis are dose-dependently decreased in cells treated by chenpi extract (**Figure 3.6B**), suggesting that chenpi extract could directly repress lipogenesis in differentiating adipocytes.

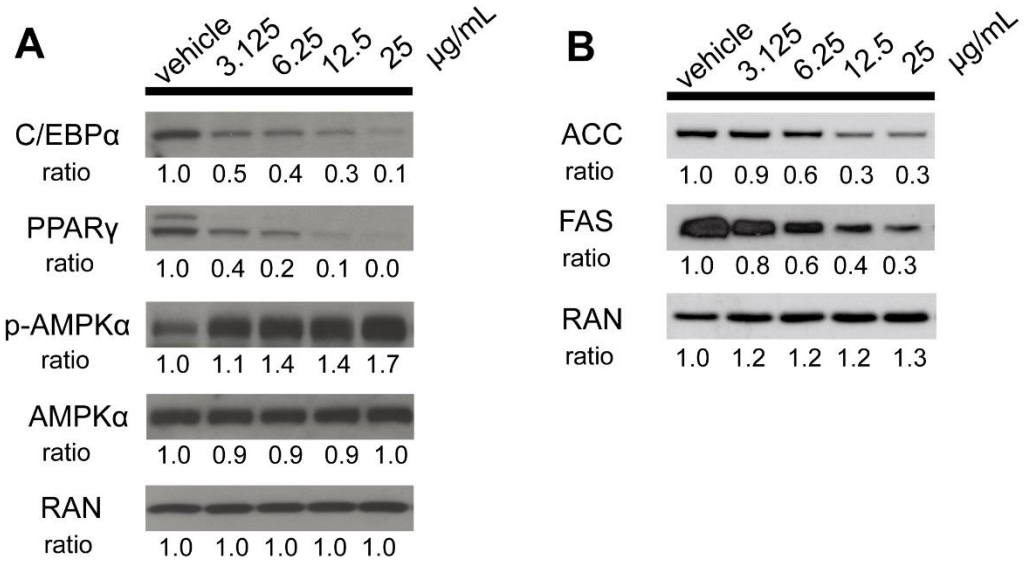

Figure 3. 6 Effect of chenpi extract on adipogenic gene expression and lipogenic gene expression. 3T3-L1 cells were induced to differentiation in the absence or presence of chenpi extract for 8 days. At the end of the treatment, the expression levels of p-AMPK, AMPK, PPARγ, C/EBPα (A), ACC and FAS (B) were determined by immunoblotting analysis, as indicated. The expression level of the nuclear protein RAN was used as a loading control.

4. Discussion

Chenpi is a food ingredient traditionally used in China. Our previous animal study showed that chenpi extract prevents diet-induced adiposity and adipocyte hypertrophy [178], which is associated with improvement in glycemic control. Obesity is usually caused by increased lipid deposition and/or increased adipocyte number in adipose tissue. It is not clear whether natural extract from chenpi would have a direct impact on adipose tissue. Here we tested the direct effect of chenpi extract on adipogenesis using the 3T3-L1 adipocyte differentiation model. In the present study, we demonstrated that two types of chenpi extract could consistently lower the intracellular lipid accumulation in differentiating adipocytes at pharmacologically relevant concentrations [179, 180]. The results show that the adipose tissue might be a direct target for the anti-obesity effect of chenpi extract, and provide strong support for using chenpi extract as nutraceuticals for anti-obesity/diabetic purpose.

We analyzed the possible mechanism of action of chenpi extract. The maturation of adipocytes basically involves growth arrest, mitotic clonal expansion and terminal differentiation [181]. Treatment with chenpi extract reduces lipid accumulation in individual differentiating adipocytes without affecting post-confluent mitotic clonal expansion and pre-confluence cell proliferation, suggesting chenpi extract might affect lipogenesis or lipid metabolism in adipocytes. Consistently, chenpi extract down-regulated the expression of two principle adipogenic transcription factors, PPARγ and C/EBPα, and induced AMPK activation. PPARγ and C/EBPα play a critical role in regulating the terminal differentiation process of adipcyte, switching on the expression of downstream adipogenic genes and lipogenic genes [172]. AMPK, in addition to being energy sensor, could act as upstream signal of PPARγ in 3T3-L1 adipocytes [182]. It is possible that chenpi may affect adipogenesis and lipogenesis by activating AMPK, which in turn affects PPARγ and C/EBPα. Moreover, activation of AMPK could inhibit the expression of FAS and ACC [183], which directly reduce fatty acid synthesis and increase beta-oxidation.

Chenpi extract contains higher 5-OH PMFs content compared to fresh citrus peel extract. In our studies, we compared the effect of two types of chenpi extract. H-chenpi extract has markedly lower PMFs (54.1% vs. 72.6%) but higher 5-OH PMFs content (9.2% vs. 4.2%) as compared to L-chenpi extract. However, they have comparable effect in lowering lipid accumulation in differentiating adipocytes. This result suggests that the content of 5-OH PMFs may be critical for the lipid lowering activity. Interestingly, recent studies showed that 5-OH PMFs have better anti-inflammation and anti- cancer activity than PMFs [93]. It will be interesting to further investigate if these activities of 5-OH PMFs share a similar molecular mechanism.

In summary, we demonstrated that natural extract from chenpi is efficacious in inhibiting lipogensis in differentiating adipocytes. This is associated with activation of AMPK and down-regulation of adipogenic transcription factors as well as lipogenic genes. Together with our previous study in mice, these results provide direct evidence supporting the beneficial anti-obesity and anti-diabetic effect of this nutraceutical.

Chapter IV. Determine the effect of casticin, a novel 5-OH polymethoxyflavone on lipid metabolism in differentiating mouse adipocytes

The work of Chapter IV is going to be submitted to Journal of Functional Food with the title of 'Casticin inhibits adipogenesis in differentiating mouse adipocytes'

Casticin inhibits adipogenesis in differentiating mouse adipocytes

Jingjing Guo[1,2], Xiaoqi Wang[1], Chi-tang Ho, Shengkan Jin[2], Qingrong Huang[1]

[1]Department of Food Science, Rutgers University, 65 Dudley Road, New Brunswick, New Jersey 08901, USA

[2]Department of Pharmacology, Rutgers University-Robert Wood Johnson Medical School, Piscataway, New Jersey 08854, USA

1. Introduction

The global epidemic of obesity poses medical challenge and socioeconomic burden in modern society. Obesity, along with overweight, affects over one third of world adult population now and is projected to reach 58% in adult population till 2030 [184]. Morbid obesity is highly associated with a wide spectrum of metabolic disorders including insulin resistance, type 2 diabetes, nonalcoholic fatty liver diseases, cardiovascular diseases, and etc. [143]. Accordingly, dietary or lifestyle intervention that is capable of reducing excessive fat accumulation improves insulin resistance, hyperglycemia and hepatic steatosis [185].

Obesity is characterized by imbalance between the interplay of energy intake and consumption, resulting in excessive body fat accumulation, with most profound presentation in adipose tissue. The increased adipose tissue mass is accompanied with increased cell number

(adipocyte hyperplasia) and/or increased cell size (adipocyte hypertrophy) [186]. 3T3-L1 differentiating mouse adipocyte is a well-established in vitro model system that recapitulates the growth mechanism of adipocytes in obesity. Upon differentiation induction, 3T3-L1 preadipocytes consecutively undergo proliferation and differentiation stages to form lipid-loaded mature adipocytes [187]. Adipogenesis process is well-regulated by a cascade of transcription factors, among which peroxisome proliferator-activated receptor γ(PPARγ) and CCAAT-enhancer binding protein α(C/EBPα) are the major determinants of adipocyte fate [188]. PPARγ and C/EBPα further induces the downstream genes expression that are involved in lipogenesis, lipolysis and glucose transport [189], which give rise to the lipid-laden phenotype and metabolic features of adipocytes.

Casticin(3',5-dihydroxy-3,4',6,7-tetramethoxyflavone) is a major flavonoid of the active constituents of Viticis Fructus (Manjingzi in Chinese).[111] Viticis Fructus is the dry fruit of *Vitex rotundifolia* plant, which has been used anciently for treatment of inflammation and pain-relief.[111] It has been shown that casticin exhibits diverse bioactivities, including anti-inflammation, anticancer, immunoregulatory, and other complimentary properties [190]. However, no study has been reported regarding the activity of casticin in modulating lipid metabolism.

Casticin can be structurally recognized as a 5-OH PMF derivative with one extra hydroxyl group on 3'-postions. Our recent study demonstrated that 5-OH PMFs-enriched chenpi extract is effective to prevent high fat diet-induced obesity and type 2 diabetes symptoms in mice [178]. Consistent with its anti-obesity activity in mice, 5-OH PMFs-enriched chenpi extract dramatically reduced lipid accumulation in differentiating mouse adipocytes and the lipid-reducing effect is positively correlated with the 5-OH PMFs content of the extract, suggesting that 5-OH PMFs might play critical role against lipogenesis in adipocytes [191]. In addition, oral administration of synthetic 5-OH PMFs ameliorated HFD-induced adiposity in mice and reduced

lipid accumulation in differentiating mouse adipocyte [109, 192]. Encouraged by the potent activity of 5-OH PMFs against obesity and metabolic disorders, here we determined the effect of casticin, as a 5-OH PMF derivative, on lipid metabolism in 3T3-L1 cell model system.

2. Material and Methods

2.1 Reagents

We used following reagents: antibodies including Acetyl-CoA Carboxylase (ACC) mAb and fatty acid synthase mAb were from Cell Signaling Technology (Danvers, MA, USA), all diluted 1: 1,000 for immunoblotting analyses. β-Actin mAb, PPARγ mAb, and C/EBPα pAb were from Santa Cruz Biotechnology (Dallas, TX, USA), diluted 1: 1,000 for immunoblotting analyses. 3-Isobutyl-1-methylxanthine (IBMX), insulin, dexamethasone, RNAse A and Propidium iodide were from Sigma (St. Louis, MO, USA). Dulbecco's modified Eagle's medium (DMEM), 100 U/mL of penicillin and 0.29 mg/mL of L-glutamine were from ThermalFischer (Carlsbad, CA, USA). Fetal bovine serum was from Atlanta Biologicals (Flowery Branch, GA). 10% neutral buffered formalin was from Surgipath Medical Industries Inc. (Richmond, IL, USA). The mini-complete protease inhibitor cocktail was from Roche Diagnostics (Indianapolis, IN, USA). 12% tris-glycine mini gels and 3-8% tris-acetate mini gel were from Life Technologies (Carlsbad, CA, USA). ECL western blotting reagents used for chemiluminescent detection were from Amersham (Buckinghamshire, UK).

2.2 Sample preparation and characterization

Continuous phase transition extraction method was employed in extraction procedure of casticin. Fruit of *Vitex rotundifolia* was first grinded to 40 mesh, and then underwent flavone extraction by continuous 85% (v/v) ethanol in a 20 L extraction vessel for 4 h at 60 °C under 0.1~0.2 MPa. Then the obtained solution was subjected to vacuum rotary evaporation, and the resulted sticky extract was redissolved in small amount of 70% (v/v) ethanol, followed by

extracting with three times volume of petroleum ether for three times to remove the oil. After evaporating the ethanol with rotary evaporator, the flavone components were further enriched by extracting the residue with three times volume of ethyl acetate for three times and subsequently washed with water. The organic phase was then concentrated again with rotary evaporator and finally received the flavone extract.

Column chromatography was utilized for the separation of casticin from flavone extract, and the mixture of petroleum ether and ethyl acetate was selected as the eluent. The crude sample was loaded on column as solid by first dissolving the obtained extract with small amount of methanol, and then uniformly mixing the sample with proper amount of silica gel, followed by the evaporation of methanol in oven. Gradient elution was applied during the separating process, starting from petroleum ether: ethyl acetate = 4: 1 (v/v), and casticin can be detected when the volume ratio of petroleum ether: ethyl acetate is 3: 2 (Rf = 0.35). The casticin-contained eluent was then collected and subjected to vacuum rotary evaporation, afterwards the separated casticin was obtained.

The purity of the casticin fine extract was analyzed by the Waters Alliance HPLC system (Milford, MA, USA) with a Phenomenex® Luna C18(2) column, 250 x 4.6 mm, 5 μ, 100A (Torrance, CA, USA), connected to a Photodiode Array detector (PDA). Two solvents were used: Solvent A, Water + 0.1% Formic Acid; Solvent B, Acetonitrile + 0.1% Formic Acid. A linear gradient elution was carried out at flow rate of 1 ml/min as follows: 0min, 100% A; 5min, 70% A and 30% B; 8min, 60% A and 40% B; 12min, 30% A, 70% B; 18min, 30% A, 70% B; 22-30 min, 100% B.

2.3 Cell culture

3T3-L1 cells were cultured and differentiated according to the protocol described before. Briefly here, 3T3-L1 mouse preadipocyte fibroblasts were seeded in 6-well plate and then

cultured in DMEM complete medium to 100% confluence. Two days after confluence, cells were incubated in differentiation medium containing cocktail inducers for three days. Cells were then switched to insulin-containing maintenance medium for another 5 days. For treatment, casticin was first prepared in DMSO stock and then administrated to the cells at indicated time points with the dilution factor of 1:1000.

2.4 MTS cell proliferation assay

For pre-confluent preadipocytes proliferation study, 3T3-L1 cells were seeded in the 96-well plate with the density of 1×10^4 cells/well and incubated in complete DMEM medium in the presence of DMSO or serious concentrations of casticin for 24 or 48 hours. For post-confluent preadipocytes proliferation study, two days after 3T3-L1 cells reaching confluence, cells were incubated with differentiation medium in the presence of different concentrations of casticin for 24, 48 or 72 hours. At the end of each treatment, cell number were determined by CellTiter 96 AQueous nonradioactive cell proliferation assay kit (Promega, Madison, WI, USA). Cell viability were interpreted as the readout ratio of the cells treated with casticin to cells treated with DMSO alone.

2.5 Cell cycle analysis

3T3-L1 cells were cultured in 6-well plate and induced to differentiate according to the protocol. Cells were harvested at indicated time point by trypsinization and then fixed in ice-cold 70% ethanol for 30 min. The ethanol-fixed cells were washed with ice-cold PBS and digested with RNAse A solution, followed by addition of propidium iodide (PI) solution, which were analyzed by flow cytometry.

2.6 Oil red O staining

After 8 days of differentiation, cells were washed with PBS twice, followed by fixation in 10% neutral buffered formalin for 15 min. The fixed cells were stained with oil red o dye for 30min. After staining, cells were washed with PBS for three times and ready for lipid quantification. The intracellular lipid accumulation was imaged by Nikon Eclipse Ni-U imaging system, and quantified with absorbance reading of the oil red o stain elution. The intracellular lipid content was interpreted as the ratio between absorbance readouts of casticin-treated cells over DMSO-treated cells.

2.7 Protein extraction and immunoblotting analysis

Cells were homogenized with lysis buffer containing 10 mM TRIS-HCl (pH 7.9), 10% glycerol, 0.1 mM ethylenediaminetetraacetic acid (EDTA), 100 mM KCl, 0.2% NP-40, 0.5 mM PMSF, 1 mM DTT and mini-complete protease inhibitor cocktail. The cell homogenates were then centrifuged and the supernatant was collected for immunoblotting analyses.

2.8 Statistics

Data are presented as the means ± SD. One-way ANOVA was used for all the statistical comparison among groups.

3. Results

3.1 Characterization of casticin

The HPLC profile of casticin extract was shown in Figure 4.1A. The retention time of casticin was identical with the casticin standard curve shown in Figure 4.1B. The purity of casticin extract was estimated to be over 96.5%.

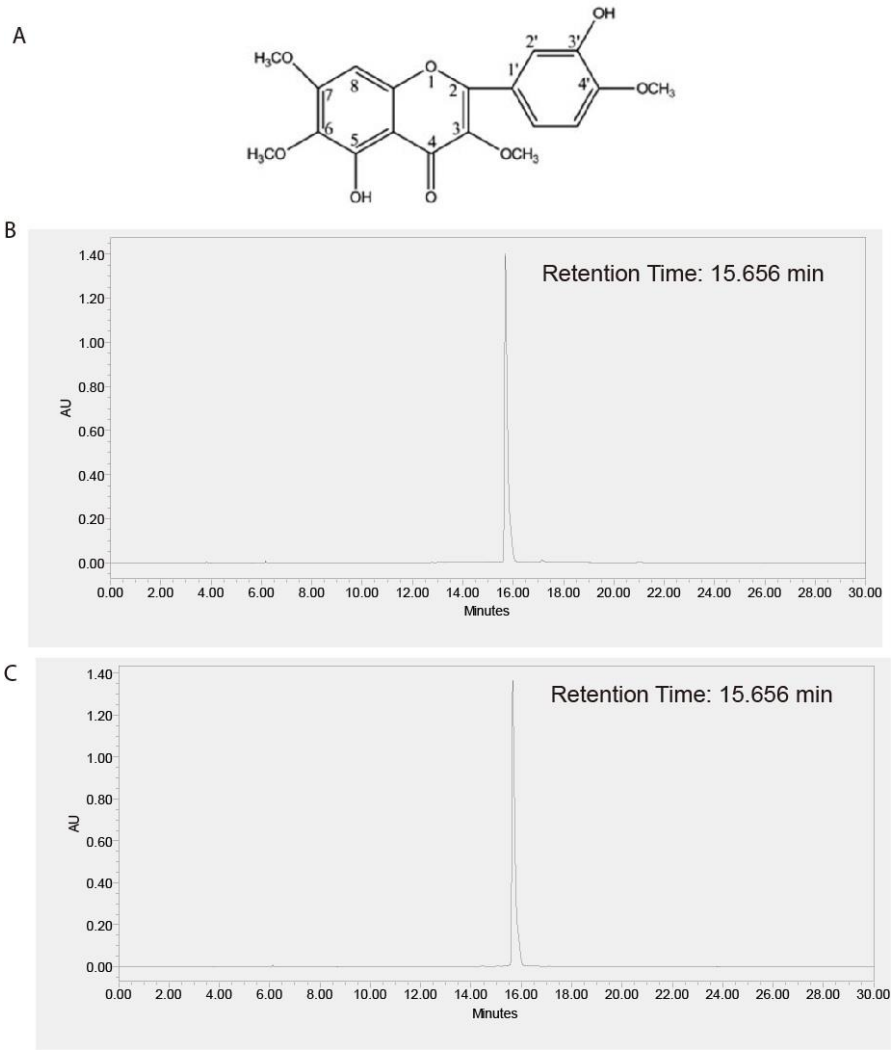

Figure 4. 1 Characterization of casticin extract. (A) Chemical structure of casticin. (B) HPLC profile of casticin extract. (C) HPLC profile of casticin commercial standard.

3.2 Casticin treatment reduced lipid accumulation in differentiating adipocytes

We investigated the effect of casticin on intracellular lipid accumulation in differentiating adipocytes. Post-confluent 3T3-L1 cells were incubated in the differentiation medium with or without serious doses of casticin for 8 days. As shown in **Figure 4.2A and B**, after eight days of induction, vehicle treated differentiated cells developed massive intracellular lipid droplets compared to the cells without differentiation induction. Comparatively, casticin treatment reduced

lipid content in a dose-dependent manner starting from 2.5μM and decreased the lipid accumulation by 77% at 20μM after 8 days of treatment.

It is well documented that adipogenesis process in differentiating 3T3-L1 cells is initiated by mitotic clonal expansion during first 72 hours, followed by differentiation stage in which cells express specific adipogenic and lipogenic genes [193]. To dissect the effect of casticin on different stages of adipogenesis, we further examined the lipid content levels of the differentiated 3T3-L1 cells when 20μM casticin was added at different time points. As shown in **Figure 4.2C** and 2D, lipid-depletion effect of casticin was most profound when the cells were incubated with casticin treatment throughout the differentiation process. Interestingly, cells treated with casticin within first 72 hours presented much lower lipid content compared to those with casticin treatment during the last 5 days of differentiation. The differential lipid-reducing effect of casticin suggests that casticin might affect the proliferation and lipogenesis of differentiating 3T3-L1 cells.

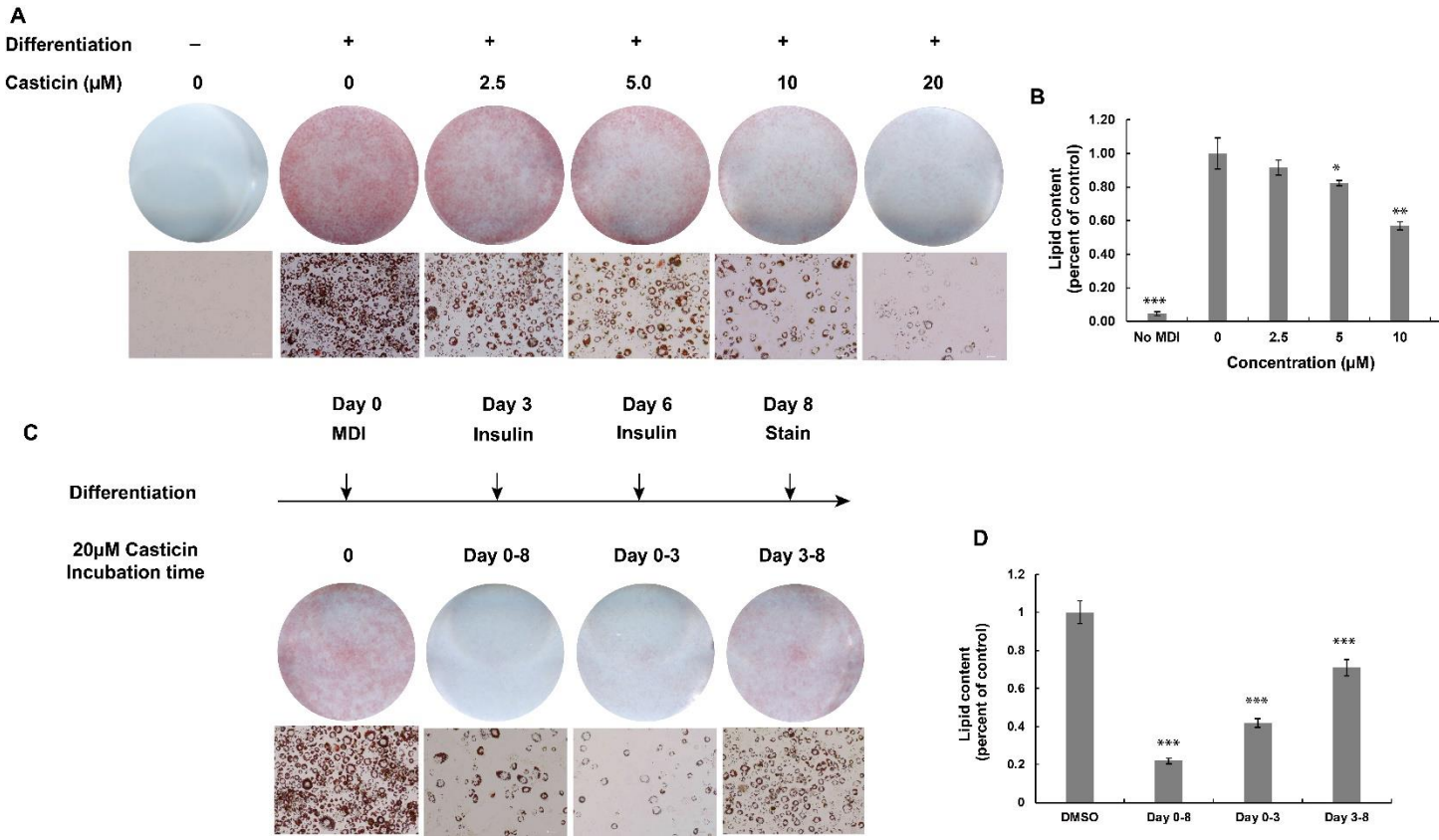

Figure 4. 2 Casticin reduced intracellular lipid accumulation in differentiating mouse adipocytes. Two-day post-confluent 3T3-L1 cells were incubated with differentiation medium in presence of DMSO or different concentrations of casticin for 8 days, followed by Oil Red O staining for microscope observation (A) and quantification (B). Differentiating 3T3-L1 cells were incubated with 20μM casticin across different time frames during eight-days differentiation, followed by Oil Red O staining for imaging (C) and quantification (D). Data shown reflect the means ± SD of 3 experiments. (*) $P<0.05$, (**) $P<0.01$, and (***) $P<0.001$ compared to DMSO treated cells. All error bars, SD.

3.3 Casticin treatment inhibited 3T3-L1 cell proliferation in adipogenesis

We performed cell proliferation assay (MTS assay) on post-confluent 3T3-L1 cells to further understand whether casticin can affect the cell number during adipogenesis. Post-confluent 3T3-L1 preadipocytes were incubated with differentiated medium in the presence of

casticin for 24, 48 or 72 hours, followed by MTS incubation. The activity of MTS assay represents the total number of living cells. As shown in **Figure 4.3A**, casticin inhibited the cell proliferation of differentiating 3T3-L1 cells in a time and dose-dependent manner, suggesting that casticin reduced the cell number during adipogenesis in differentiating 3T3-L1 cells. Consistently, casticin inhibited cell proliferation of pre-confluent 3T3-L1 cells within the dose range of 2.5μM to 20 μM (**Figure 4.3B**).

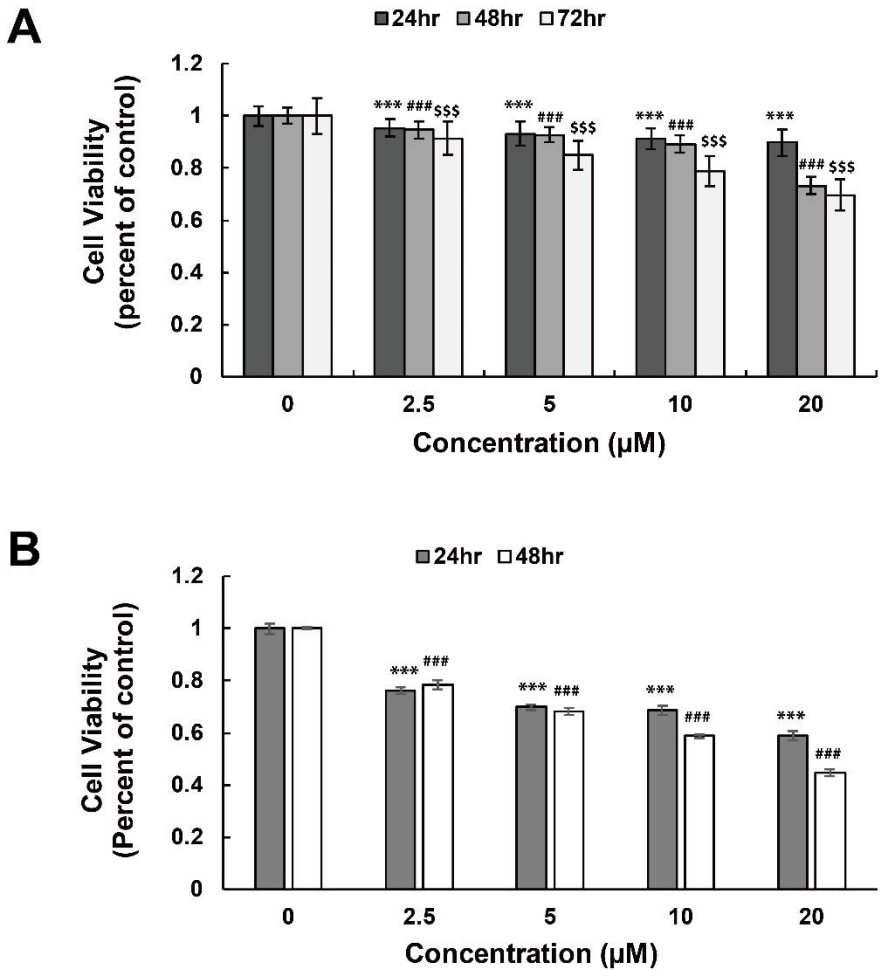

Figure 4. 3 The effect of casticin on post-confluent and pre-confluent 3T3-L1 cell proliferation. (A) Two-day post-confluent 3T3-L1 cells were incubated with differentiation inducer cocktails

(MDI) in the presence of DMSO or different doses of casticin for 24, 48 or 72 hours. (B) pre-confluent 3T3-L1 cells were incubated in complete DMEM medium in the presence of DMSO or casticin for 24 or 48 hours. Cell viability was examined at indicated time points with colorimetric proliferation assay. Data were interpreted as percent of control treated with DMSO vehicle. Data shown reflect the means ± SD of 6 experiments. (*) $P<0.05$, (**) $P<0.01$, and (***) $P<0.001$ compared to the DMSO-treated differentiated cells. All error bars, SD.

3.4 Casticin treatment slowed down the cell cycle progression in differentiating adipocytes

We then performed cell cycle analysis to understand how casticin impact the cell proliferation during adipogenesis. Two-day post-confluent 3T3-L1 cells were activated by differentiation inducer (MDI cocktail) in the presence of DMSO or casticin. After 18 to 24 hours of differentiation induction, cells treated with MDI alone quickly progressed from S phase to G2 phase whereas casticin treatment dramatically slowed down the MDI-induced cell cycle progression, resulting in higher percent of cells present in G0/G1 phase in casticin-treated cells (**Figure 4.4**).

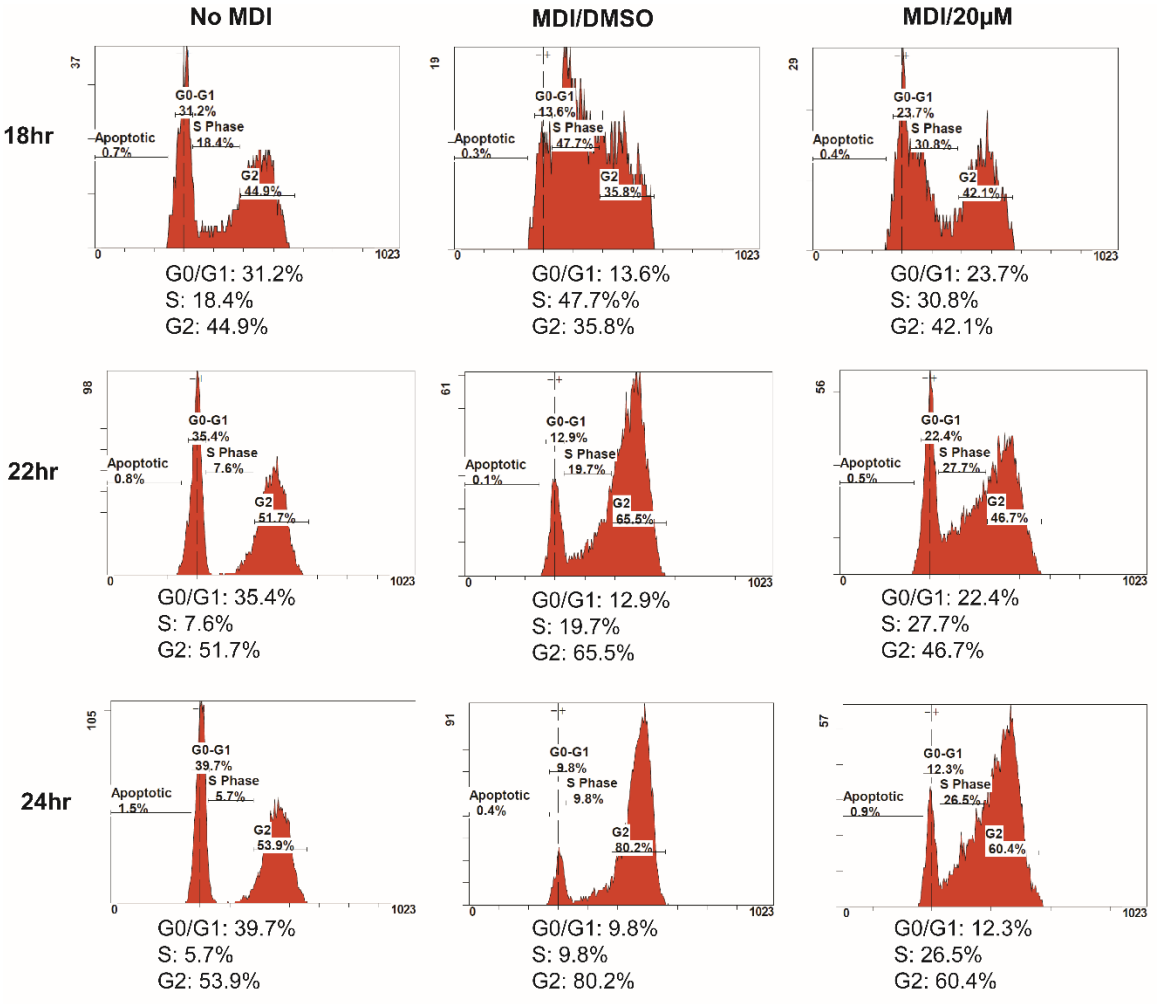

Figure 4. 4 Effect of casticin on cell cycle of differentiating 3T3-L1 cells. Two-day post-confluent 3T3-L1 cells were incubated in culture medium, or activated by differentiation inducer cocktail (MDI) with or without casticin treatment up to 24 hours.

3.5 Casticin treatment induced down-regulation of adipogenic genes expression

We further investigated the effect of casticin on the adipogenic transcription cascade and cellular metabolism regulators. PPARγ and CEBPα are the key adipogenic transcription factors that work sequentially and cooperatively to regulate downstream adipogenesis and lipogenesis events. The results showed that casticin treatment down-regulated expression levels of PPARγ and CEBPα (**Figure 4.5**). Consistently, casticin treatment reduced the expression levels of ACC

and FAS (**Figure 4.5**), suggesting that casticin inhibited fatty acid synthesis and increased fatty acid oxidation in differentiating adipocytes, which is casually related to the reduction in lipogenesis.

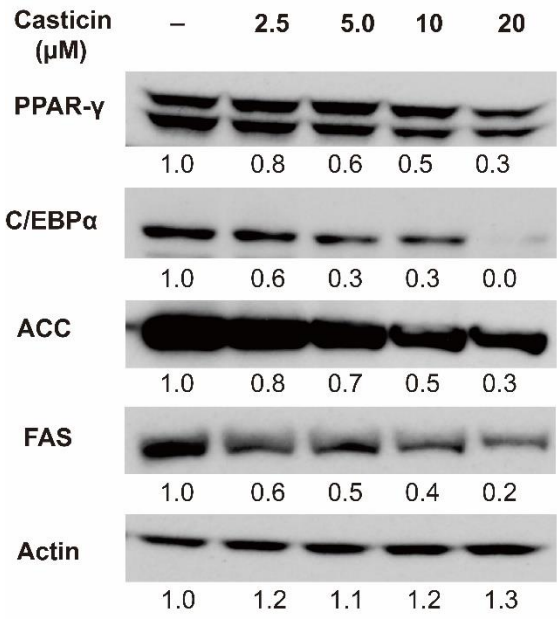

Figure 4. 5 Effect of casticin on the expression levels of adipogenic transcription factors and lipogenic genes. Two-day post-confluent 3T3-L1 cells were incubated in differentiation medium supplemented with or without casticin for 8 days. At the end of treatment, the expression levels of PPARγ, C/EBPα, ACC, FAS and β-Actin were determined by immunoblotting analysis. The protein expression level of β-Actin was used as the internal control.

4. Discussion

Accumulating studies demonstrate that 5-OH PMFs exhibit potent bioactivity in modulation of lipid metabolism and therefore provides a novel therapeutic approach for preventing and treating obesity-related metabolic disorders [109, 192, 194]. Casticin is a 5-OH PMF with one additional hydroxyl group substitution on C3' position. In current study, we evaluated the efficacy of casticin, as a novel 5-OH PMF, on adipogenesis using differentiating

3T3-L1 mouse adipocyte model. The result showed that casticin is effective to reduce intracellular lipid accumulation in differentiating mouse adipocytes within the dose-range of 2.5μM to 20μM. In addition, casticin inhibited cell proliferation and slowed down the cell cycle progression as well as down-regulated the expression levels of critical adipogenic and lipogenic genes during adipogenesis in differentiating 3T3-L1 cell model. The data support that casticin simultaneously affect the total cell number and lipid amount in each individual cells of differentiated adipocytes.

The adipogenesis of 3T3-L1 preadipocytes basically involves multiple consecutive stages including growth arrest, mitotic clonal expansion, initial differentiation and terminal differentiation [193]. Our results showed that casticin presented more potent lipid-reducing effect when dosed during early differentiation stage compared to the latter stage, which implies that casticin has more pronounced impact on the early events of adipogenesis. Accordingly, cell cycle analysis showed that casticin antagonized cell cycle progression and resulted in more cells staying in G0/G1 phase compared to cells treated with differentiation inducer alone during mitotic clonal expansion stage of differentiation. The anti-proliferation effect of casticin we observed here is in accordance with the anti-cancer properties demonstrated previously in multiple cancer cell lines [195, 196].

Casticin can be structurally recognized as the analog of 5-OH nobiletin which has only one hydroxyl group on C5 position. Previous study showed that 5-OH nobiletin is effective to reduce lipid accumulation in 3T3-L1 differentiating mouse adipocytes starting from 2.5μM and reduced the lipid amount by 35% at 20μM. Comparatively, casticin reduced lipid content by 77% at 20μM, suggesting a more potent lipid-reducing efficacy of casticin than 5-OH nobiletin. In addition, it is reported that 5-OH nobiletin did not affect the cell proliferation or cell cycle in the early stage of differentiation [192], which is different from the working mechanism of casticin. Interestingly, it is reported that C-3’hydroxyl group plays critical role in the anti-proliferative

activity of PMFs [190, 197, 198]. The differential impact of casticin and 5-OH nobiletin on cell proliferation could be attributed to the specific structure-activity relationship of PMFs.

One recent study reported that casticin is effective to inhibit hepatic stellate cell proliferation and transdifferentiation in vitro and in vivo, resulting in lower liver fibrosis deposition [199]. Similarly, our results demonstrated that casticin inhibited the growth factor induced adipocytes proliferation and differentiation, resulting in lower lipid deposition. The dual impacts of casticin on lipid metabolism and fibrogenesis provides the rationale that casticin might be a great natural product for preventing and treating non-alcoholic steatohepatitis (NASH) which is an advanced stage of NAFLD with the presence of lipid accumulation and fibrosis [200]. It is interesting to further determine the effect of casticin on NASH treatment in relevant animal models.

The original content of casticin inside the raw material, fruit of Vitex rotundifolia, is so low as 0.379‰ according to our detection, which may largely restrict the exploration and application of this potent polymethoxyflavone compound in either mitigating or treating various malicious diseases. However, with the aid of continuous phase transition extraction method, flavone-contained extract can be collected from bulky raw material preliminarily with enhanced efficacy and reduced manpower input. Moreover, the relatively low extracting temperature that adopted also avoided the possible decomposition of flavone compounds during the whole extracting process.

The purification procedure facilitated the enrichment of casticin within mass extract. By removing the oil and water-soluble impurities, the casticin content inside purified extract can be increased to 3%, which is more proper for further separation by column chromatography. In this way, up to 30 kg of Vitex rotundifolia fruit can be handled within the extraction vessel at one time, which enabled the gram-scale production of casticin after separation.

In summary, we demonstrated that casticin, a novel 5-OH PMF extracted from Vitex rotundifolia fruit, is effective to reduce cell proliferation and lipid accumulation in differentiating mouse adipocytes. To the best of our knowledge, this is the first report regarding the effect of casticin on lipid metabolism. Our data support that casticin has the potential to be developed as an active ingredient in the functional foods.

Author contribution

JG, SJ and QH designed the experiment. JG performed the experiments and wrote the manuscript; XW provided the casticin extract and contributed to the writing of extraction method and the novelty of extraction method. SH, QH and CH revised the manuscript.

Chapter V. Determine the effect of safe mitochondrial chemical uncoupler on preventing and treating obesity, diabetic symptoms and hepatic lipid accumulation

The work of Chapter V was published in the tile of 'Niclosamide piperazine prevents high-fat diet-induced obesity and diabetic symptoms in mice' on Eating and Weight Disorders-Studies on Anorexia, Bulimia and Obesity, 2017, pp.1-6.

Niclosamide piperazine prevents high-fat diet-induced obesity and diabetic symptoms in mice

Jingjing Guo[1,2], Hanlin Tao[1], Amer Alasadi[1], Qingrong Huang[2], Shengkan Jin[1,*]

[1] Department of Pharmacology, [3] Department of Physiology, Rutgers University–Robert Wood Johnson Medical School, Piscataway, New Jersey, USA

[2] Department of Food Science, Rutgers University, New Brunswick, New Jersey, USA

*Corresponding author: victor.jin@rutgers.edu

Abstract

Purpose: Obesity and type 2 diabetes (T2D) have become a major public health challenge globally. Mitochondrial uncoupling, which reduces intracellular lipid loads and corrects the underlying cause of insulin resistance, has emerged as a promising anti-obese and anti-diabetic intervention. Niclosamide is an anthelmintic drug approved by the US FDA with the mechanism of action that uncouples mitochondria of parasitic worms. Recently, niclosamide ethanolamine salt (NEN) was found to be a safe and effective hepatic mitochondrial uncoupler for the

prevention and treatment of obesity and T2D in mouse models. The striking features of NEN prompt us to examine the anti-obese and anti-diabetic efficacy of other salt forms of niclosamide, with the ultimate goal to identify a suitable salt formulation for future clinical development. Here we report the study with niclosamide piperazine salt (NPP), another salt form of niclosamide with documented safety profile.

Methods: Mitochondrial uncoupling activity of NEN and NPP were determined by oxygen consumption assay with Seahorse XF24 Analyzer, as well as by membrane potential measurement in cultured cells. The *in vivo* anti-diabetic and anti-obesity activity were determined in C57BL/6J mice fed high-fat diet (HFD) or HFD containing 2,000ppm NPP for 11 weeks.

Results: NPP showed a comparable mitochondrial uncoupling activity to NEN. Oral administration of NPP significantly reduced HFD-induced obesity, hyperglycemia and hepatic steatosis, and sensitized the insulin responses in mice.

Conclusion: NPP may hold the promise to become an alternative to NEN as a drug lead for the treatment of obesity and T2D.

1. Introduction

The obesity and obesity-related diseases, in particular, type 2 diabetes (T2D) have become the major medical challenges to all the nations [11]. In United States, over 78.6 million adults are obese and approximately 29.1 million people have T2D [201, 202]. T2D is a progressive disease characterized by insulin resistance and disrupted glucose and lipid metabolism. Insulin resistance, which precedes the development of T2D, is attributed to the major cause of T2D and other obesity-related metabolic disorders including fatty liver diseases, dyslipidemia, cardiovascular diseases [203, 204]. However, medications available nowadays are not effective in correcting the underlying cause of insulin resistance and bear inherent limitations

[144, 205]. Therefore, anti-diabetic pharmacotherapies which target the cause of insulin resistance are preferable to improve T2D treatment.

The association between obesity and T2D has been recognized for decades. Several mechanisms have been proposed that ectopic lipid accumulation in liver and muscle plays causal role in insulin resistance and T2D [143, 146, 161, 206, 207]. Recently, a new class of compounds, mitochondrial uncouplers was found to be promising as anti-obese and anti-diabetic pharmacotherapy with a novel mechanism [133, 140]. Mitochondrial uncoupling dissipates the energy from mitochondrial oxidation as heat without effectively producing ATP [208, 209]. The resultant cellular energy inefficiency in turn increases lipid catabolism and then reduces intracellular lipid loads [210, 211], which improves insulin sensitivity and obesity [185, 212].

Niclosamide is an anthelmintic drug approved by United States Food and Drug Administration [213]. Previous study showed that NEN, the ethanolamine salt of niclosamide, is a moderate hepatic mitochondrial uncoupler for treating obesity and T2D in animal models [140]. A more recent research showed that niclosamide itself also has effect on obesity [214]. Oral administration of NEN in mice significantly improved obesity, hyperglycemia, insulin resistance and hepatic steatosis symptoms by reducing cellular energy efficiency and increasing lipid oxidation in liver [140]. Niclosamide piperazine (NPP) is the other niclosamide salt form with known safety profile [215]. NPP has higher water solubility than niclosamide free base but lower water solubility than NEN. The higher water solubility of the salt formulation usually leads to the higher oral bioavailability hence potency [216]. However, increased bioavailability may also enhance toxicity. For clinical drug development, it is important to identify the best salt formulation with proven efficacy and lower toxicity. In current study, we determined the efficacy of NPP, as the other salt formulation of niclosamide on preventing the development of obesity and diabetic symptoms in high-fat diet (HFD)-induced obese/diabetic mice.

2. Materials and Methods

2.1 Reagent

Niclosamide piperazine salt (NPP, 5-chloro-salicyl-(2-chloro-4-nitro) anilide piperazine salt) was purchased from BOC Sciences (Shirley, NY); ethanolamine salt (NEN, niclosamide 5-chloro-salicyl-(2-chloro-4-nitro) anilide 2-aminoethanol salt) from 2A PharmaChem (Lisle, IL).

2.2 Measurement of mitochondrial membrane potential

NIH-3T3 cells were plated in 6-well plate and cultured in DMEM medium supplemented with 10% (vol/vol) fetal bovine serum, 100 U/mL of penicillin, 100 μg/mL of streptomycin and 0.29 mg/mL of L-glutamine at 37°C in a humidified atmosphere of 5% CO_2. For treatment, NPP or NEN was dissolved in DMSO as stock solutions, and then was added into medium to reach final desired concentrations by 1:1,000 dilutions. Cells were incubated with vehicle (DMSO), NPP or NEN at indicated final concentration for 2 hours followed by PBS wash for twice. Cells were then stained with tetramethylrhodamine ethyl ester (TMRE) at final concentration of 100 nM for 10 minutes followed by PBS wash. Afterwards cells were subjected to florescence microscope for determination of membrane potential indicated by florescence strength.

2.3 Mitochondrial Respiration Measurement

Mitochondrial respiration rate was evaluated by measuring oxygen consumption rate (OCR) under mitochondrial stress condition using XF24 Extracellular Flux Analyzer (Seahorse Bioscience Inc., MA). One day before seahorse study, human liver carcinoma HepG2 cells were plated into XF24 microplate at the density of 50,000 cells/well in complete Minimum Essential Medium containing 10% (vol/vol) fetal bovine serum, 100 U/mL penicillin, 100 μg/mL of streptomycin and 0.29 mg/mL of L-glutamine. The plate was placed at 37°C in a humidified atmosphere of 5% CO_2 for overnight. On the day of assay, cells were washed twice with fresh

complete DMEM medium and the volume of each well was brought up to 525 μL. Cells were then placed in a CO_2- free incubator for 1 hour before the OCR assay. The OCR profile was measured at four consecutive stages, including baseline, injection of part A (2.5μM oligomycin), injection of port B (2.5 μM NEN or 2.5 μM NPP), and injection of port C (2.5μM antimycin and 2.5μM rotenone). For each stage, the OCR was measured for 2 to 3 times; and for each measurement, there is a 2min mix followed by a 2min wait time to restore oxygen retention and a 3min measure. The seahorse data was interpreted by Wave 2.3 software.

2.4 Animal and treatment

Four-week-old male C57BL/6J mice were purchased from Jackson Laboratory (Bar Harbor, ME) and shipped to the vivarium of Rutgers-Robert Wood Johnson Medical School. All the experimental protocols were approved by Institutional Animal Care and Use Committees (IACUCs). Mice were maintained in temperature/humidity-controlled room with 12h light/dark cycle. Starting at age of five weeks, mice were randomized into two groups with matched body weights (n=9), and were fed either HFD (60% fat calories; Research Diet, New Brunswick, NJ) or HFD containing 2,000 p.p.m. NPP (mixed and formulated by Research Diet using NPP supplied by the Jin lab), respectively for 11 weeks. Mice were allowed free access to water and food throughout the experiment period. Body weight was measured weekly, and food intake was recorded daily.

2.5 Blood glucose and plasma insulin measurement

Glucose level was determined by tail vein bleed from 16 hour-fasted mice with a glucometer (OneTouch UltraSmart blood glucose monitoring system, Lifescan, Milpitas, CA). For measuring plasma insulin, mice were fasted 5 hours before experiment. Blood samples were then collected and subjected to ultra-sensitive mouse insulin ELISA kit (Crystal Chem Inc., Downers Grove, IL)

2.6 Glucose tolerance assay and insulin sensitivity assay

Mice were fasted 16 hours before glucose tolerance test. Glucose load was given by intraperitoneal injection of 20% D-glucose (Sigma Aldrich, St. Louis, MO) at a dosage of 2 g/kg body weight. Blood glucose levels were measured initially and at designated time points after administration (15, 30, 60, 90, and 120 min).

For insulin sensitivity assay, 5 hour-fasted mice were intraperitoneally injected with recombinant human insulin (Eli Lilly, Indianapolis, IN) at a dosage of 0.75 U/kg body weight. Blood glucose concentrations were measured at the same time points indicated in glucose tolerance assay.

2.7 Histology of liver

At the end of treatment, mice were sacrificed by decapitation. Liver tissues were dissected and fixed with 10% neutral buffered formalin (Surgipath Medical Industries Inc., Richmond, IL). Tissue sections were then prepared and stained with hematoxylin and eosin (H&E). Images were captured by Nikon Eclipse Ni-U imaging system.

3. Results

3.1 NPP uncouples mitochondria in mammalian cells

The structures of NPP and NEN are listed in ***Fig 5.1a and b***, respectively. NPP is another well- documented active salt form of niclosamide that has been used in veterinary medicine to control tapeworm infections through uncoupling mitochondria of the parasites [217]. To determine if NPP has mitochondrial uncoupling activity, we first analyzed mitochondrial membrane potential in two mammalian cell lines upon treatment with NPP. In cultured cells, the mouse fibroblast cell line NIH-3T3 and human hepatic cell line, HepG2, NPP decreased mitochondrial membrane potential starting at the concentration of 500nM and reached 50%

reduction of membrane potential over concentration of 1μM, which is comparable to that of NEN (***Fig 5.1c***). The hallmark of mitochondrial uncoupling is the ability to increase mitochondrial oxygen consumption in the presence of a mitochondrial ATP synthase inhibitor such as oligomycin. We did oxygen consumption studies with Seahorse instrument in HepG2 cells. As shown in ***Fig 5.1e***, similar to NEN, NPP treatment stimulates mitochondrial oxygen consumption in the presence of oligomycin, indicating that NPP has mitochondrial uncoupling activity.

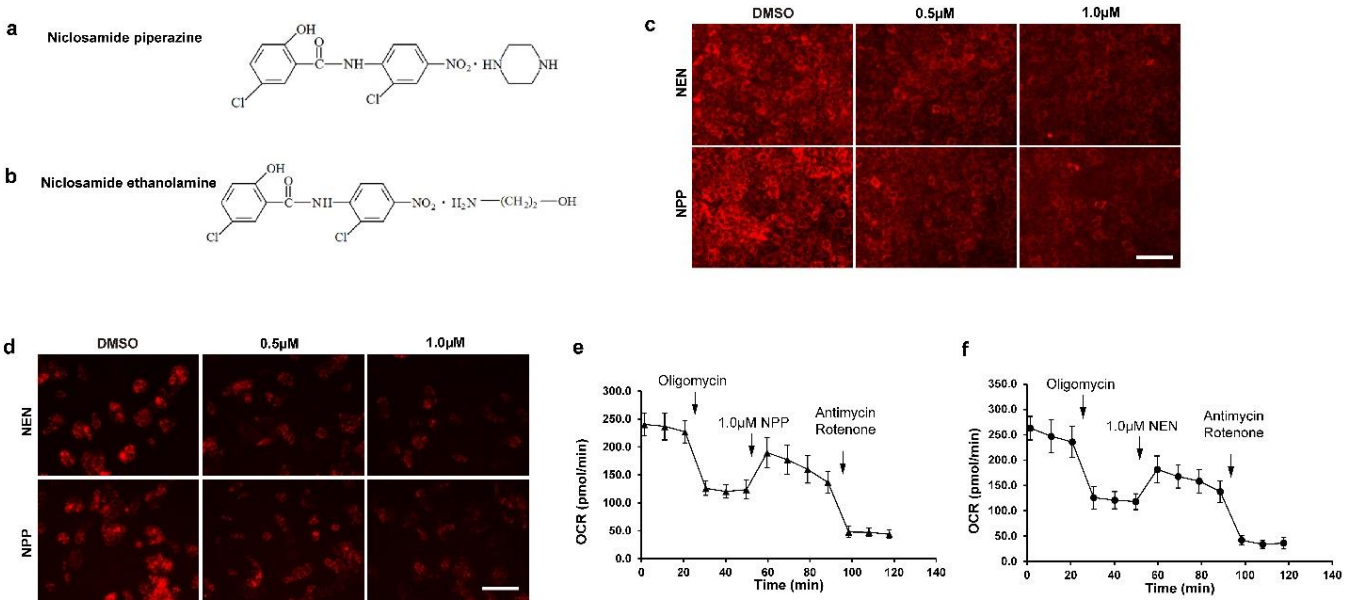

Figure 5. 1 NPP uncouples mitochondria in mammalian cells. (a) Structures of 5-chloro-salicyl-(2-chloro-4-nitro) anilide piperazine salt (NPP), and (b) 5-chloro-salicyl-(2-chloro-4-nitro) anilide 2-aminoethanol salt (NEN). Effect of NPP and NEN on mitochondrial membrane potential determined by TMRE staining in NIH-3T3 cells (c) and in HepG2 cells (d). Cells were treated with vehicle (DMSO), NPP or NEN alone at indicated final concentration for 2 hours. Cells were then stained with TMRE (100nM) for 15 min to detect mitochondrial membrane potential. After washed twice with PBS, cells were observed under microscope. Scale bars, 200μm. (e), oxygen consumption rate (OCR) profile of HepG2 cells treated with 2.5 μM NEN or 2.5 μM NPP. Data are presented as mean value ± SD (n=3)

3.2 NPP reduced diet-induced body weight gain

We further evaluated the efficacy of NPP on metabolism in animals. Long-term high-fat diet (HFD) feeding induces obesity, hyperglycemia, insulin resistance and hepatic steatosis in C57BL/6 mice. We either fed the C57/BL/6 mice HFD alone for 8 weeks to induce metabolic symptoms, or HFD containing 2,000 p.p.m. NPP (125 mg/kg/day) during the same period of time. We found that despite the similar average initial body weight (***Fig 5.2a***), mice treated with NPP exhibited slower rate of gaining body weight than the control group fed HFD alone, and ended with 25% less body weight gain after 8 weeks of treatment. The less body weight gain of NPP-treated mice was not caused by the less food intake, as shown in ***Fig 5.2b***.

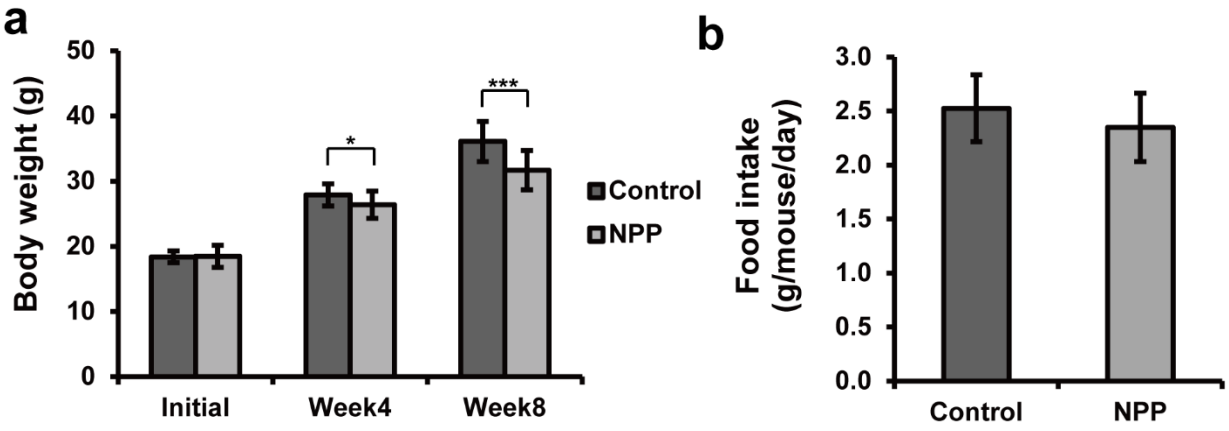

Figure 5. 2 Chronic oral treatment of NPP reduced body weight gain in high-fat diet (HFD)-induced obese/diabetic mice. (a) Body weights, (b) daily food intake of mice fed HFD (60% fat calories) or HFD containing 2,000 p.p.m. NPP for 11 weeks. Data are mean value ± SD (n=9). * P<0.05, ** P<0.01, *** P<0.001

3.3 NPP improved glycemic control and insulin resistance

We further determined the effects of NPP on glycemic control and insulin sensitivity. After 4-week HFD feeding, fasting blood glucose level of the control mice increased to ~122

mg/dL (***Fig 5.3a***) which reaches prediabetic range [218], while the age-matched mice treated with NPP showed significantly lower blood glucose levels which are still within the normal range [218]. At the end of 8-week treatment, control mice fed HFD alone developed hyperglycemia to ~158 mg/dL and hyperinsulinemia to ~2.18 ng/mL, which reaches diabetic level [218]. Comparatively, NPP treatment significantly reduced blood glucose level and plasma insulin by 22% and 61%, respectively (***Fig 5.3b***). To further investigate the effects of NPP on insulin resistance, intraperitoneal glucose tolerance assay and insulin resistance assay were performed. Consistent with the better glycemic control in NPP treatment group, mice treated with NPP showed significantly improved glucose tolerance and better insulin sensitivity in response to glucose and insulin load, respectively (***Fig 5.3c and d***).

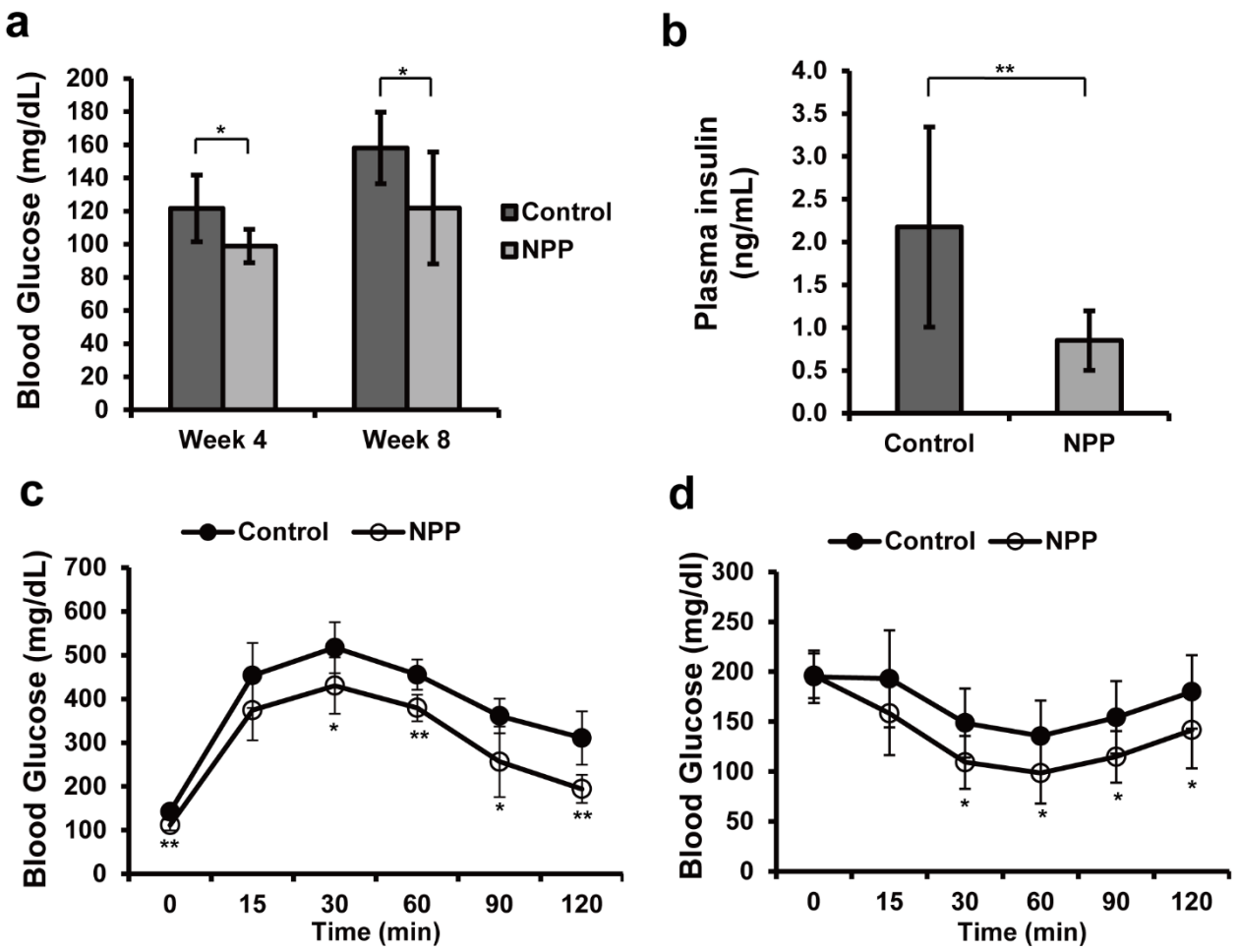

Figure 5. 3 Chronic oral treatment of NPP improved glycemic control and insulin resistance in high-fat diet (HFD)-induced obese/diabetic mice. (a) Fasting blood glucose levels of mice fed HFD (60% calories) or HFD containing 2,000 p.p.m. NPP measured at week 4 and 8 of treatment; (b) plasma insulin level measured at week 9; (c) glucose tolerance assay and (d) insulin sensitivity assay performed at week 10 and 11, respectively. Data are mean value ± SD (n=9). * P<0.05, ** P<0.01, *** P<0.001

3.4 NPP prevented diet-induced hepatic steatosis

To determine whether NPP impacts hepatic lipid metabolism, we performed hepatic histology study. As shown in ***Fig 5.4***, the hepatocytes of control mice fed HFD alone had significant vacuolation composed of massive lipid droplets, which indicates severe hepatic

steatosis. In contrast, fewer intracellular lipid droplets and regular shape of hepatocytes were found in the NPP-treated mice under same HFD feeding conditions. The histology results suggested that, similar to its analog NEN, NPP treatment prevented the HFD-induced hepatic lipid accumulation in mice.

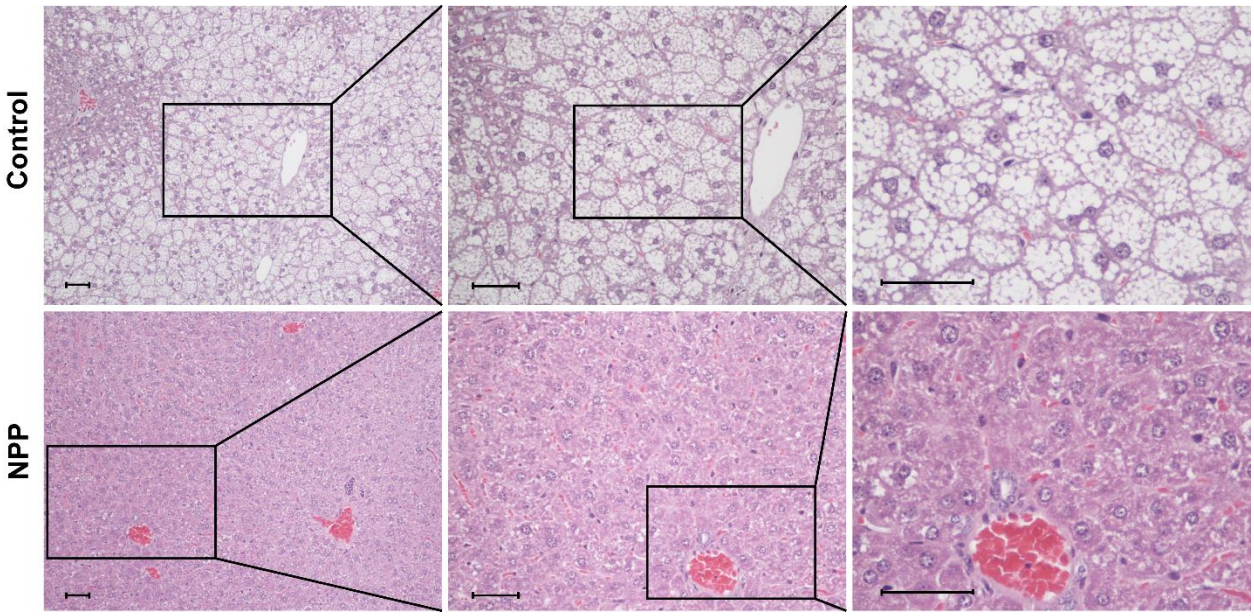

Figure 5. 4 Chronic oral treatment of NPP reduced hepatic lipid accumulation. Representative pictures of H&E stained liver tissues from mice fed high-fat diet (HFD) alone or HFD containing 2000 ppm NPP for 11 Weeks. The white areas in hepatocytes are cells with high lipid content. Scale bar, 50 μM

4. Discussion

Niclosamide is practically insoluble in water compared to its two salt forms, NEN and NPP [213]. For oral administration, it is mostly likely that NEN and NPP are more bioaccessible than niclosamide free base due to their higher water solubility, which gives rise to higher oral bioavailability and anti-diabetic efficacy of NEN and NPP. Thus, compared to niclosamide, the two salt forms exhibit higher potential for therapeutics development.

Previous study demonstrated that NEN is efficacious in correcting obesity, insulin resistance and diabetic symptoms [140]. The water solubility of NPP is between NEN and niclosamide. The current study addressed the question whether NPP could serve as an alternative to NEN as drug candidate for future clinical development. We demonstrated that NPP is effective in improving HFD-induced obesity, hyperglycemia, insulin resistance and hepatic steatosis at a dose similar to NEN in mice. The result provided evidence that NPP has comparable efficacy for treating obesity and T2D as NEN. Further studies, particularly the comparison in toxicity profile between NPP and NEN, will determine which salt form has a better therapeutic window. This would help us select a better lead compound for development of a therapeutic for treatment of obesity and T2D.

5. Conclusion

In brief, we found that NPP, a salt form of niclosamide, is efficacious in reducing HFD-induced obesity and improving HFD-induced diabetic symptoms and hepatic steatosis in mice. Its anti-obesity and anti-diabetic effect, together with our previous studies [140], confirmed the effectiveness of mitochondria uncoupling for prevention or treatment of obesity and T2D. Moreover, based on result from the current animal study, NPP may hold the promise to become an alternative to NEN as a drug lead for treating obesity and T2D. Future pre-clinical studies are required to compare the therapeutic window of the two drugs.

Chapter VI. Determine the effect of safe mitochondrial uncoupler on treating advanced fatty liver disease

The work of Chapter VI is currently under manuscript preparation in the title of 'Niclosamide ethanolamine ameliorates steatosis, inflammation and fibrosis in western diet-induced nonalcoholic steatohepatitis mice'

Niclosamide ethanolamine ameliorates steatosis, inflammation and fibrosis in western diet-induced nonalcoholic steatohepatitis mice

Hanlin Tao[†1], Jingjing Guo[†1], Justin Schumacher[2], Amer Alasadi[1], Juan Collantes[1], Xiaoyang Su[3], Grace L. Guo[2], and Shengkan Jin[1]*

[1]Department of Pharmacology, Rutgers, The State University of New Jersey–Robert Wood Johnson Medical School, 675 Hoes Lane West, Piscataway, NJ 08854, USA; [2]Department of Pharmacology and Toxicology, School of Pharmacy, EOHSI, Rutgers University, Piscataway, NJ 08854, United States; [3]Endocrinology, Rutgers, The State University of New Jersey–Robert Wood Johnson Medical School, 89 French Street, New Brunswick, NJ 08901

[†] J.G. and H.T. contributed equally to this work

*Corresponding Author: victor.jin@rutgers.edu

1. Introduction

Nonalcoholic steatohepatitis (NASH), the advanced stage of nonalcoholic fatty liver disease (NAFLD), has been a major public health issue globally.[219, 220] Progression of the disease from simple fatty liver leads to hepatic inflammation and fibrosis, and ultimately life-threatening outcomes such as cirrhosis or liver cancer – both requiring a liver transplantation at end stage.[221, 222] There is no approved medication for NASH so far.

The pathogenesis of NASH was initially described as the “two-hit hypothesis” in 1998.[223] The “first hit” refers to ectopic lipid accumulation in liver, which causes hepatocyte degeneration and makes the tissue more vulnerable to injury mediated by other factors that constitute the "second hit". The “second hit” may include oxidative stress, mitochondrial dysfunction, proinflammatory cytokines and insulin resistance etc., which further promote hepatic injury leading to steatohepatitis and fibrosis.[224, 225] As the knowledge of new pathogenic factors and the interplay between these factors have greatly increased over the last decade,[226-228] the “two-hit” theory has been modified recently to a “multiple hits” hypothesis, which demonstrates multiple parallel factors acting synergistically in genetically predisposed individuals to induce NASH.[59]

Among all these factors, fat accumulation in liver plays a fundamental role in initiating the disease progress of NASH.[62, 229, 230] High level fatty acids, free cholesterol and other lipid metabolites may accumulate in the fatty liver due to excess intake of nutrients or altered lipid metabolism, leading to lipotoxicity which causes dysfunction and death of hepatocytes. The prolonged damage to liver induces a low grade, chronic inflammatory state in the tissue characterized by the activation of hepatic Kupffer cells (KCs) and induction of mixed inflammatory cell infiltration, a critical feature that distinguishes NASH from simple fatty liver.[231-234] Chronic inflammation promotes further injury of hepatocytes, creating a feed-forward regulatory loop.[235] Long-term injury and inflammation in liver promotes the transdifferentiation (often referred to as “activation”) of hepatic stellate cells (HSCs) to

myofibroblasts, which produces extracellular matrix leading to the formation of fibrosis.[236, 237] The HSCs, also known as perisinusoidal cells or Ito cells, reside in the perisinusoidal space of the liver. In a health liver, the HSCs represent 5-8% of the total number of liver cells and remain in a quiescent state.[238] In NASH, the quiescent HSCs are induced into an activated state characterized by proliferation, contractility, and chemotaxis. The activation is mediated by multiple stimuli from resident and infiltrating inflammatory cells.[239] Upon activation, multiple signaling pathways inside the HSCs have been shown to be highly activated and drive the process of fibrogenesis. The core pathways mediating HSC activation and hepatic fibrogenesis include the platelet-derived growth factor (PDGF), the transforming growth factor β (TGFβ), integrins and some other growth factor pathways.[240-242]

Mitochondrial uncoupling is a process by which the mitochondrial electron transport chain (ETC) activity is de-coupled from production of ATP by FoF1-ATP synthase. It is usually mediated by proton "leaking" back across mitochondrial inner membrane. Mitochondrial uncoupling can be induced by the expression of uncoupling proteins (UCPs), such as UCP1. It can also be mediated by a chemical uncoupler, usually a lipophilic weak acid that is protonated at the outer side of the membrane and de-protonated at the inner side of the membrane, catalyzing the influx of proton across the mitochondrial inner membrane. As a result, mitochondrial uncoupling creates a futile cycle of mitochondrial oxidation: the energy extracted from oxidation is dissipated as heat rather than for ATP production. Mitochondrial uncoupling is a powerful way of facilitating free fatty acid oxidation and reducing lipid load in cells and tissues. Moreover, mild mitochondrial uncoupling is well documented to reduce mitochondrial ROS production. In fact, UCP2 is usually upregulated in cellular oxidative stress to mitigate the increase of cellular ROS. Moreover, we have previously demonstrated that safe mitochondrial uncoupler niclosamide ethanolamine (NEN) is effective to reduce hepatic steatosis and improve insulin sensitivity in high-fat diet-induced diabetic mice, and protect hepatocytes form ballooning or cell death,[243]

which suggests a potential of mitochondrial uncoupling in treating NASH as it targets the root cause of the disease.

The carbon tetrachloride (CCl_4) induced-fibrosis in mouse liver is a classic mouse model used in the study of liver injury and fibrosis. NASH induced by a western style diet with high fat and cholesterol content in small rodent animals is another important animal model, which has been well established and widely used in NASH drug development researches.[244-248] This animal model recapitulates very well the pathological features of NASH in human, such as insulin resistance, hepatic steatosis, inflammation and fibrosis. In the present study we tested the effect of mitochondrial uncoupler NEN and its derivative compound on NASH in these mouse models.

2. Material and Methods

2.1 Reagents.

NEN (niclosamide 5-chloro-salicyl-(2-chloro-4-nitro) anilide 2-aminoethanol salt) was from 2A PharmaChem (Lisle, IL); Recombinant Human TGF-beta 1 (TGFβ, 240-B-002) was from R & D systems (Minneapolis, MN); Platelet-Derived Endothelial Cell Growth Factor from human platelets (PDGF, P5208) was from Sigma-Aldrich. AMPK-α monoclonal antibody (mAb) (#2793) and pAMPK-α (Thr172) mAb (#2535), Phospho-Smad2 (Ser465/467)/Smad3 (Ser423/425) (D27F4) Rabbit mAb (#8828), PDGF Receptor β (28E1) Rabbit mAb (#3169) were from Cell Signaling Technology. β-catenin polyclonal antibody (sc-65483) was from Santa Cruz Biotechnology. Collagen I polyclonal antibody (ab34710) was from Abcam. F4/80 mAb (MCA497GA) was from AbD Serotec. Desmin polyclonal antibody (#PIPA519063) was from Fisher Scientific.

2.2 Animals and treatments.

Male C57BL6 mice were from the Jackson Laboratory. The mice were housed in the vivarium of Rutgers University-Robert Wood Johnson Medical School with free access to diet and water. Mouse study protocol was approved by the Institutional Animal Care and Use Committees (IACUCs) at the Rutgers University. For Western Diet induced NASH study, the mice were randomized into two groups and fed either Western Diet (D09032705G, Research Diet, Inc., New Brunswick, NJ), or the same Western Diet containing 2,000 p.p.m. NEN (D16012604, Research Diet, Inc., New Brunswick, NJ) for 8 months. The dose is around 200 mg/kg NEN per day to each mouse. For carbon tetrachloride (CCl_4) induced fibrosis study, the mice were randomized into 6 groups, which are the vehicle control, CCl_4 positive, NEN prevention on CCl_4-injected mice (the drugs were administered since the beginning of CCl4 injection), NEN treatment on CCl_4-injected mice (the drugs were administered after 2 weeks CCl_4 injection). The CCl_4 were injected into the mice intraperitoneally at a dose of 1 ml/kg, twice a week for 4 weeks. The drugs were mixed into the diet as 2,000 p.p.m. for NEN (D13101902, Research Diet, Inc.), which gave around 150 mg/kg NEN to the mice. Animal sample size for each group in the study was chosen based on literature documentation of similar studies. The animal studies were not blinded to investigators.

2.3 Blood parameters

Blood glucose levels of the mice were determined using OneTouch UltraSmart blood glucose monitoring system (Lifescan, Milpitas, CA) after 16 hours fast. Blood samples of the mice were collected from lateral tail vein of the mice after 5 hours or 16 hours fast as indicated in the individual experiment. The blood samples were centrifuged at 1,500×g for 10 min at 4°C, and then the plasma were recovered and stored at −70°C. Plasma lipid profile including free fatty acid, triglyceride and total cholesterol; plasma insulin, and the levels of aspartate transaminase (AST) and alanine transaminase (ALT) were determined by the US National Mouse Metabolic Phenotyping Center (MMPC) at University of California, Davis (Davis, CA).

2.4 Hepatic lipid profile and immunohistochemistry

For the Western Diet fed mice, the mice were sacrificed after 8 months' treatment, and the liver tissues were dissected and frozen in liquid nitrogen immediately, or fixed within neutral buffered formalin 10% (Surgipath Medical Industries, Inc.). The hepatic lipid profiles in these mice were determined by MMPC at UC Davis. The fixed tissues were embedded in paraffin, and tissue sections were prepared and stained with hematoxylin and eosin (H&E) by the Histopathology Core at the Rutgers University-Cancer Institute of New Jersey. The liver sections were stained by the Mason's trichrome blue and Picro-Sirius red for showing hepatic fibrosis, using staining kits from the IHC WORLD, LLC. The liver sections were also stained with anti-F4/80 and anti-Desmin mAb.

2.5 Cell culture and treatments

LX-2 Human Hepatic Stellate Cell Line (SCC064) was purchased from EMD Millipore (Temecula, CA). The cells were thawed in DMEM High Glucose media containing 10% FBS, 1X Pen/Strep, and 1X Glutamine; then the cells were cultured in the same media but with only 2% FBS. For the in vitro activation assay, the cells were cultured in 2% FBS media until semi-confluent, then the cells were cultured in FBS free media for 24 hours; to induce the proliferation and trans differentiation of the cells, the culture media were replaced with 2% FBS media and treated with 10 ng/ml TGFβ or 50 ng/ml PDGF for indicated time.

Cell cycle analyses were determined by flow cytometry following standard procedure.

For the metabolomics study, LX-2 cells were cultured on 6-well plate in FBS-free media for 24 hours and then switched to media supplemented with 2% dialyzed serum (SH3007903 from ThermoFisher) for another 2 hours. After the 2 hour-preincubation, cells were incubated in fresh 2% dialyzed serum media containing in the presence of TGFb and/or NEN for indicated treatment time. At the end of drug incubation, cells were immediately quenched with 400μL/well

ice-cold quenching buffer (40:40:20 methanol:acetonitrile:water w/ 0.5% formic acid). Cell plates were then immediately incubated on ice for 5 min with the addition of 20μL 15% NH_4HCO_3. Cell lysates were collected by scraping the cells with cell lifters and then subjected to centrifugation at 15,000g for 10 minutes in cold room to pellet cell debris and protein. The supernatant was collected and stored at -80C for further LC/MS/MS analysis.

2.6 LC-MS analysis

LC−MS analysis the cellular metabolites was performed on the Q Exactive PLUS hybrid quadrupole-orbitrap mass spectrometer (Thermo Scientific) coupled to hydrophilic interaction chromatography (HILIC). The LC separation was performed on UltiMate 3000 UHPLC system with an XBridge BEH Amide column (150 mm × 2.1 mm, 2.5 μM particle size, Waters, Milford, MA) with the corresponding XP VanGuard Cartridge. The liquid chromatography used a gradient of solvent A (95%:5% H_2O: acetonitrile with 20mM ammonium acetate, 20 mM ammonium hydroxide, pH 9.4), and solvent B

(20%:80% H2O: acetonitrile with 20 mM ammonium acetate, 20 mM ammonium hydroxide, pH 9.4). The gradient was 0 min, 100% B; 3 min, 100% B; 3.2 min, 90% B; 6.2 min, 90% B; 6.5 min, 80% B; 10.5 min, 80% B; 10.7 min, 70% B; 13.5 min, 70% B; 13.7 min, 45% B; 16 min, 45% B; 16.5 min, 100% B. The flow rate was 300 μl/min. Injection volume was 5 μL and column temperature 25 °C. The MS scans were in negative ion mode with a resolution of 70,000 at m/z 200. The automatic gain control (AGC) target was 3 × 10 6 and the scan range was 75−1000. Metabolite features were extracted in MAVEN (Cite: PMID 21049934) with the labeled isotope specified and a mass accuracy window of 5 ppm. The 13 C isotope natural abundance and impurity of labeled substrate was corrected using AccuCor written in R (Cite: PMID 28471646).

2.7 Protein extraction and immunoblotting

Cells or tissues were collected and homogenized within lysis buffer containing 10 mM TRISHCl (pH 7.9), 10% glycerol, 0.1 mM EDTA, 100 mM KCl, 0.2% NP40, 0.5 mM PMSF, 1 mM dithiothreitol (DTT), minicomplete protease inhibitor cocktail (Roche, 11836153001) and phosphatase inhibitor cocktail (Roche, 04906845001), if required. Nuclei and insoluble debris were pelleted in an Eppendorf microcentrifuge at 10,000 r.p.m. for 5 min at 4°C. Cell extracts were then stored at −20 °C or immediately subjected to SDS/PAGE. For SDS/PAGE, protein extracts were mixed with 5× Laemmli loading buffer and heated at 95 °C for 5 min before electrophoresis. For immunoblotting, proteins were transferred to polyvinylidene difluoride (PVDF) membranes (Millipore, IPVH00010). The membranes were blocked with 5% milk in PBS supplemented with 0.1% (v/v) Tween 20 for 1 hr at room temperature, and then blotted with the specific antibodies. Chemiluminescent detection was performed with enhanced chemiluminescent (ECL) western blotting reagents (95038566, Amersham). Quantification was determined by measuring band intensities using ImageJ software and calculating the ratio of the protein of interest to an internal loading control.

2.8 Quantitative PCR analyses of gene expression

Total RNAs were extracted from mouse liver or cultured cells using TRIzol reagent (Invitrogen, Carlsbad, CA). The cDNA was amplified using TaqMan® Reverse Transcription Reagents (N8080234, Applied Biosystems). Quantitative PCR (qPCR) were performed following standard SYBR® Green dye based method. The primers used for gene expression analyses are listed below.

2.9 Statistical analyses

Student's t-test and the one-way analysis of variance (ANOVA) were used for the statistical analyses in the studies as indicated. Data were presented as the means ± s.d., and statistical significance is denoted as *$P < 0.05$, **$P < 0.01$ and ***$P < 0.001$.

3. Results

3.1 NEN improved metabolic symptoms in high-fat and high-cholesterol diet-induced NASH mice

NASH symptoms including hepatic steatosis, inflammation and fibrosis were induced in C57BL6 mice by feeding high-fat and high-cholesterol western style diet for 6-8 months (the formulation of the diet is described in **Table 6.1**).

Table 6. 1 Diet composition. Modified western diet (40% kcal as mostly hydrogenated coconut oil plus 1.22% cholesterol), formulated by Research Diets, Inc., D09032705G.

Component	g%	kcal%
Protein	20	17
Carbohydrate	49	43
Fat	21	40

Ingredient	g/kg	kcal /kg
Coconut Oil, Hydrogenated	200	1800
Cholesterol	12.2	0
Corn Starch	50	200
Sucrose	341	1364
Casein	195	780

NEN was mixed into the diet; and our previous study showed that oral NEN is primarily distributed to and reaches an effective concentration in liver.[243] After 6-8 months feeding the Western Diet, the mice became obese with increased blood glucose and cholesterol levels. The biochemical indexes of the mice were summarized in **Table 6.2**. NEN treatment slightly

increased daily food intake of the mice, however, the body weight, blood glucose and cholesterol of the mice were significantly lower when compared to the control mice.

Table 6. 2 Biochemical indexes of the mice fed HF HC diet with or without NEN treatment

	Control (n=8)	NEN (n=9)	p-value
Body weight (g)	40.0±4.4	33.8±2.6	<0.01
Food intake (g/mouse.day)	3.0±0.5	3.4±0.6	<0.05
Blood glucose (mg/dl)	103.1±15.5	85.6±8.5	<0.05
Plasma insulin (ng/ml)	1.1±0.4	1.7±0.8	0.20
Plasma triglyceride (mg/dl)	47.7±7.2	56.3±5.1	<0.05
Plasma cholesterol (mg/dl)	355.1±27.6	278.9±42.0	<0.0001
Plasma FFA (mEq/l)	1.0±0.18	1.0±0.17	0.48

The Western Diet induced severe hepatic steatosis in the control mice. The average liver weight of these mice became abnormally high (**Fig 6.1A**), and histological analyses revealed tremendous lipid accumulation in the liver (**Fig 6.1D**, **left panel**). In contrast, the average liver weight of the NEN-treated mice was significantly lower and very close to liver weight in a heathy mouse. Consistently, the hepatic lipid accumulation was either dramatically (50 % of the mice, **Fig 6.1D, middle panel**), or completely resolved (50 % of the mice, **Fig 6.1D**, **right panel**). Histopathology analyses scored 3.75 for steatosis in the liver of control mice, which was decreased to 2.67 in the liver of NEN-treated mice (**Table 6.3**).

Table 6. 3 Histopathology scoring

	Control	NEN	p value
Steatosis	3.75	2.67	<0.01

Inflammation	1.50	1.11	0.08
Fibrosis	2.00	0.89	<0.01

A further quantification analysis of hepatic lipid content showed that NEN treatment significantly reduced the total triglyceride level in the mouse livers (**Fig 6.1B**). In the mice fed the Western Diet with high cholesterol content, the hepatic total cholesterol level became extremely high (3-4 folds higher than normal level); while the NEN treatment significantly reduced the level of hepatic cholesterol (**Fig 6.1C**).

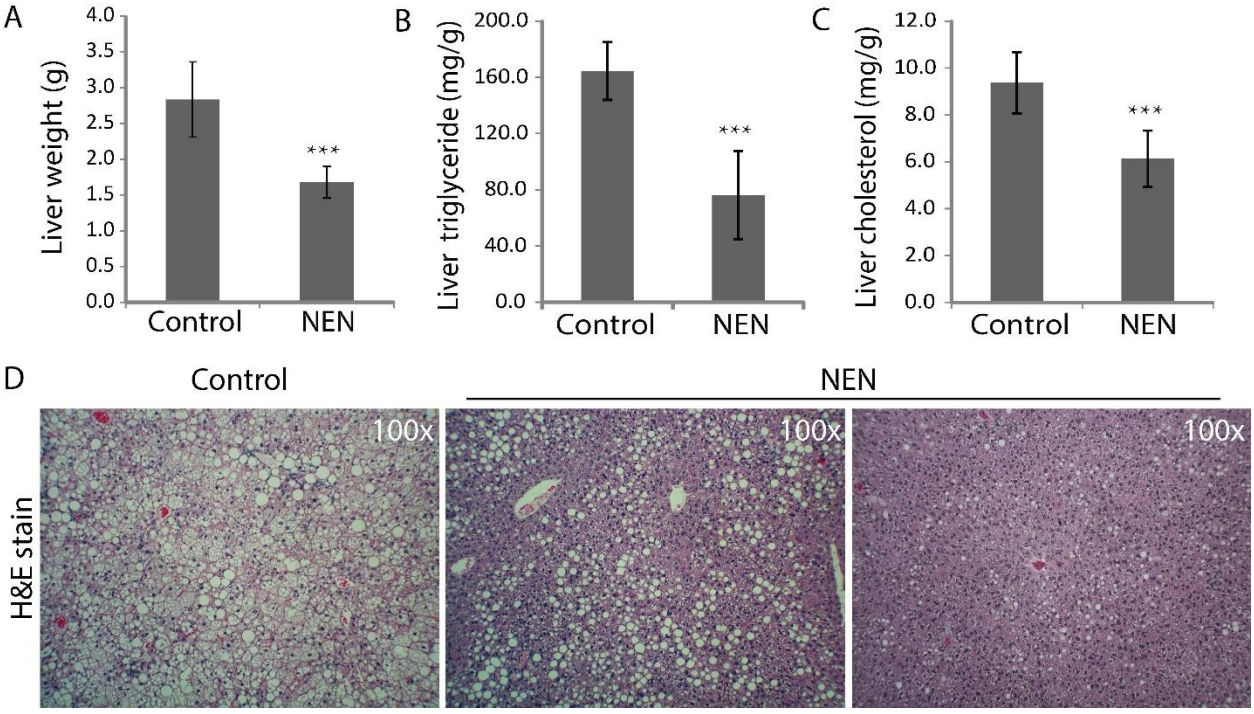

Figure 6. 1 Effect of NEN treatment on hepatic steatosis in western diet-induced NASH mice model. (A) average liver weight, (B) hepatic triglycerides content, (C) hepatic total cholesterol content and (D) liver histology manifested by representative liver sections stained with H&E. Control, the mice were fed on western diet for 8 months; NEN, the mice were fed on western diet containing 2,000 p.p.m. NEN for 8 months.

3.2 NEN reduced hepatocyte ballooning and hepatic inflammation in high-fat and high-cholesterol diet-induced NASH mice

Hepatocellular ballooning is a key feature indicating liver damage in NASH which is characterized by cell swelling and loss of cytoplasm content [249]. As shown in the hematoxylin-eosin (H&E) stained liver sections, cellular ballooning appeared widespread in the liver of the control mice, while NEN treatment dramatically reduced the extent of cellular ballooning (**Fig 6.2A, upper panel**). Ballooning degeneration reflects cell death of hepatocytes, therefore we further examined the levels of aspartate transaminase (AST) and alanine transaminase (ALT) in the blood of the mice, which are liver enzymes released into blood due to liver cell injury or death. Consistently, NEN treatment significantly reduced the plasma ALT and AST levels (**Fig 6.2B & C**).

Hepatic inflammation is a hallmark of NASH as well. Both the activation of Kupffer cells and infiltration of circulating immune cells are involved in mediating the inflammatory state in NASH.[234, 250] In the liver sections of NEN-treated mice, we found the population of monocytes were reduced as compared to the control mice, especially in lobular area (**Fig 6.2A, lower panel**). Quantification analyses of the expression of macrophage specific marker F4/80 in the liver tissues also revealed that NEN treatment reduced F4/80 expression to about half of that in the control mice (**Fig 6.2D**). In response to liver damage signals, monocyte chemoattractant protein 1 (MCP1/CCL2) is induced in NASH liver and plays a key role in regulating migration and infiltration of monocytes/macrophages.[251] As shown in **Fig 6.2E**, NEN treatment significantly reduced MCP1 expression to about one third of the level in the liver of control mice. The levels of tumor necrosis factor alpha (TNFα) and interleukin-1 beta (IL-1β), which are produced mainly by activated macrophages as key cytokine involved in systemic inflammation in NASH, were also significantly lower in the liver of NEN-treated mice (**Fig 6.2F**). Taken together,

the NEN treatment effectively reduced hepatic cell damage and inflammation in the Western Diet-induced NASH mice.

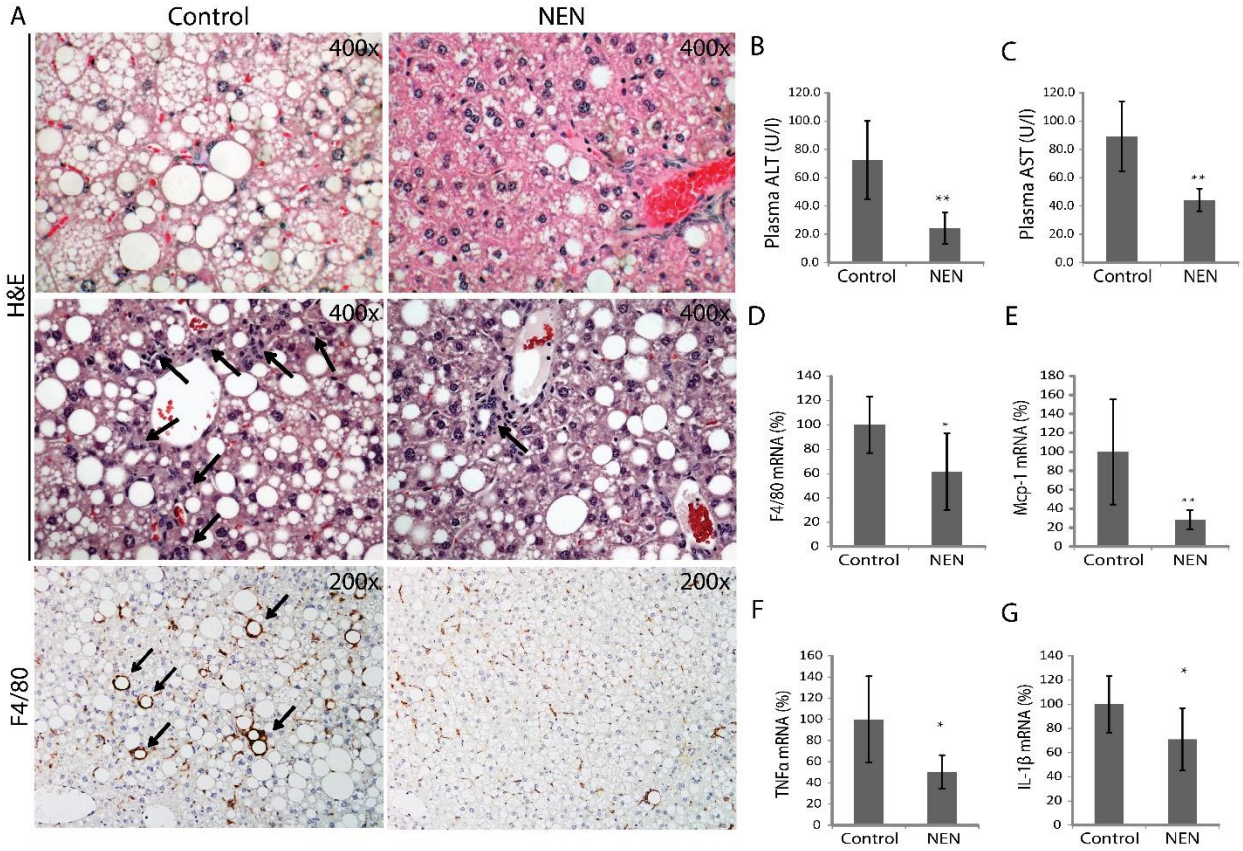

Figure 6. 2 Effect of NEN treatment on liver damage and hepatic inflammation. (A) Representative liver histology of hepatocyte ballooning (upper panel), inflammatory cell population (middle panel) and F4/80 immunohistochemical staining (bottom panel). (B) Plasma ALT. (C) Plasma AST. Hepatic mRNA expression levels of (D) F4/80, (E) Mcp-1, (F) TNFα, and (G) IL-1β. Control, n=8, the mice were fed on western diet for 8 months; NEN, n=9, the mice were fed on western diet containing 2,000 p.p.m. NEN for 8 months. *P < 0.05, **P < 0.01, ***P < 0.001. Statistical significance (P) was determined by Student's t test. All error bars, s.d.

3.3 NEN reduced hepatic fibrosis and inhibited hepatic stellate cell activation in high-fat and high-cholesterol diet-induced NASH mice

Hepatic fibrosis was induced in the mice after long-term Western Diet feeding. The hepatic fibrosis manifested by both the Mason's trichrome blue stain and the Picro-Sirius red stain became evident in periportal and lobular areas of the liver in control mice, while NEN treatment dramatically reduced the formation of fibrosis (**Fig 6.3A**). Accordingly, histopathology analyses scored 2.00 for fibrosis in the liver of control mice, while NEN treatment decreased the score to 0.89 (**Table 6.3**). As the hepatic fibrosis is largely composed of collagen types I[252, 253], we determined the expression of collagen type I, alpha 1 chain (Col1a1) in liver of the mice. As shown in **Fig 6.3B**, the expression of Col1a1 in the NEN-treated mice liver was only about one-fifth of the levels of the control mice.

The hepatic stellate cells (HSCs) are the key cellular mediator of fibrosis in NASH. The quiescent HSCs are activated and differentiated into myofibroblasts in response to liver damage in NASH, which then produce extracellular matrix like fibril-forming collagens.[236, 254] Increased desmin expression and formation of desmin-containing intermediate filaments is one of the hallmarks of HSCs activation.[255, 256] As shown in **Fig 6.3C**, immunohistochemical stain with desmin specific antibody showed clearly a large amount of HSCs in the liver of control mice, and vast majority of the HSCs exhibited an elongated filament morphology. In contrast, the density of HSCs in the liver of NEN-treated mice was apparently lower, and the morphology of the HSCs was still in round/oval shape indicating these cells were not activated. Quantification of the desmin-positive cells showed that the HSCs population increases to approximately 11% of total liver cells in control mice, while it is decreased significantly to ~5% in the NEN-treated mice (**Fig 6.3D**), which reaches to a normal level as it has been well documented that HSCs constitute 5-8% of the total liver cell population.[257, 258] In addition, the percentage of activated HSCs in total liver cells was dramatically reduced as well (**Fig 6.3E**).

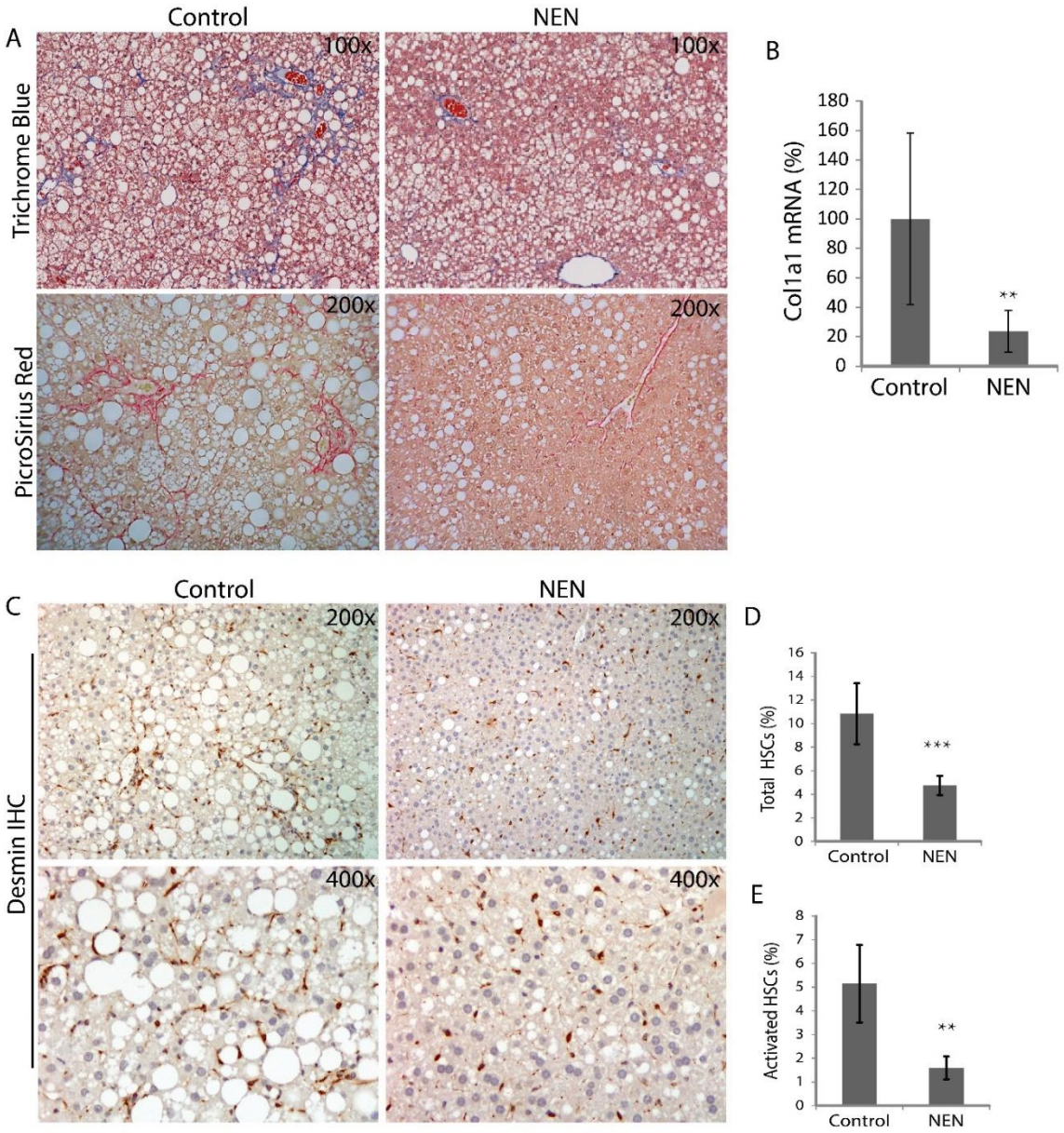

Figure 6. 3 Effect of NEN treatment on liver fibrosis and hepatic stellate cell (HSC) activation. (A) Representative liver sections stained with Trichrome Blue (upper panel) and PicroSirius Red (bottom panel). (B) Hepatic mRNA expression of Col 1a1. (C) Representative liver sections of Desmin immunohistochemical staining. (D) Quantification of total HSC population of total liver cells. (E) Quantification of activated HSC population of total liver cells. Control, the mice were fed on western diet for 8 months; NEN, the mice were fed on western diet containing 2,000

p.p.m. NEN for 8 months. *P < 0.05, **P < 0.01, ***P < 0.001. Statistical significance (P) was determined by Student's t test. All error bars, s.d.

3.4 NEN prevented and reversed CCl_4-induced fibrosis in mice

The inhibitory effect of NEN in HSCs activation suggests it may work directly to antagonize the formation of fibrosis. Therefore, we further tested NEN on the carbon tetrachloride (CCl_4) induced-fibrosis in mice. All the mice fed a chow diet with/without intraperitoneal injection of CCl_4, which causes damage to the liver without induction of steatosis. As shown in **Figure 6.4A**, CCl_4 induced perisinusoidal fibrosis and bridging fibrosis in the liver of control mice, which are more severe than that induced by Western Diet. NEN was given to mice at the beginning of CCl_4 injection, or after 2 weeks of CCl_4 injection. Although NEN is not supposed to prevent the damage induced by CCl_4 (**S. Fig 6.3**), NEN were effective to reduce the fibrosis in both cases. CCl_4 caused bile duct damage leading to biliary hyperplasia in control mice, which contributes to the formation of fibrosis as well. Clearly our results showed that NEN treatment reduced the formation of biliary hyperplasia (**Fig 6.4B**). In addition, NEN significantly reduced the accumulation of hemosiderin-laden macrophages in liver of CCl_4-treated mice (**Fig 6.4B**). Taken together, mitochondrial uncoupler NEN exhibited direct inhibitory effect on liver fibrosis, aside from the lipid depletion effect. Moreover, NEN are effective to prevent and reverse fibrosis.

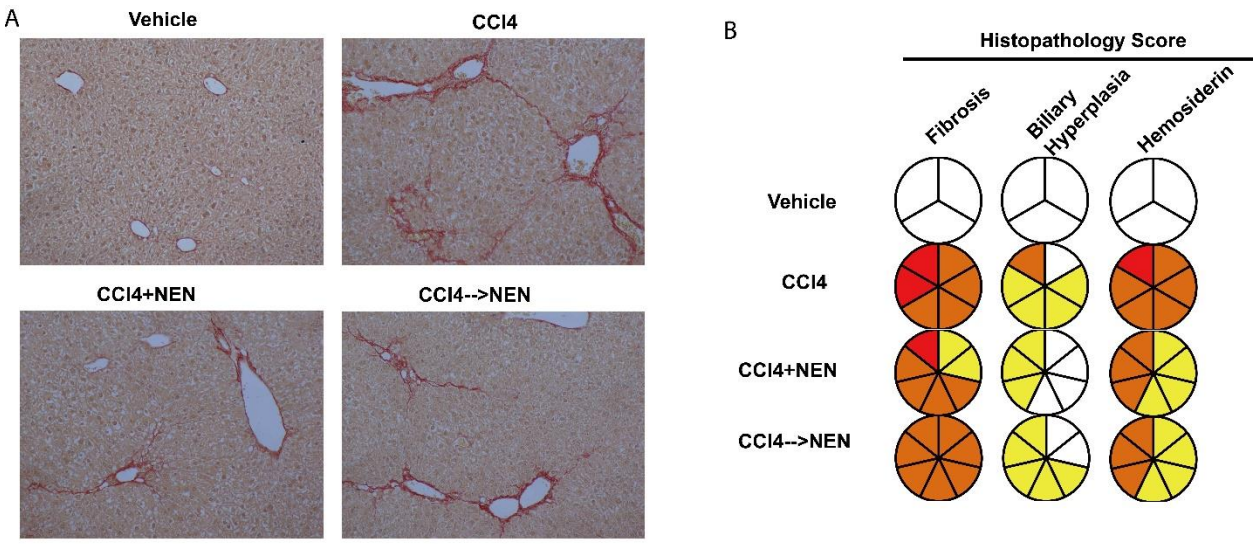

Figure 6. 4 Effect of NEN treatment on CCl4-induced fibrosis in mice. Liver fibrosis was manifested by Sirius red stain (A) and quantified by histopathology scoring (B). In the histopathology scoring system, white=0, yellow=1, brown=2, and red=3. Vehicle, mice received vehicle injection and chow diets for 6 weeks; CCl_4, mice with CCl_4 injection and chow diets for 6 weeks; CCl_4+NEN, mice with CCl_4 injection and chow diet containing 2,000 p.p.m NEN for 6 weeks; CCl_4→NEN, mice with CCl_4 injection for 6 weeks during which mice were fed chow diet for 2 weeks and switched to NEN chow diet for the rest of 4 weeks.

3.5 NEN inhibits HSC activation and antagonizes the PDGF and TGFβ signaling pathways in vitro

To further understand the functional mechanism of how NEN inhibited fibrosis, we further evaluated whether NEN could directly inhibit the activation of cultured HSC in vitro. Activation of HSCs, such as the human HSC cell line LX-2, can be triggered by TGFβ or PDGF treatment *in vitro*. The activated LX-2 cells presented the phenotypes resembling activated HSCs in vivo including cell amplification, contractile property and production of extracellular matrix. We then tested the effect of NEN on inhibiting the activation of LX-2 cells with TGFβ treatment. The experimental procedure was described as **Fig 6.5A**. The LX-2 cells exhibited a distinctive

"ring"-shape morphology after TGFβ treatment, exhibiting the contractile property of activated HSCs.[259] NEN treatment is effective to prevent this morphologic change of LX-2 cells with TGFβ treatment (**Fig 6.5B**). Quantitative-PCR analyses and western blotting analysis also confirmed that NEN treatment reduced the expression of Col1a1 and alpha smooth muscle actin (SMAα), which represent the major components of hepatic fibrosis in NASH (**Fig 6.5C- E**).

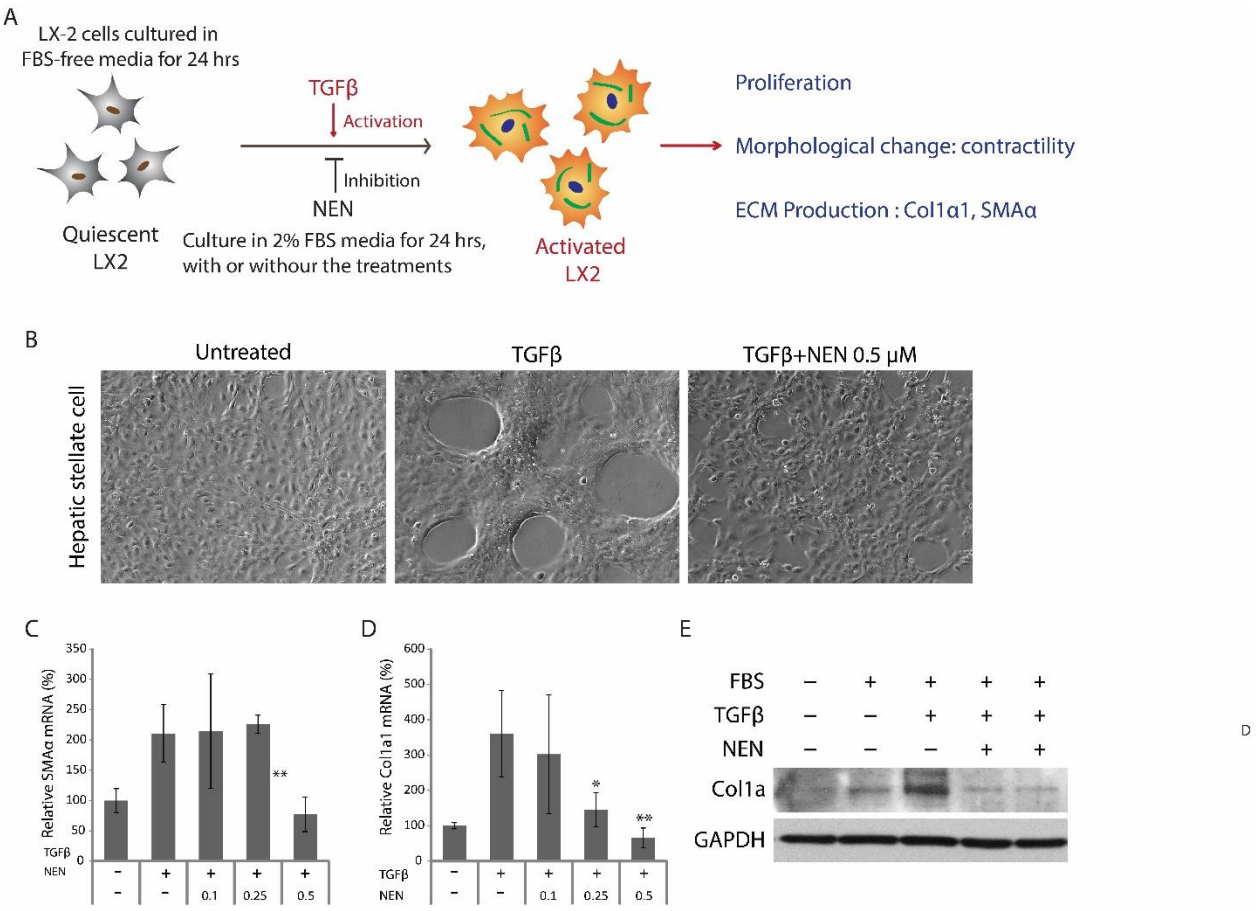

Figure 6. 5 Effect of NEN on TGFβ-induced human HSC LX-2 cell activation. (A) Schematic diagram of the experimental procedure. (B) Bright field images of LX-2 cell morphological change. (C) qPCR quantification of cellular SMAα expression. (D) qPCR quantification of cellular Col 1a1 expression. (E) Immunoblotting analysis of collagen I expression. *P < 0.05, **P < 0.01, ***P < 0.001. Statistical significance (P) was determined by Student's t test. All error bars, s.d.

Moreover, NEN treatment arrested the cell cycle progression of LX-2 cells induced by PDGF or TGFβ treatment. As shown by the cell cycle analyses (**Fig 6.6A**), either PDGF (**middle left**) or TGFβ (**bottom left**) treatment effectively induced proliferation of LX-2 cells as compared to the cells cultured in quiescent condition (**upper left**); while NEN treatment dramatically reduced the profile of dividing cells in the presence of PDGF or TGFβ treatment and induced G1 arrest (**middle and bottom right**). Consistently, metabolomics analysis showed that NEN treatment significantly reduced the ribose-phosphate (**Fig 6.6B**) and UTP (**Fig 6.6C**) contents in TGFβ-treated LX2 cells, suggesting NEN inhibited the generation of building blocks that are required for nucleotide biosynthesis.

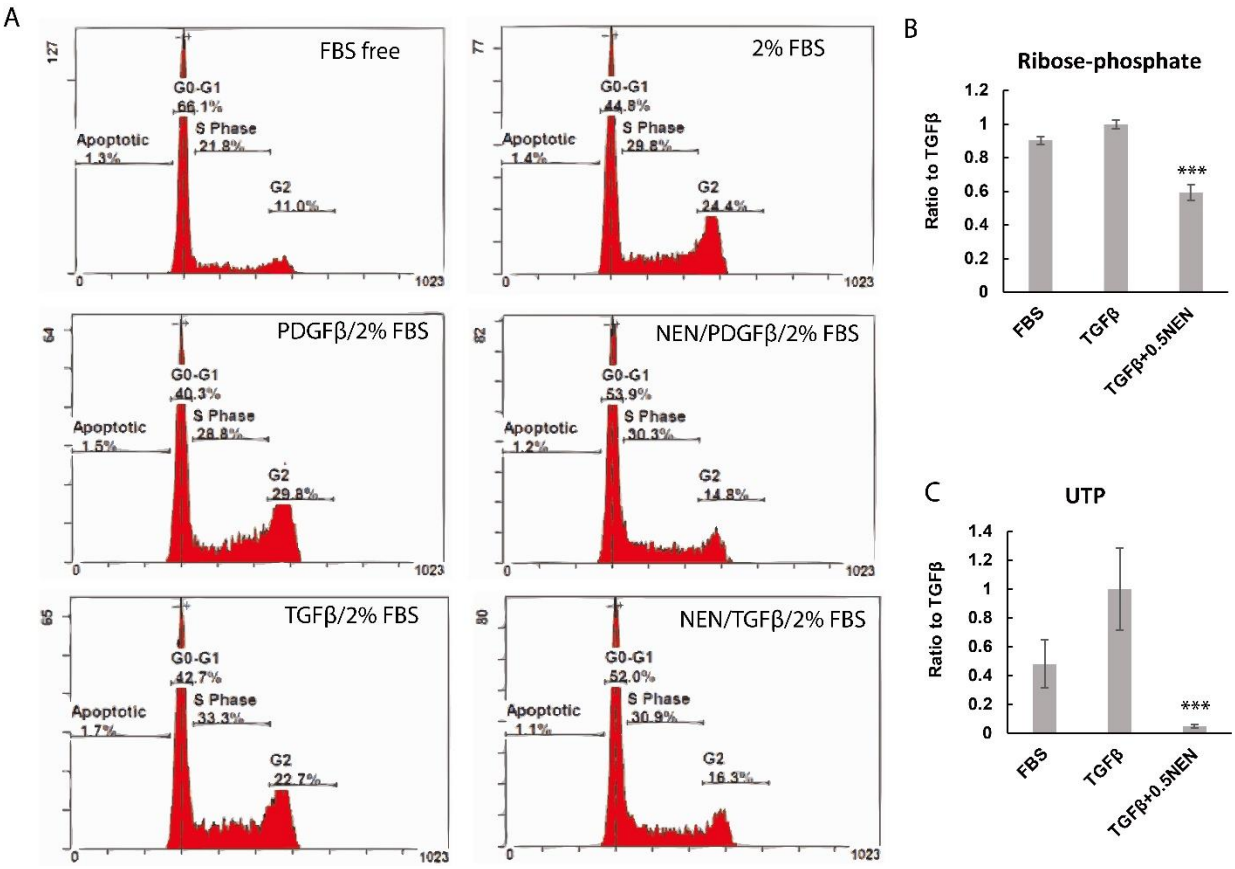

Figure 6. 6 Effect of NEN on TGFβ-induced human HSC LX-2 cell proliferation. (A) LX2 cells were cultured in FBS free condition for overnight and then switched to 2% FBS medium. Cells

were then incubated with TGFβ or PDGF in the presence or absence of NEN. (A) Effect of NEN on TGFβ or PDGF induced cell cycle progression. Quantification of intracellular ribose-phosphate (B) and UTP (C) in TGFβ-treated LX-2 cells with LC/MS/MS metabolomics studies. *P < 0.05, **P < 0.01, ***P < 0.001 compared to TGFβ alone group. Statistical significance (P) was determined by Student's t test. All error bars, s.d.

We further examined the effect of NEN on PDGF and TGFβ signaling. Firstly, NEN treatment downregulated the expression of the PDGF receptor (PDGFR) in the TGFβ-treated LX-2 cells (**Fig 6.7A**); consistently, the expressions of PDGFR were also reduced in the liver of NEN-treated mice as compared to control mice (**S Fig 6.2**). In cultured LX-2 cells, NEN was effective in inhibiting the phosphorylation of Smad2 in response to TGFβ, and the expressions of Smad 2/3 proteins were also reduced upon NEN treatment (**Fig 6.7A**). The Wnt signaling pathway, which is known to be induced downstream of TGFβ in HSCs activation, plays an important profibrotic and proinflammatory role in NASH[260]. Consistently, we found NEN induced downregulation of β-catenin expression in TGFβ-treated LX-2 cells, indicating an inhibitory effect on the Wnt pathway (**Fig 6.7A**). Glycine and proline are the two dominant amino acids present in collagen. Recent study demonstrated that de novo serine synthesis pathway contributes to the biosynthesis of glycine, which is required for TGFβ-induced collagen production [261]. We further determined the effect of NEN on the amino acids synthesis. Our results showed NEN treatment inhibited the biosynthesis of serine, glycine and proline (**Fig 6.7B-D**) and down-regulated mTOR signaling downstream effector, the ribosomal protein S6 kinase (p70S6K) (**Fig 6.7A**) in TGFb-treated LX-2 cells. The inhibition of protein synthesis is in line with the reduction in collagen expression (**Fig 6.5 D and E**). Recent studies revealed that AMPK activation is a negative relator of TGF-b signaling by inhibiting the phosphorylation of Smad2/3 and activating inhibitory Smad7 [262]. Our data showed that NEN-induced mitochondrial

uncoupling immediately induced AMP/ATP accumulation (**Figure 6.7F-H),** which directly activated AMPK (**Fig 6.7E**) and potentially down-regulated the TGF-β/Smad signaling.

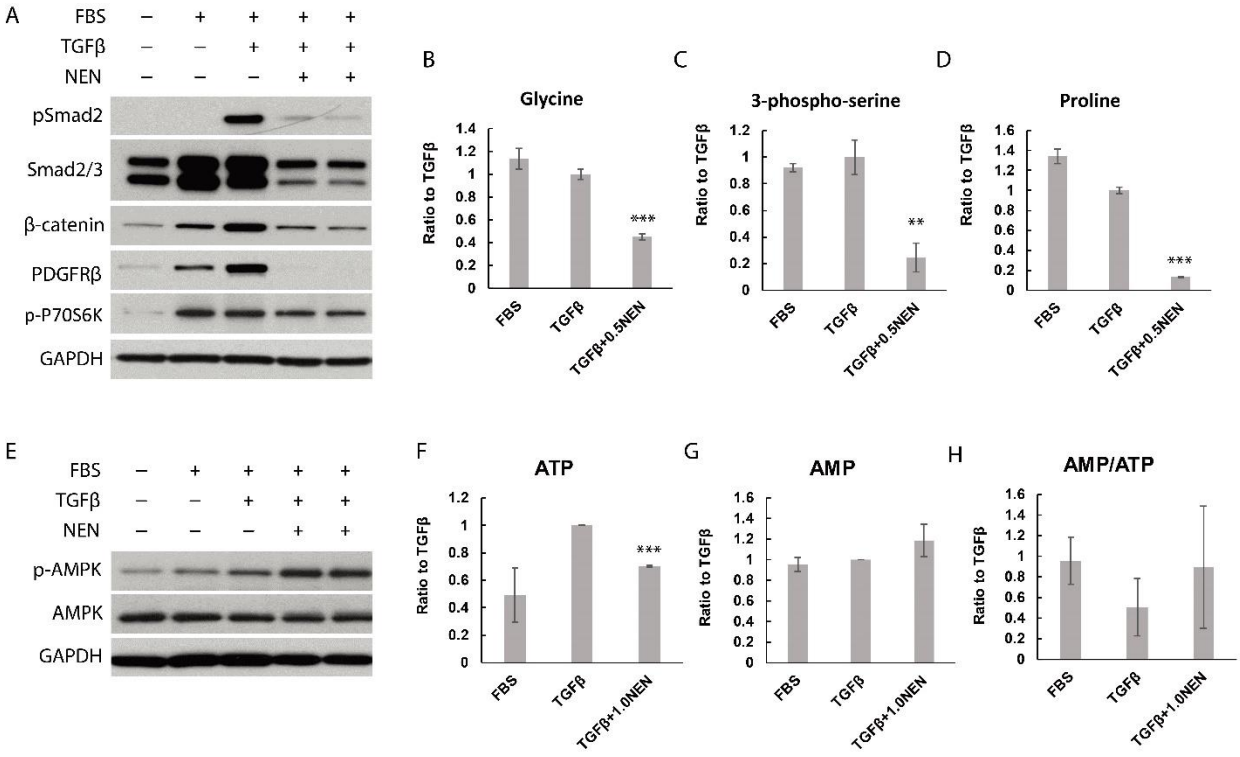

Figure 6. 7 Effect of NEN on PDGF and TGFβ signaling in TGFβ-treated human HSC LX-2 cells. Quiescent LX-2 cells were treated with TGFβ in the presence of absence of NEN for 24 hours or 30 min (ATP and AMP were quantified after 30min-treatment). (A) Immunoblotting analysis of downstream effectors of PDGF and TGFβ signaling. Quantification of intracellular amino acids required for collagen production, including (B) glycine, (C) 3-phospho-serine, and (D) proline with metabolomics studies. (E) Immunoblotting analysis of TGFβ-induced AMPK activation. Quantification of intracellular (F)ATP, (G) AMP, and (H) AMP/ATP with metabolomics studies. *P < 0.05, **P < 0.01, ***P < 0.001 compared to TGFβ alone group. Statistical significance (P) was determined by Student's t test. All error bars, s.d.

4. Conclusion

Our results support that NEN is effective in ameliorating high-fat and high-cholesterol diet induced NASH symptoms, including steatosis, inflammation and fibrosis. Moreover, NEN treatment directly reversed the CCl_4-induced bridging fibrosis. The mechanistic characterizations support that NEN may impact on NASH through two mechanisms. First, NEN uncouples mitochondria in hepatocytes, increasing lipid oxidation, reducing ectopic lipid accumulation and thus liver damage. Second, NEN has a direct effect on inhibiting HSC activation. It antagonizes TGFβ and PDGF signaling pathways. The impact of NEN on hepatic lipid metabolism and steatosis can be well explained by inducing mitochondrial uncoupling in hepatocytes with the treatment of oral NEN. Current research is ongoing to elucidate the mechanism underlying the effect of NEN on HSC activation. Our preliminary metabolomic studies support that NEN uncouples mitochondria of stellate cells, leading to AMP/ATP accumulation, which directly induces AMPK activation. AMPK cross talk with TGF and PDGF signaling, thus inhibiting proliferation and transdifferentiation of HSCs. Activated HSCs is the major source of extracellular matrix production. The reduction in activated HSCs population directly ameliorates the fibril deposition.

The reduction and reversal of fibrosis is the competitive feature and hurdle in the NASH drug development. NEN-induced mitochondrial uncoupling provides an effective approach to treat fibrosis and other major symptoms in NASH, suggesting the therapeutic potential of mitochondrial uncoupling strategy to treat NASH.

In summary, our work demonstrated that safe mitochondrial uncoupler is an effective pharmacotherapy to treat NASH with a novel mechanism.

Supplementary Figures

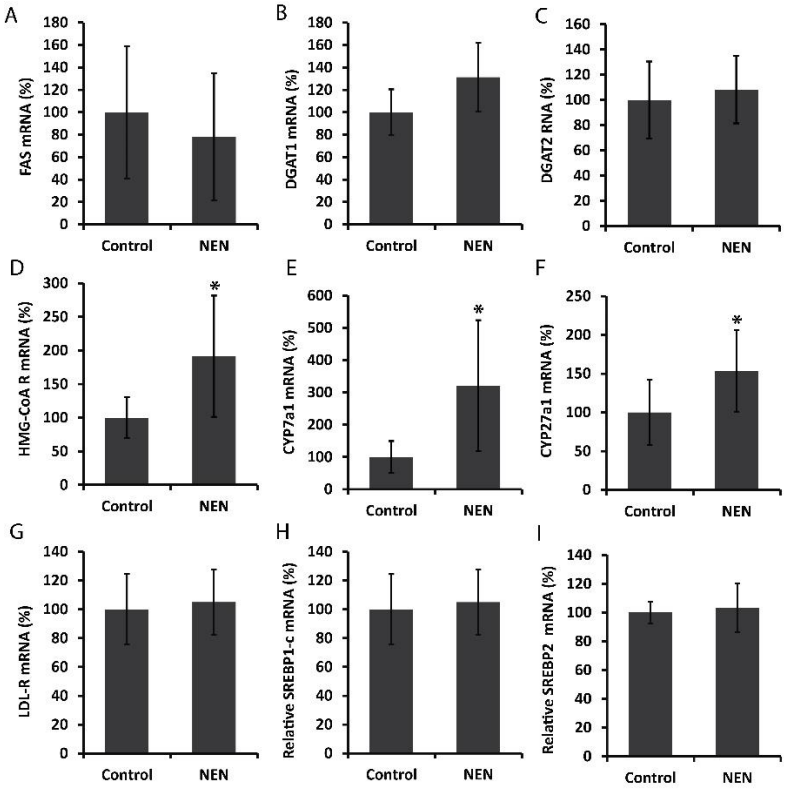

Supplementary Figure 6. 1 Effect of NEN on metabolic genes expression in liver. Control, the mice were fed on western diet for 8 months; NEN, the mice were fed on western diet containing 2,000 p.p.m. NEN for 8 months. *P < 0.05, **P < 0.01, ***P < 0.001 compared to control. Statistical significance (P) was determined by Student's t test. All error bars, s.d.

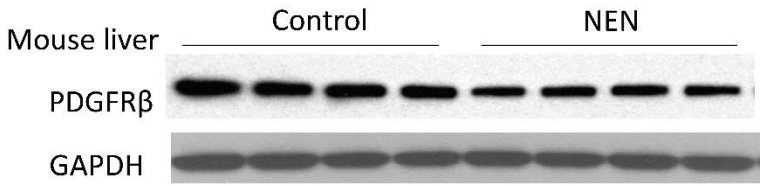

Supplementary Figure 6. 2 Effect of NEN on hepatic PDGFRβ expression in mice. Control, the mice were fed on western diet for 8 months; NEN, the mice were fed on western diet containing 2,000 p.p.m. NEN for 8 months. *P < 0.05, **P < 0.01, ***P < 0.001 compared to control. Statistical significance (P) was determined by Student's t test. All error bars, s.d.

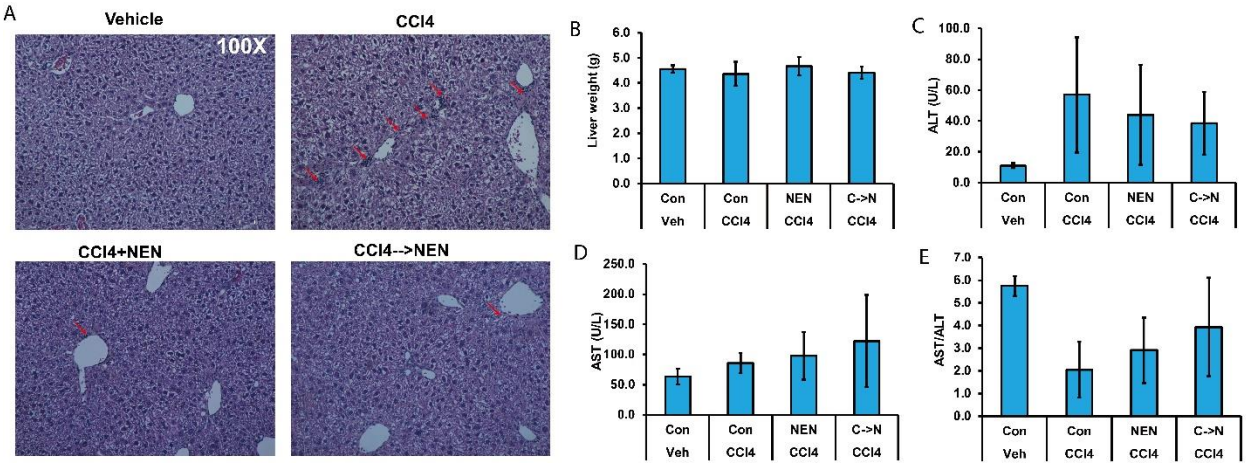

Supplementary Figure 6. 3 Effect of NEN on liver damage and inflammation in CCl4-induced fibrosis mouse model. Vehicle, mice received vehicle injection and chow diets for 6 weeks; CCl4, mice with CCl4 injection and chow diets for 6 weeks; CCl4+NEN, mice with CCl4 injection and chow diet containing 2,000 p.p.m NEN for 6 weeks; CCl4→NEN, mice with CCl4 injection for 6 weeks during which mice were fed chow diet for 2 weeks and switched to NEN chow diet for the rest of 4 weeks.

Chapter VII. Determine the effect of safe mitochondrial uncoupler on treating hepatic lipid accumulation caused by genetic mutation

The work of Chapter VII has been submitted to Journal of Pharmacology and Experimental Therapeutics in the title of 'Mitochondrial uncoupler niclosamide ethanolamine in treating lysosomal acid lipase deficiency in mice'.

Mitochondrial uncoupler niclosamide ethanolamine in treating lysosomal acid lipase deficiency in mice

Jingjing Guo[1,2†], Hanlin Tao[1†], Amer Alasadi[1], Juan Collantes[1], Cong Yan[3], Hong Du[3], Qingrong Huang[2], Shengkan Jin[1]*

[1]Department of Pharmacology, Rutgers University-Robert Wood Johnson Medical School, Piscataway, New Jersey (J.G., H.T., A.A., J.C. and S.J.); [2]Department of Food Science, Rutgers University, New Brunswick, New Jersey (J.G. and Q.H.); and [3]Department of Pathology and Medicine Laboratory, Indiana University, Indianapolis, Indiana (H.D. and C.Y.)

*Corresponding Author: victor.jin@rutgers.edu

Abstract

Lysosomal acid lipase deficiency (LAL-D) is an autosomal recessive disease caused by *LIPA* gene mutations and consequent loss of LAL activity, resulting in massive accumulation of triglycerides and cholesterol esters in the lysosomes of liver, spleen and other organs. Hepatosplenomegaly, progressive liver impairment and lipid abnormalities are common presentations in LAL-D patients. Niclosamide is a FDA-approved anthelmintic drug, with the mechanism of action of inducing mitochondrial uncoupling in parasitic worms. We previously showed that the ethanolamine salt form of niclosamide (NEN) uncouples mammalian

mitochondria. Oral treatment with NEN effectively reduces hepatic lipid accumulation in mice by increasing β- oxidation and decreasing lipid synthesis. Here we investigated if NEN is efficacious for treating LAL-D, using a lysosomal acid lipase deficient (*lal-/-)* mouse model. We showed that NEN markedly improves hepatosplenomegaly in *lal-/-* mice. Moreover, NEN reduces the levels of plasma alanine transaminase and aspartate transaminase, indicating decrease in liver damage. Importantly, NEN treatment dramatically increases the lifespans of the *lal-/-* mice. The beneficial effect of NEN is associated with a reduction in hepatic apolipoprotein B-containing very low density lipoprotein (VLDL) production and a lower plasma VLDL/low density lipoprotein (LDL) cholesterol level. Together, our data support a novel strategy for treating LAL-D and identified a prototype experimental drug NEN for further investigation.

1. Introduction

Lysosomal acid lipase (LAL), encoded by *LIPA* gene, is an essential enzyme responsible for the hydrolysis of cholesterol esters (CE) and triglycerides (TG) into free cholesterol and fatty acids in lysosome [263]. Lysosomal acid lipase deficiency (LAL-D) is a rare autosomal recessive lysosomal storage disease resulting from the mutations of *LIPA* gene [264]. It is estimated that the prevalence of LAL in general population is around 1/130000 [265]. The loss of LAL activity causes sequestration of CE and TG in lysosome, resulting in pronounced lipids accumulation in multiple organs including liver, spleen and small intestine [82]. Hepatomegaly, progressive liver damage and dyslipidemia are the most important symptoms in the clinical course of LAL-D [265, 266], which may lead to liver fibrosis, cirrhosis, atherosclerosis and cardiovascular diseases in a large proportion of the LAL-D patients [267, 268]. The resultant premature morbidity and mortality calls for early diagnosis and efficacious therapy.

For the disease management, sebelipase alfa (a recombinant form of human LAL enzyme) was recently approved by FDA as enzyme replacement therapy for LAL-D [269].

However, hypersensitivity reactions including anaphylaxis have been reported in enzyme-treated patients [90, 91]. Alternative or complementary therapies for LAL-D are therefore still in demand. Currently several lipid-lowering drugs are clinically used for treating LAL-D [265-267, 270], among which the statins are the most commonly used. Statins reduced plasma LDL-cholesterol in LAL-D patients but their efficacy on LAL-D remains unclear [266], as progressive liver damage or even liver failure in LAL-D patients are not affected by statin treatment [82, 92, 264].

Mitochondrial uncoupling allows proton gradient bypassing ATP synthase across the inner membrane of mitochondria [120]. The proton leakage results in lower energy efficiency and elevated lipid oxidation [271]. Our previous study showed that niclosamide ethanolamine (NEN), a salt form of niclsoamide (an FDA approved anthelmintic drug), is a mitochondrial uncoupler primarily targeting liver [140]. In mice, NEN was shown to be efficacious to deplete hepatic lipid accumulation, which results in significant improvement in hepatic steatosis, insulin resistance, glycemic control [140] and diabetic dyslipidemia symptoms (data not published). The striking efficacy of NEN in reducing lipid accumulation in liver as well as its excellent safe profile prompted us to evaluate its potential for treating LAL-D. *Lal* -/- mouse is a well-characterized model in which LAL activity is totally absent by targeted disruption of the mouse lysosomal acid gene [272]. The model closely recapitulates LAL-D clinical symptoms including hepatosplenomagly, progressive liver damage and hypercholesterolemia [273, 274]. Here we investigate the effectiveness of NEN for treating LAL-D in *lal-/-* mice.

2. Material and Methods

2.1 Chemicals and reagents

Niclosamide ethanolamine was from 2A PharmaChem (Lisle, IL). Antibodies including Ran polyclonal antibody (pAb), Actin pAb and Apolipoprotein B pAb were from Santa Cruz

Biotechnology (Dallas, TX); LDL-receptor mAb was from Abcam (Cambridge, MA). Medium Essential Medium (MEM), trypsin, penicillin and streptomycin were purchased from ThermoFischer Scientific. Fetal bovine serum was from Atlanta Biologicals Inc. (Flowery Branch, GA).

2.2 Animals and treatment

The *lal*+/+ and *lal*-/- mice were generated from *lal*+/- breeding stock on FVB/N background which were generated by the laboratory of Dr. Hong Du [272, 273]. The litters were weaned and genotyped at the age of 19-21 days, according to the methods developed by Dr. Du's lab. Mice were maintained in the temperature/moisture controlled room with 12h light/dark cycle in the vivarium of Rutgers-Robert Wood Johnson Medical School. All the experimental protocols were approved by Institutional Animal Care and Use Committees (IACUCs). For four-week treatment study, starting from 3 weeks of age, *lal*-/- mice were randomized into two groups based on body weight, each containing 7 males and 6 females. One group of mice were fed AIN-93M diet, the other group fed AIN-93M diet containing 2,000 p.p.m. NEN, for 4 weeks. In the same period, age-matched *lal*+/+ mice (5 males and 3 females) were fed AIN-93M diet alone. Food and water were given ad libitum throughout the experiment period. Body weight was monitored weekly and daily food intake was recorded in week 2 and week 4.

For longevity study, four *lal*-/- mice (2 males and 2 females) in control group were fed AIN-93M diet, and five *lal*-/- mice (1 male and 4 females) in NEN-treated group fed AIN-93M diet containing 2,000 p.p.m. NEN.

2.3 Plasma and liver biochemical analysis

Plasma triglycerides (TG), total cholesterol (TC), nonesterified fatty acid (NEFA), alanine transaminase (ALT), aspartate transaminase (AST), hepatic TG, hepatic TC and hepatic NEFA were analyzed by the Metabolic Core of U.S. National Mouse Metabolic Phenotyping

Center (MMPC) at the University of California-Davis.The plasma samples were collected after 5-hour fast. The liver samples were dissected and froze in liquid nitrogen immediately.

2.4 Immunoblotting analyses

Protein extraction and immunoblotting analyses were performed according to the protocol described previously. Briefly here, tissue or cells were homogenized with lysis buffer containing 10mM TRIS-HCl (pH 7.9), 10% glycerol, 0.1mM EDTA, 100mM KCl, 0.2% NP-40, 0.5mM PMSF, 1mM DTT and mini-complete protease inhibitor cocktail (Roche Diagnostics, Indianapolis, IN, USA). Lysates were then syringed with 26 gauge ½ inch needles on ice. Supernatants collected from micro-centrifuge (12,000 rpm for 15 min at 4°C) were subjected to SDS polyacrylamide gel electrophoresis (SDS-PAGE). Proteins were then transferred to polyvinylidene difluoride (PVDF) membranes (Millipore, Belgium) for overnight. All primary and secondary antibodies were used as 1:1,000 dilutions. Chemiluminescent detection was completed with ECL western blotting reagents (Amersham, Buckinghamshire, UK). Quantification of protein level was determined by measuring band intensity using ImageJ software and calculating the ratio of protein of interest to an internal loading control.

2.5 Cell culture and cellular Apolipoprotein B (ApoB) secretion assay

HepG2 cells were plated in 6-well plate and cultured to 100% confluence in Medium Essential Medium (MEM) containing 1.0 g/L glucose, 10% (vol/vol) fetal bovine serum, 100 U/mL of penicillin, 100 µg/mL of streptomycin and 0.29 mg/mL of L-glutamine at 37°C in a humidified atmosphere of 5% CO_2. For ApoB secretion assay, cells were incubated with NEN (0.1 µM, 0.5µM, 1.0µM), or insulin (100nM) for 24 hours. At the end of treatment, culture medium was collected, adjusted to 0.1% EDTA, and centrifuged at 1,500 rpm for 10min at 4°C to remove cell debris. The supernatant fraction was then subjected to immunoblotting for the

determination of net secretion of ApoB into media. NEN was dissolved in DMSO as stock solutions and added to medium to reach final designated concentrations by 1:1,000 dilutions.

2.6 Statistics

Data are presented as the mean ± standard deviation (SD). One-way ANOVA was used for all of the statistical comparisons among groups. Statistical significance is denoted. Survival curves were compared by log-rank test using an online application for survival analysis (OASIS2) [275].

3. Result

3.1 NEN treatment ameliorates hepatosplenomegaly in *lal-/-* mice

Lal-/- mice spontaneously develop progressive enlargement of liver and spleen regardless of calorie challenge. At the age of 7 weeks, the average liver mass of *lal-/-* mice compared to *lal+/+* mice was 2.3 fold higher (**Figure 7.1A**), which represents 11% of body weight of *lal-/-* mice (data not shown). The average spleen weight of *lal-/-* mice was 2.6 fold over that of *lal+/+* mice (**Figure 7.1B**). In contrast, treatment with NEN for 4 weeks significantly decreased the weight of liver and spleen by 18% and 36% in *lal-/-* mice (**Figure 7.1A and B**), respectively. The average body weight and food consumption were not significantly different despite of genotype and treatment (**Figure 7.1G and H**). Thus, NEN treatment effectively ameliorates the abnormal enlargement of liver and spleen and slows down the progression in *lal-/-* mice.

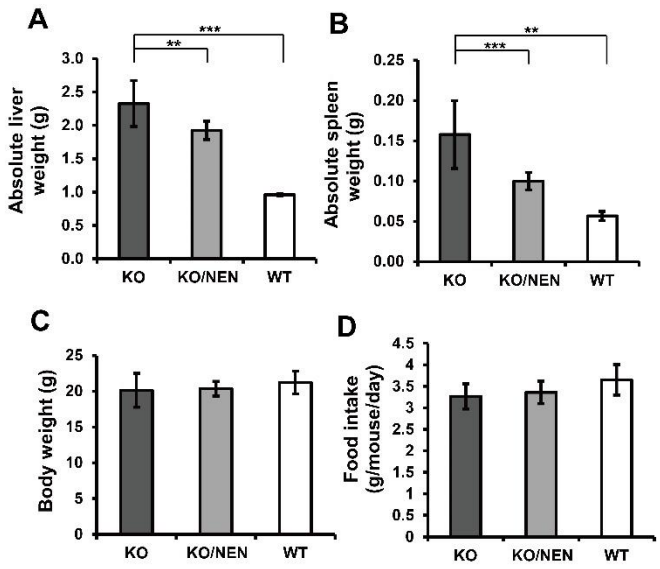

Figure 7. 1 Oral treatment of NEN reduced hepatosplenomegaly. (A) Liver weight, (B) spleen weight, (C) body weight, and (D) daily food intake of lal-/- or lal+/+ mice under various feeding conditions. Starting at 21 days of age, lal-/- mice were fed AIN-93M diet (KO) or AIN-93M diet containing 2,000 p.p.m. NEN (KO/NEN) and matching lal+/+ mice (WT) were fed AIN-93M diet alone for 4 weeks. Data are presented as mean ± SD (n = 13 including 7 males and 6 females in KO and KO/NEN, respectively, n=8 including 5 males and 3 females in WT). Games-Howell post-hoc test was used for statistical comparisons between KO and KO/NEN, and KO and WT group. (∗) $P < 0.05$, (∗∗) $P < 0.01$, and (∗∗∗) $P < 0.001$ denote significant difference; all error bars, SD.

3.2 NEN treatment reduces liver damage in *lal-/-* mice

The abnormal accumulation of CE and TG in the liver of *lal-/-* mouse results in hepatomegaly and remarkable liver damage. By promoting hepatic lipid catabolism, NEN treatment has been shown to effectively reduce hepatic lipid accumulation in HFD-induced obese mouse models [140]. We quantified hepatic triglycerides and cholesterol content. As shown in **Figure 7.2A and B,** NEN treatment has a tendency of reducing hepatic triglyceride and total

cholesterol (although there is no statistical significance, P=0.10 for both). We further measured plasma ALT and AST level in *lal-/-* mice (**Figure 7.2C and D**). NEN treatment significantly reduced ALT and AST levels, indicating a decrease of hepatic damage.

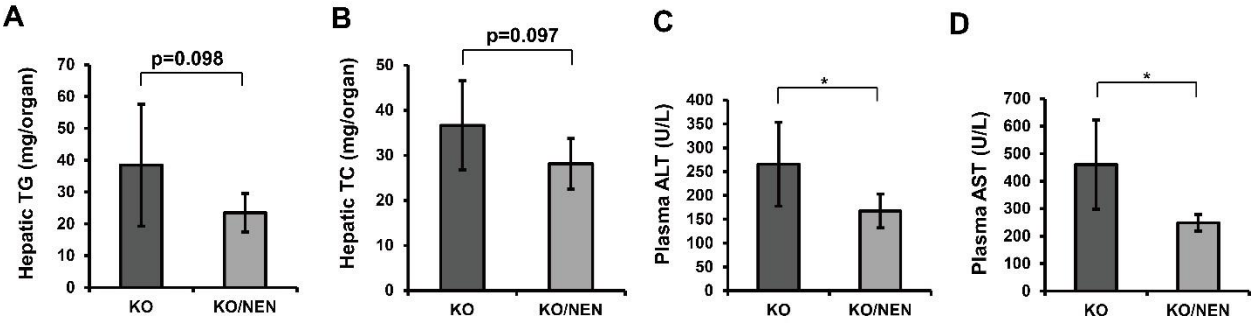

Figure 7. 2 Oral treatment of NEN reduced liver damage and hepatic lipid content. (A) Hepatic total triglycerides content (TG), (B) hepatic cholesterol content (TC), (C) plasma ALT, and (D) plasma AST of lal-/- mice fed AIN-93M diet (KO) or AIN-93M diet containing 2,000 p.p.m. NEN (KO/NEN) for 4 weeks starting from 21 days of age. Data are presented as the mean ± SD (n = 6). Student's t test was used for statistical comparisons among groups. (*) $P < 0.05$, (**) $P < 0.01$, and (***) $P < 0.001$ denote significant difference between lal-/- mice with and without NEN treatment; all error bars, SD.

3.3 NEN treatment reduces plasma very low density lipoprotein/low density lipoprotein (VLDL/LDL) cholesterol in *lal-/-* mice

The *lal-/-* mice exhibited elevated levels of VLDL- and LDL-cholesterol (VLDL/LDL-C) and lower levels of HDL-cholesterol (HDL-C) relative to *lal+/+* counterparts [273]. As shown in **Figure 7.3A**, NEN treatment significantly reduced plasma VLDL/LDL-C in *lal-/-* mice. There is no significant change in plasma HDL-C levels between NEN treated and non-treated *lal-/-* mice (**Figure 7.3B**). The plasma total cholesterol (TC) levels of *lal-/-* mice treated with NEN were slightly lower than the non-treated *lal-/-* mice (**Figure 7.3C**), which resulted from the lower fraction of VLDL/LDL cholesterol (the HDL cholesterol levels were slightly higher in NEN

treated group). As shown in **Figure 7.3D and E**, no significant difference in plasma TG and NEFA was observed between the NEN treated and non-treated *lal-/-* mice.

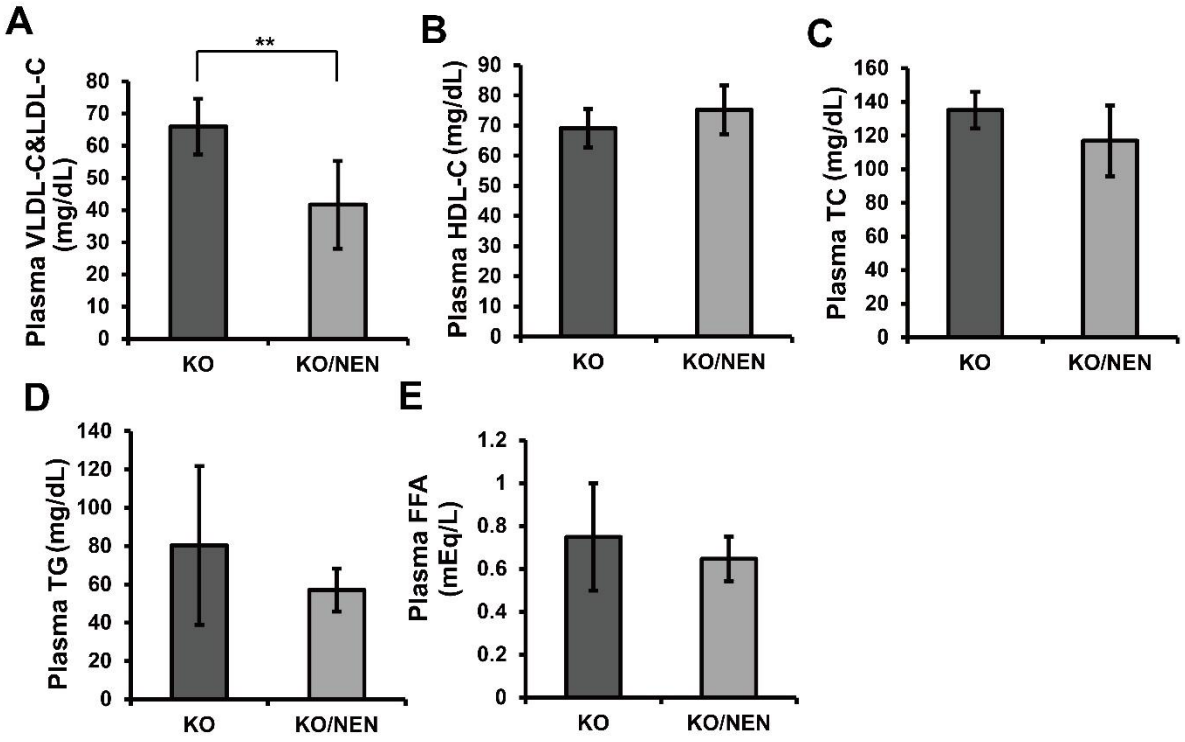

Figure 7. 3 Oral treatment of NEN improved plasma lipid profile. (A) Plasma VLDL&LDL cholesterol (VLDL&LDL-C), (B) plasma HDL-cholesterol (HDL-C), (C) plasma total cholesterol (TC), (D) plasma triglycerides (TG) and (E) plasma non-esterified fatty acids (FFA) of lal-/- mice fed AIN-93M diet (KO) or AIN-93M diet containing 2,000 p.p.m. NEN (KO/NEN) for 4 weeks starting from 21 days of age. Data are presented as the mean value ± SD (n = 6). Student's t test was used for statistical comparisons among groups. (*) $P < 0.05$, (**) $P < 0.01$, and (***) $P < 0.001$ denote significant difference between lal-/- mice with and without NEN treatment; all error bars, SD.

3.4 NEN treatment prolongs the lifespan of *lal-/-* mice

The disease of LAL-D dramatically reduces the lifespan of *lal-/-* mice [273]. We then measured the impact of NEN on the overall health of *lal-/-* mice by measuring the lifespan. As

shown in **Figure 7.4**, NEN treatment markedly reduced the mortality of *lal-/-* mice ($p<0.0027$, Log- Rank test). The median and maximal lifespan of the non-treated *lal-/-* mice were 259 and 308 days respectively, while the median and maximal lifespan of NEN treated *lal-/-* mice were 469 and 489 days, respectively. The results support that NEN dramatically improves the overall health of *lal-/-* mice and is efficacious for treating LAL-D.

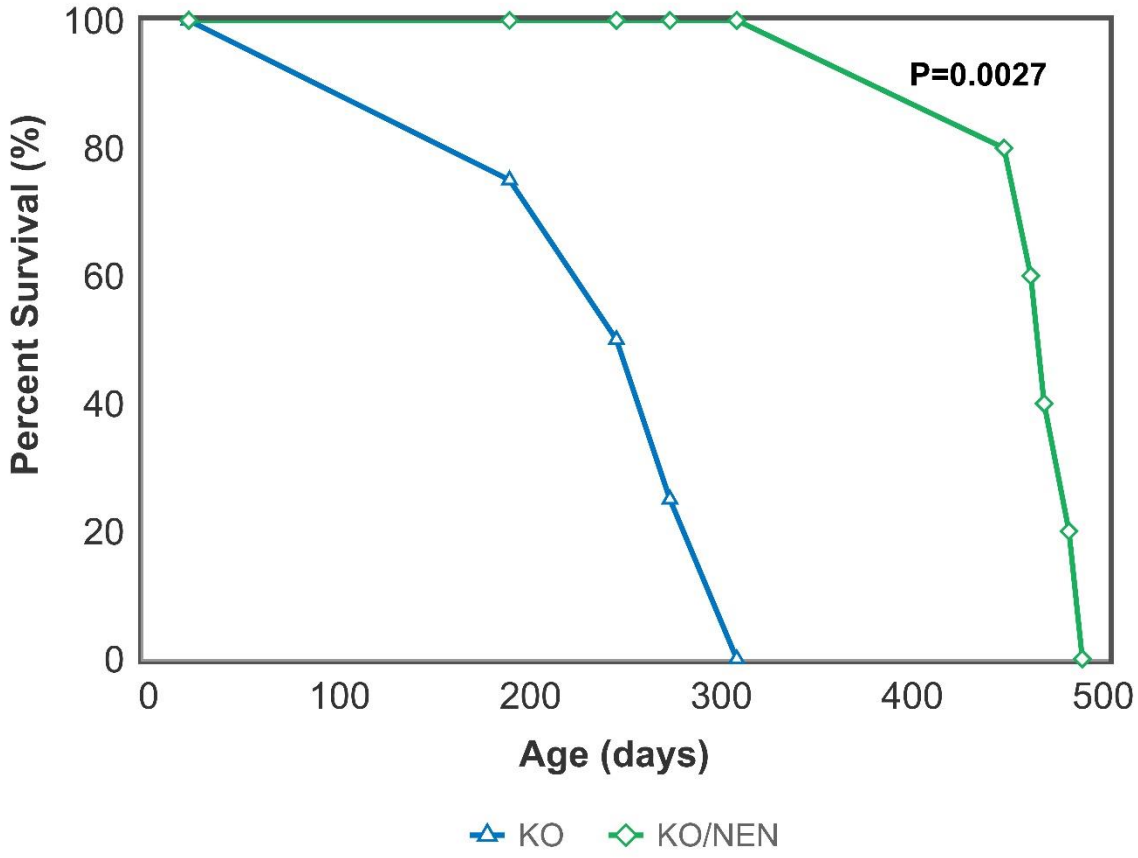

Figure 7. 4 NEN extended the lifespan of lal-/- mice. Starting at 21 days of age, lal-/- were fed AIN-93M diet (KO, n=4) or AIN-93M diet containing 2,000 p.p.m. NEN (KO/NEN, n=5). Survival curves were made and compared by log-rank test using an online application for survival analysis (OASIS2).

3.5 The effect of NEN is associated with reduction in hepatic VLDL/LDL production and secretion

Previous studies demonstrated that NEN reduces hepatic lipid accumulation by inducing mitochondrial uncoupling and consequent increasing lipid oxidation and decreasing lipid synthesis [140]. To understand how NEN affects plasma lipids, we performed cellular apolipoproteinB (ApoB-100) secretion assay in human liver carcinoma HepG2 cells. We found that NEN reduced ApoB-100 net secretion into medium in a dose-dependent manner, starting at the dose of 0.1µM (**Figure 7.5A**). In *lal-/-* mice, the hepatic apoB-100 content is significantly lower (**Figure 7.5B and C**) in NEN-treated group compared to the non-treated one, which could contribute to the lower level of circulating VLDL and LDL (**Figure 7.3A**).

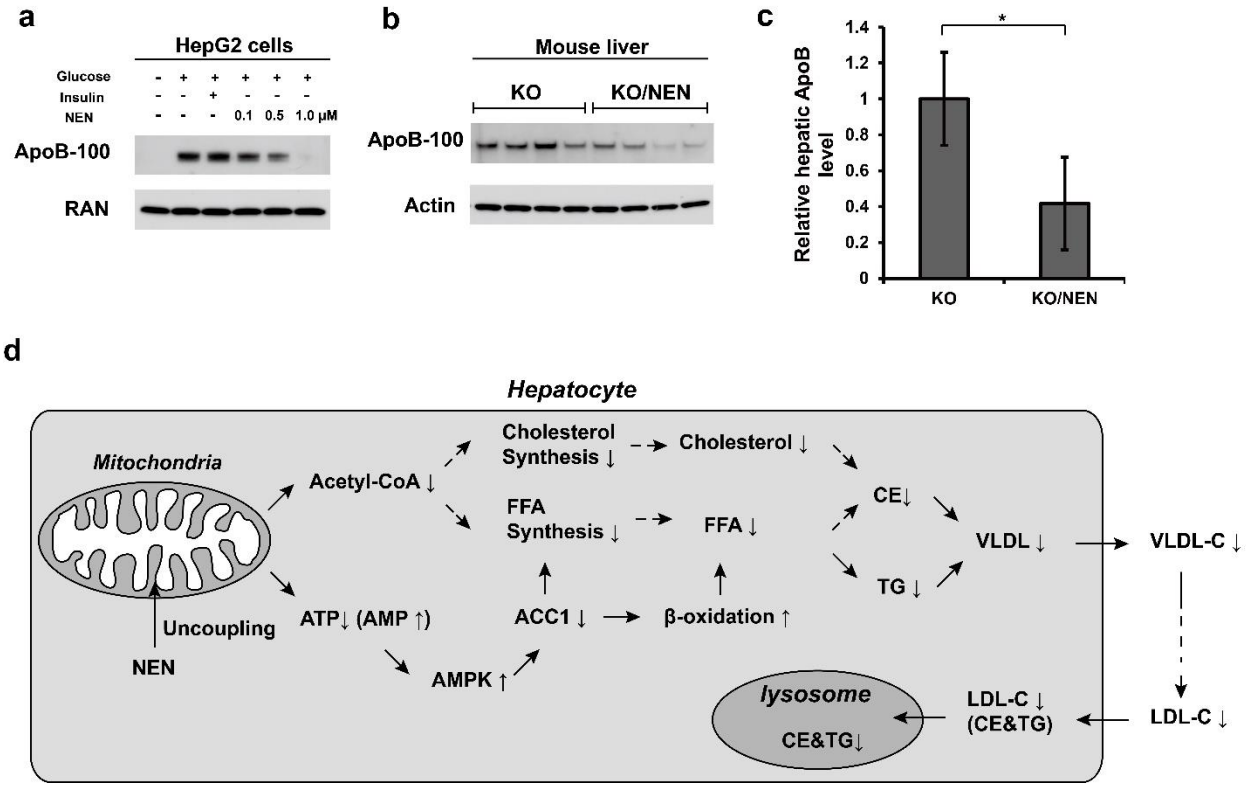

Figure 7. 5 NEN reduced apoB-100 secretion from HepG2 cells and liver. (A) Immunoblot analyses of apoB-100 secreted from HepG2 cells treated with insulin (100ng/mL), 0.1µM NEN,

0.5μM NEN, or 1.0μM NEN in the absence or presence of 1.0g/L glucose, as indicated, for 24 hours. (B) Immunoblot analyses of hepatic apoB-100 in lal-/- mice fed AIN-93M diet (KO) or AIN-93M diet containing 2,000 p.p.m. NEN (KO/NEN) for 4 weeks starting from 21 days of age. (C) Quantification of relative hepatic apoB-100 level. (D) Schematics of mechanism of action of NEN in liver, Acetyl-CoA carboxylase (ACC), Free fatty acid (FFA), Triglyceride (TG), Cholesterol ester (CE).

4. Discussion

In LAL deficiency patients, loss of LAL activity due to *LIPA* gene mutations causes sequestration of TG and CE in liver lysosomes. The ectopic lipid accumulation results in progressive liver enlargement and liver cell death, which further leads to inflammation, fibrosis, liver failure or even death in affected individuals. In addition to hepatomegaly and liver damage, LAL-D causes significant increase in *de novo* synthesis of CE and TG in liver due to reduced release of free fatty acids and free cholesterols from lysosomal lipid hydrolysis [274]. This leads to elevated output of VLDL particles from liver, not only resulting in hypercholesterolemia symptom but also exacerbating the liver symptoms in LAL-D. As ectopic lipid accumulation in liver is the causal factor of the pathogenesis and various symptoms of LAL-D, dissipating hepatic lipid accumulation could be an efficacious treatment strategy. Mitochondrial uncoupling is an effective approach for treatment of hepatic steatosis [133, 140, 276, 277]. NEN induces mitochondrial uncoupling in liver and consequently almost depletes hepatic steatosis in mice [140]. In current study, we examined whether NEN is effective in treating LAL-D using the *lal-/-* mouse model. The results showed that NEN treatment significantly reduced liver weight as well as lowered the levels of ALT and AST in *lal-/-* mice, indicating the effectiveness of NEN treatment in reducing liver damage in LAL-D. Meanwhile, NEN treatment reduces plasma VLDL/LDL-C, suggesting NEN is efficacious to improve lipid abnormalities in *lal-/-* mice. Most

strikingly, we found long-term treatment of NEN significantly reduces the mortality of *lal-/-* mice, supporting that NEN improves overall health condition of LAL-D.

Lal-/- mouse model was created by disrupting of the *LIPA* gene, resulting in total disappearance of LAL mRNA, protein or enzyme activity. The pathogenesis and phenotypes of *lal-/-* mice recapitulates those in LAL-D, which makes *lal-/-* mouse a clinical relevant model for drug development of treating LAL-D. *Lal-/-* mouse model has been used for preclinical analysis of recombinant human LAL for treating LAL-D [278-281], which laid the foundation for subsequent clinical trials and development. The efficacy of NEN demonstrated in *lal-/-* mice in current study therefore strongly supports the potential of NEN for treating LAL-D.

Recent progress in the understanding of molecular mechanism underlying the pathogenesis of LAL-D includes the upregulation of SREBPs-mediated cholesterol synthesis and fatty acid synthesis due to compromised feedback inhibition of cholesterol and fatty acid released from lysosomes, and increased hepatic secretion of ApoB-containing VLDL particles [87, 266]. The detail molecular mechanism by which NEN improves LAL-D symptoms was not fully examined in our study. Our data support a working model shown in **Figure 5D**. By uncoupling mitochondria, NEN increases the oxidation of acetyl-CoA, the substrate for synthesis of cholesterol and fatty acid, which lowers the level of newly synthesized cytosolic cholesterol esters and triglycerides in the hepatocytes [140]. Meanwhile, NEN-induced mitochondrial uncoupling reduces ATP production and increases AMP/ATP ratio, which activates AMPK-ACC pathway. Phosphorylation of ACC by activated AMPK reduces fatty acid synthesis and elevates fatty acid catabolism through beta-oxidation, which further contributes to the lower synthesis of TG and CE in the liver [140]. In addition, the results show that NEN treatment markedly reduced hepatic ApoB level and plasma VLDL/LDL-C level in *lal-/-* mice and lowered the net secretion of ApoB from HepG2 cells. It is most likely that NEN improves the hypercholesterolemia symptoms in *lal-/-* mice by lowering production of ApoB-containing plasma VLDL from liver.

And the lower circulating VLDL-C leads to lower amount of LDL-C delivered back to lysosomes of liver, which ameliorates the ectopic lipids accumulation in lysosomes and slows down the liver damage in *lal-/-* mice. The action on reducing the production of VLDL particles were also proposed in the treatment of *lal-/-* mice with cholesterol esterification inhibitor [282] or intestinal cholesterol absorption inhibitor [283].

NEN is a safe mitochondrial uncoupler with documented safety profile. The oral LD_{50} of NEN is similar or even higher compared to that of niclosamide in mammals. In rats, oral LD_{50} of NEN is over 10,000mg/kg body weight and rats fed 25,000 p.p.m NEN in diets for over one year showed no adverse effects [141, 284, 285]. The dosage of NEN used in *lal-/-* mice is 2000 p.p.m. (~150mg/kg.day), which is less than 2% of LD_{50} of NEN and less than 10% of the safe dosage of NEN documented in long-term toxicity study. The high therapeutic window of oral NEN makes it a promising prototype for treating LAL-D.

In summary, our study demonstrates that NEN treatment is effective in reducing the progressive liver damage and dyslipidemia symptoms of LAL-D in a clinically relevant mouse model. The underlying mechanism of NEN is associated with its effects on reducing lipids biosynthesis, lowering hepatic VLDL-C production, decreasing recycled LDL-C to liver and subsequently ameliorating progressive lipids accumulation in lysosome of liver. NEN has well-documented safety profile, which makes NEN a promising alternative experimental drug for treating LAL-D.

Summary and Significance

T2D is a chronic disease with large population and diverse diabetic complications. Unfortunately, anti-diabetic medications available currently are not effective in correcting underlying cause of the disease and patients present refractory responses to long-term treatment. Thus, developing new alternatives that target the cause of insulin resistance with good tolerance is necessary to improve diabetes therapy.

Chenpi has been anciently applied for anti-digestion and anti-inflammation with unidentified active constituents. Previous study showed an aging-dependent enrichment of 5-OH PMFs, which coincides with a general observation of an age-dependent increase in medicinal efficacy of *chenpi*. Encouraged by the unique profile of *chenpi* extract, we determined the effect of 5-OH PMFs enriched constituents on preventing the development of obesity and T2D. Our results showed that 5-OH PMFs enriched *chenpi* extract is effective in preventing obesity and diabetic symptoms, which provides strong evidence that 5-OH PMFs enriched constituents are the active ingredients in *chenpi* for anti-obesity and anti-diabetes. Moreover, the beneficial effect on glycemic control and insulin resistance is accompanied by the dramatic reduction in ectopic lipid accumulation in liver and abdominal adipose tissue, which has been demonstrated as a major cause of insulin resistance. Therefore, the 5-OH PMFs-enriched *chenpi* extract is expected to be a novel anti-diabetic nutraceutical with cause-correcting potential, which is a top-hit feature for diabetes therapy. Additionally, both glycemic control and lipid management are important for diabetes management. The comprehensive efficacy of 5-OH PMFs-enriched *chenpi* extract on metabolic profile is appealing to the development of T2D therapy. Furthermore, the fruit-derived character facilitates the commercialization of *chenpi* extract into not only anti-diabetes pharmacotherapy but also medicinal food or dietary supplements.

The preliminary work on lipid-reducing efficacy of casticin is also promising. As a 5-OH PMF derivative, casticin reduced intracellular lipid accumulation in differentiating mouse adipocytes. The potency of casticin on inhibiting lipogenesis is higher than that of 5-OH nobiletin. Moreover, the inhibitory effect of casticin on adipogenesis results from the reduction in cell amplification and lipogenesis. Comparatively, previous studies showed that 5-OH nobiletin did not impact on cell proliferation process of adipogenesis. The discrepancy of the two 5-OH PMF in their impacts on cell dividing could arise from the specific structure-activity relationship. 3'-OH is reported to be the functional group of inducing potent anti-proliferative property of PMFs. Future pharmacology study of evaluating the effect of casticin on the suppression of adiposity and improve diabetic symptoms is warranted.

Safe mitochondrial uncouplers have attracted intensive research interests regarding their therapeutic potential to treat T2D, fatty liver diseases, neurodegenerative diseases and aging. For treating T2D and fatty liver diseases, one striking feature of mitochondrial uncoupler is to target the causal factor of these diseases by elevating lipid oxidation. In current research, we identified two representative safe mitochondrial uncouplers by repurposing the FDA-approved drug. The liver target property as well as their excellent safety profile accounts for their translational value. Previous work showed that NEN-induced mitochondrial uncoupling is effective to treat insulin resistance and diabetic symptoms in mice. My work substantiated and further explored the therapeutic value of safe mitochondrial uncouplers: I identified NPP as an alternative drug with NEN for treating T2D and I successfully revealed the therapeutic potential of NEN on treating advanced fatty liver diseases either developed in the context of metabolic syndromes or caused by genetic mutation.

NASH is also a chronic disease which has great socioeconomic impacts but lacks disease-specific therapies. Our work provides an effective approach with novel mechanism for treating NASH by targeting lipid metabolism and hepatic stellate cell activation. The striking

efficacy of NEN on resolving fibrosis is the key competitive feature of NASH drug development. Our work reveals several important features of NEN for treating NASH including documented safety property, cause-targeting strategy as well as fibrosis-resolving efficacy.

LAL-D is a rare disease with similar clinical presentation as NASH, including hepatic lipid accumulation, inflammation and liver damage. The working principle of NEN for treating NASH was transferred to treat LAL-D. Our preliminary results demonstrated NEN is effective to ameliorate critical LAL-D symptoms and dramatically prolonged the lifespan of *lal-/-* mice. The efficacy of NEN for treating LAL-D provides strong evidence that mitochondrial uncoupling is an appealing therapeutic approach to treat lipid accumulation caused by genetic mutations.

Currently, there is unmet need for the treatment of T2D and fatty liver diseases. Discovery and development of novel therapeutic approaches is expected and needed. My dissertation research demonstrated practical therapeutic approaches to treat T2D and fatty liver diseases by targeting the causal factors of these chronic diseases, which not only provides the potential to cure the diseases but also presents great impact on improving the health and life quality of the patients.

Reference

1. Racette, S.B., S.S. Deusinger, and R.H. Deusinger, *Obesity: overview of prevalence, etiology, and treatment.* Phys Ther, 2003. **83**(3): p. 276-88.
2. *Obesity: preventing and managing the global epidemic. Report of a WHO consultation.* World Health Organ Tech Rep Ser, 2000. **894**: p. i-xii, 1-253.
3. Kumar, V.F., Nelson; Abbas, Abul K.; Cotran, Ramzi S. ; Robbins, Stanley L., *Robbins and Cotran Pathologic Basis of Disease (7th Ed.)*. 2005, Philadelphia, Pa. : Elsevier Saunders, c2005. p. 1194-1195.
4. Saltiel, A.R. and C.R. Kahn, *Insulin signalling and the regulation of glucose and lipid metabolism.* Nature, 2001. **414**(6865): p. 799-806.
5. Boden, G. and M. Laakso, *Lipids and glucose in type 2 diabetes: what is the cause and effect?* Diabetes Care, 2004. **27**(9): p. 2253-9.
6. Pessin, J.E. and A.R. Saltiel, *Signaling pathways in insulin action: molecular targets of insulin resistance.* J Clin Invest, 2000. **106**(2): p. 165-9.
7. Kahn, S.E., *The relative contributions of insulin resistance and beta-cell dysfunction to the pathophysiology of Type 2 diabetes.* Diabetologia, 2003. **46**(1): p. 3-19.
8. Prentki, M. and C.J. Nolan, *Islet beta cell failure in type 2 diabetes.* J Clin Invest, 2006. **116**(7): p. 1802-12.
9. DeFronzo, R.A., R.C. Bonadonna, and E. Ferrannini, *Pathogenesis of NIDDM. A balanced overview.* Diabetes Care, 1992. **15**(3): p. 318-68.
10. Rosolova, H., et al., *[Macrovascular and microvascular complications in type 2 diabetes patients].* Vnitr Lek, 2008. **54**(3): p. 229-37.
11. Chen, L., D.J. Magliano, and P.Z. Zimmet, *The worldwide epidemiology of type 2 diabetes mellitus--present and future perspectives.* Nat Rev Endocrinol, 2012. **8**(4): p. 228-36.
12. Prevention, C.f.D.C.a., *National Diabetes Statistics Report: Estimates of Diabetes and Its Burden in the United States, 2014.* 2014: Atlanta, GA: U.S. Department of Health and Human Services; 2014.
13. Samuel, V.T. and G.I. Shulman, *Mechanisms for insulin resistance: common threads and missing links.* Cell, 2012. **148**(5): p. 852-71.
14. Randle, P.J., et al., *The glucose fatty-acid cycle. Its role in insulin sensitivity and the metabolic disturbances of diabetes mellitus.* Lancet, 1963. **1**(7285): p. 785-9.
15. Kumashiro, N., et al., *Cellular mechanism of insulin resistance in nonalcoholic fatty liver disease.* Proc Natl Acad Sci U S A, 2011. **108**(39): p. 16381-5.
16. Fabbrini, E., et al., *Intrahepatic fat, not visceral fat, is linked with metabolic complications of obesity.* Proc Natl Acad Sci U S A, 2009. **106**(36): p. 15430-5.
17. Petersen, K.F., et al., *Reversal of nonalcoholic hepatic steatosis, hepatic insulin resistance, and hyperglycemia by moderate weight reduction in patients with type 2 diabetes.* Diabetes, 2005. **54**(3): p. 603-8.
18. Krssak, M., et al., *Intramyocellular lipid concentrations are correlated with insulin sensitivity in humans: a 1H NMR spectroscopy study.* Diabetologia, 1999. **42**(1): p. 113-6.
19. Shoelson, S.E., J. Lee, and A.B. Goldfine, *Inflammation and insulin resistance.* J Clin Invest, 2006. **116**(7): p. 1793-801.
20. Yin, M.J., Y. Yamamoto, and R.B. Gaynor, *The anti-inflammatory agents aspirin and salicylate inhibit the activity of I(kappa)B kinase-beta.* Nature, 1998. **396**(6706): p. 77-80.
21. Gao, Z., et al., *Serine phosphorylation of insulin receptor substrate 1 by inhibitor kappa B kinase complex.* J Biol Chem, 2002. **277**(50): p. 48115-21.

22. Shoelson, S.E., J. Lee, and M. Yuan, *Inflammation and the IKK beta/I kappa B/NF-kappa B axis in obesity- and diet-induced insulin resistance.* Int J Obes Relat Metab Disord, 2003. **27 Suppl 3**: p. S49-52.
23. Ozcan, U., et al., *Endoplasmic reticulum stress links obesity, insulin action, and type 2 diabetes.* Science, 2004. **306**(5695): p. 457-461.
24. Ozcan, U., et al., *Chemical chaperones reduce ER stress and restore glucose homeostasis in a mouse model of type 2 diabetes.* Science, 2006. **313**(5790): p. 1137-40.
25. Gregor, M.F., et al., *Endoplasmic Reticulum Stress Is Reduced in Tissues of Obese Subjects After Weight Loss.* Diabetes, 2009. **58**(3): p. 693-700.
26. Tuncman, G., et al., *Functional in vivo interactions between JNK1 and JNK2 isoforms in obesity and insulin resistance.* Proceedings of the National Academy of Sciences of the United States of America, 2006. **103**(28): p. 10741-10746.
27. Qatanani, M. and M.A. Lazar, *Mechanisms of obesity-associated insulin resistance: many choices on the menu.* Genes Dev, 2007. **21**(12): p. 1443-55.
28. Goossens, G.H., *The role of adipose tissue dysfunction in the pathogenesis of obesity-related insulin resistance.* Physiol Behav, 2008. **94**(2): p. 206-18.
29. Despres, J.P. and I. Lemieux, *Abdominal obesity and metabolic syndrome.* Nature, 2006. **444**(7121): p. 881-7.
30. Berg, A.H., et al., *The adipocyte-secreted protein Acrp30 enhances hepatic insulin action.* Nat Med, 2001. **7**(8): p. 947-53.
31. Kubota, N., et al., *Disruption of adiponectin causes insulin resistance and neointimal formation.* J Biol Chem, 2002. **277**(29): p. 25863-6.
32. Diez, J.J. and P. Iglesias, *The role of the novel adipocyte-derived hormone adiponectin in human disease.* Eur J Endocrinol, 2003. **148**(3): p. 293-300.
33. Fernandez-Real, J.M. and W. Ricart, *Insulin resistance and chronic cardiovascular inflammatory syndrome.* Endocr Rev, 2003. **24**(3): p. 278-301.
34. Montgomery, M.K. and N. Turner, *Mitochondrial dysfunction and insulin resistance: an update.* Endocr Connect, 2015. **4**(1): p. R1-R15.
35. Mootha, V.K., et al., *PGC-1alpha-responsive genes involved in oxidative phosphorylation are coordinately downregulated in human diabetes.* Nat Genet, 2003. **34**(3): p. 267-73.
36. Patti, M.E., et al., *Coordinated reduction of genes of oxidative metabolism in humans with insulin resistance and diabetes: Potential role of PGC1 and NRF1.* Proc Natl Acad Sci U S A, 2003. **100**(14): p. 8466-71.
37. Hawley, J.A., *Exercise as a therapeutic intervention for the prevention and treatment of insulin resistance.* Diabetes Metab Res Rev, 2004. **20**(5): p. 383-93.
38. King, D.S., et al., *Insulin action and secretion in endurance-trained and untrained humans.* J Appl Physiol (1985), 1987. **63**(6): p. 2247-52.
39. Rodnick, K.J., et al., *Improved insulin action in muscle, liver, and adipose tissue in physically trained human subjects.* Am J Physiol, 1987. **253**(5 Pt 1): p. E489-95.
40. Gan, S.K., et al., *Changes in aerobic capacity and visceral fat but not myocyte lipid levels predict increased insulin action after exercise in overweight and obese men.* Diabetes Care, 2003. **26**(6): p. 1706-13.
41. Goodpaster, B.H., A. Katsiaras, and D.E. Kelley, *Enhanced fat oxidation through physical activity is associated with improvements in insulin sensitivity in obesity.* Diabetes, 2003. **52**(9): p. 2191-7.
42. Devlin, J.T., et al., *Enhanced peripheral and splanchnic insulin sensitivity in NIDDM men after single bout of exercise.* Diabetes, 1987. **36**(4): p. 434-9.
43. Hughes, V.A., et al., *Exercise increases muscle GLUT-4 levels and insulin action in subjects with impaired glucose tolerance.* Am J Physiol, 1993. **264**(6 Pt 1): p. E855-62.

44. Corpeleijn, E., et al., *Improvements in glucose tolerance and insulin sensitivity after lifestyle intervention are related to changes in serum fatty acid profile and desaturase activities: the SLIM study.* Diabetologia, 2006. **49**(10): p. 2392-401.
45. Dela, F., et al., *Insulin-stimulated muscle glucose clearance in patients with NIDDM. Effects of one-legged physical training.* Diabetes, 1995. **44**(9): p. 1010-20.
46. Kang, J., et al., *Effect of exercise intensity on glucose and insulin metabolism in obese individuals and obese NIDDM patients.* Diabetes Care, 1996. **19**(4): p. 341-9.
47. Poirier, P., et al., *Impact of moderate aerobic exercise training on insulin sensitivity in type 2 diabetic men treated with oral hypoglycemic agents: is insulin sensitivity enhanced only in nonobese subjects?* Med Sci Monit, 2002. **8**(2): p. CR59-65.
48. Schneider, S.H., et al., *Studies on the mechanism of improved glucose control during regular exercise in type 2 (non-insulin-dependent) diabetes.* Diabetologia, 1984. **26**(5): p. 355-60.
49. Haus, J.M., et al., *Improved hepatic lipid composition following short-term exercise in nonalcoholic fatty liver disease.* J Clin Endocrinol Metab, 2013. **98**(7): p. E1181-8.
50. van der Heijden, G.J., et al., *A 12-week aerobic exercise program reduces hepatic fat accumulation and insulin resistance in obese, Hispanic adolescents.* Obesity (Silver Spring), 2010. **18**(2): p. 384-90.
51. Lebovitz, H.E., *Type 2 diabetes: An overview.* Clinical Chemistry, 1999. **45**(8): p. 1339-1346.
52. Dhatariya, K., *Pharmacotherapy for type 2 diabetes in very elderly patients: practicing nihilism or pragmatism?* Age Ageing, 2015. **44**(4): p. 540-2.
53. Brunt, E.M., *Pathology of nonalcoholic fatty liver disease.* Nat Rev Gastroenterol Hepatol, 2010. **7**(4): p. 195-203.
54. Farrell, G.C. and C.Z. Larter, *Nonalcoholic fatty liver disease: from steatosis to cirrhosis.* Hepatology, 2006. **43**(2 Suppl 1): p. S99-S112.
55. Sanyal, A., et al., *Population-based risk factors and resource utilization for HCC: US perspective.* Curr Med Res Opin, 2010. **26**(9): p. 2183-91.
56. Browning, J.D., et al., *Prevalence of hepatic steatosis in an urban population in the United States: impact of ethnicity.* Hepatology, 2004. **40**(6): p. 1387-95.
57. Charlton, M.R., et al., *Frequency and outcomes of liver transplantation for nonalcoholic steatohepatitis in the United States.* Gastroenterology, 2011. **141**(4): p. 1249-53.
58. Sayiner, M., et al., *Epidemiology of Nonalcoholic Fatty Liver Disease and Nonalcoholic Steatohepatitis in the United States and the Rest of the World.* Clin Liver Dis, 2016. **20**(2): p. 205-14.
59. Buzzetti, E., M. Pinzani, and E.A. Tsochatzis, *The multiple-hit pathogenesis of non-alcoholic fatty liver disease (NAFLD).* Metabolism, 2016. **65**(8): p. 1038-48.
60. McPherson, S., et al., *Evidence of NAFLD progression from steatosis to fibrosing-steatohepatitis using paired biopsies: implications for prognosis and clinical management.* J Hepatol, 2015. **62**(5): p. 1148-55.
61. Neuschwander-Tetri, B.A., *Hepatic lipotoxicity and the pathogenesis of nonalcoholic steatohepatitis: the central role of nontriglyceride fatty acid metabolites.* Hepatology, 2010. **52**(2): p. 774-88.
62. Alkhouri, N., L.J. Dixon, and A.E. Feldstein, *Lipotoxicity in nonalcoholic fatty liver disease: not all lipids are created equal.* Expert Rev Gastroenterol Hepatol, 2009. **3**(4): p. 445-51.
63. Rotman, Y. and A.J. Sanyal, *Current and upcoming pharmacotherapy for non-alcoholic fatty liver disease.* Gut, 2017. **66**(1): p. 180-190.
64. Arab, J.P., M. Arrese, and M. Trauner, *Recent Insights into the Pathogenesis of Nonalcoholic Fatty Liver Disease.* Annual Review of Pathology: Mechanisms of Disease, Vol 13, 2018. **13**: p. 321-350.

65. Cariou, B., et al., *Dual peroxisome proliferator-activated receptor alpha/delta agonist GFT505 improves hepatic and peripheral insulin sensitivity in abdominally obese subjects.* Diabetes Care, 2013. **36**(10): p. 2923-30.
66. Neuschwander-Tetri, B.A., et al., *Farnesoid X nuclear receptor ligand obeticholic acid for non-cirrhotic, non-alcoholic steatohepatitis (FLINT): a multicentre, randomised, placebo-controlled trial.* Lancet, 2015. **385**(9972): p. 956-65.
67. Foster, D.W., *Malonyl-CoA: the regulator of fatty acid synthesis and oxidation.* J Clin Invest, 2012. **122**(6): p. 1958-9.
68. Safadi, R., et al., *The fatty acid-bile acid conjugate Aramchol reduces liver fat content in patients with nonalcoholic fatty liver disease.* Clin Gastroenterol Hepatol, 2014. **12**(12): p. 2085-91 e1.
69. Armstrong, M.J., et al., *Glucagon-like peptide 1 decreases lipotoxicity in non-alcoholic steatohepatitis.* J Hepatol, 2016. **64**(2): p. 399-408.
70. Cui, J.Y., et al., *Sitagliptin Versus Placebo in the Treatment of Non-Alcoholic Fatty Liver Disease: A Randomized Controlled Trial.* Journal of Hepatology, 2016. **64**: p. S192-S193.
71. Mu, J., et al., *FGF21 analogs of sustained action enabled by orthogonal biosynthesis demonstrate enhanced antidiabetic pharmacology in rodents.* Diabetes, 2012. **61**(2): p. 505-12.
72. Luo, J., et al., *Treatment with Ngm282 Significantly Improves Liver Histopathology in a Mouse Model of Non-Alcoholic Steatohepatitis (Nash).* Journal of Hepatology, 2015. **62**: p. S694-S694.
73. Xu, Q., et al., *miRNA-103: Molecular link between insulin resistance and nonalcoholic fatty liver disease.* World Journal of Gastroenterology, 2015. **21**(2): p. 511-516.
74. Sanyal, A.J., et al., *Pioglitazone, vitamin E, or placebo for nonalcoholic steatohepatitis.* N Engl J Med, 2010. **362**(18): p. 1675-85.
75. Friedman, S., et al., *Efficacy and safety study of cenicriviroc for the treatment of non-alcoholic steatohepatitis in adult subjects with liver fibrosis: CENTAUR Phase 2b study design.* Contemp Clin Trials, 2016. **47**: p. 356-65.
76. Shiffman, M., et al., *A Placebo-Controlled, Multicenter, Double-Blind, Randomised Trial of Emricasan in Subjects with Non-Alcoholic Fatty Liver Disease (Nafld) and Raised Transaminases.* Journal of Hepatology, 2015. **62**: p. S282-S282.
77. Traber, P.G. and E. Zomer, *Therapy of experimental NASH and fibrosis with galectin inhibitors.* PLoS One, 2013. **8**(12): p. e83481.
78. Loomba, R., et al., *GS-4997, an Inhibitor of Apoptosis Signal-Regulating Kinase (ASK1), Alone or in Combination with Simtuzumab for the Treatment of Nonalcoholic Steatohepatitis (NASH): A Randomized, Phase 2 Trial.* Hepatology, 2016. **64**(6): p. 1119a-1120a.
79. Ikonen, E., *Mechanisms for cellular cholesterol transport: defects and human disease.* Physiol Rev, 2006. **86**(4): p. 1237-61.
80. Zhang, B. and A.F. Porto, *Cholesteryl ester storage disease: protean presentations of lysosomal acid lipase deficiency.* J Pediatr Gastroenterol Nutr, 2013. **56**(6): p. 682-5.
81. Aslanidis, C., et al., *Genetic and biochemical evidence that CESD and Wolman disease are distinguished by residual lysosomal acid lipase activity.* Genomics, 1996. **33**(1): p. 85-93.
82. Bernstein, D.L., et al., *Cholesteryl ester storage disease: review of the findings in 135 reported patients with an underdiagnosed disease.* J Hepatol, 2013. **58**(6): p. 1230-43.
83. Scott, S.A., et al., *Frequency of the Cholesteryl Ester Storage Disease Common LIPA E8SJM Mutation (c.894G > A) in Various Racial and Ethnic Groups.* Hepatology, 2013. **58**(3): p. 958-965.

84. Reiner, Z., et al., *Lysosomal acid lipase deficiency - An under-recognized cause of dyslipidaemia and liver dysfunction.* Atherosclerosis, 2014. **235**(1): p. 21-30.
85. Lohse, P., et al., *Compound heterozygosity for a Wolman mutation is frequent among patients with cholesteryl ester storage disease.* Journal of Lipid Research, 2000. **41**(1): p. 23-31.
86. Horton, J.D., J.L. Goldstein, and M.S. Brown, *SREBPs: activators of the complete program of cholesterol and fatty acid synthesis in the liver.* J Clin Invest, 2002. **109**(9): p. 1125-31.
87. Cummings, M.H. and G.F. Watts, *Increased hepatic secretion of very-low-density lipoprotein apolipoprotein B-100 in cholesteryl ester storage disease.* Clin Chem, 1995. **41**(1): p. 111-4.
88. Quinn, A.G., et al., *Sustained elevations in LDL cholesterol and serum transaminases from early childhood are common in lysosomal acid lipase deficiency.* Molecular Genetics and Metabolism, 2014. **111**(2): p. S89-S89.
89. Balwani, M., et al., *Clinical effect and safety profile of recombinant human lysosomal acid lipase in patients with cholesteryl ester storage disease.* Hepatology, 2013. **58**(3): p. 950-7.
90. Bazil, C.W., et al., *Sebelipase alfa (Kanuma) for lysosomal acid lipase deficiency.* Med Lett Drugs Ther, 2016. **58**(1504): p. e126-7.
91. Friedman, M., et al., *Safety findings from 3 trials of treatment with sebelipase alfa in children and adults with lysosomal acid lipase deficiency.* Molecular Genetics and Metabolism, 2016. **117**(2): p. S47-S47.
92. Leone, L., P.F. Ippoliti, and R. Antonicelli, *Use of Simvastatin Plus Cholestyramine in the Treatment of Lysosomal Acid Lipase Deficiency.* Journal of Pediatrics, 1991. **119**(6): p. 1008-1009.
93. Li, S.M., et al., *Chemistry and health effects of polymethoxyflavones and hydroxylated polymethoxyflavones.* Journal of Functional Foods, 2009. **1**(1): p. 2-12.
94. Bok, S.H., et al., *Plasma and hepatic cholesterol and hepatic activities of 3-hydroxy-3-methyl-glutaryl-CoA reductase and acyl CoA: cholesterol transferase are lower in rats fed citrus peel extract or a mixture of citrus bioflavonoids.* J Nutr, 1999. **129**(6): p. 1182-5.
95. Kang, S.I., et al., *Immature Citrus sunki peel extract exhibits antiobesity effects by beta-oxidation and lipolysis in high-fat diet-induced obese mice.* Biol Pharm Bull, 2012. **35**(2): p. 223-30.
96. Lee, Y.S., et al., *Effects of a Citrus depressa Hayata (shiikuwasa) extract on obesity in high-fat diet-induced obese mice.* Phytomedicine, 2011. **18**(8-9): p. 648-54.
97. Miyata, Y., et al., *Regulation of adipocytokine secretion and adipocyte hypertrophy by polymethoxyflavonoids, nobiletin and tangeretin.* Life Sci, 2011. **88**(13-14): p. 613-8.
98. Onda, K., et al., *Polymethoxyflavonoids tangeretin and nobiletin increase glucose uptake in murine adipocytes.* Phytother Res, 2013. **27**(2): p. 312-6.
99. Mulvihill, E.E., et al., *Nobiletin attenuates VLDL overproduction, dyslipidemia, and atherosclerosis in mice with diet-induced insulin resistance.* Diabetes, 2011. **60**(5): p. 1446-57.
100. Lin, Y.G., et al., *Molecular Structures of Citrus Flavonoids Determine Their Effects on Lipid Metabolism in HepG2 Cells by Primarily Suppressing ApoB Secretion.* Journal of Agricultural and Food Chemistry, 2011. **59**(9): p. 4496-4503.
101. Morin, B., et al., *The citrus flavonoids hesperetin and nobiletin differentially regulate low density lipoprotein receptor gene transcription in HepG2 liver cells.* J Nutr, 2008. **138**(7): p. 1274-81.

102. Whitman, S.C., et al., *Nobiletin, a citrus flavonoid isolated from tangerines, selectively inhibits class A scavenger receptor-mediated metabolism of acetylated LDL by mouse macrophages.* Atherosclerosis, 2005. **178**(1): p. 25-32.
103. Murakami, A., et al., *In vitro absorption and metabolism of nobiletin, a chemopreventive polymethoxyflavonoid in citrus fruits.* Biosci Biotechnol Biochem, 2001. **65**(1): p. 194-7.
104. Manthey, J.A., et al., *Pharmacokinetic Study of Nobiletin and Tangeretin in Rat Serum by High-Performance Liquid Chromatography-Electrospray Ionization-Mass Spectrometry.* Journal of Agricultural and Food Chemistry, 2011. **59**(1): p. 145-151.
105. Li, S.M., et al., *Chemistry and bioactivity of nobiletin and its metabolites.* Journal of Functional Foods, 2014. **6**: p. 2-10.
106. Li, S.M., et al., *Isolation and syntheses of polymethoxyflavones and hydroxylated polymethoxyflavones as inhibitors of HL-60 cell lines.* Bioorganic & Medicinal Chemistry, 2007. **15**(10): p. 3381-3389.
107. Xiao, H., et al., *Monodemethylated polymethoxyflavones from sweet orange (Citrus sinensis) peel inhibit growth of human lung cancer cells by apoptosis.* Mol Nutr Food Res, 2009. **53**(3): p. 398-406.
108. Qiu, P., et al., *Inhibitory effects of 5-hydroxy polymethoxyflavones on colon cancer cells.* Mol Nutr Food Res, 2010. **54 Suppl 2**: p. S244-52.
109. Lai, C.S., et al., *Suppression of adipogenesis and obesity in high-fat induced mouse model by hydroxylated polymethoxyflavones.* J Agric Food Chem, 2013. **61**(43): p. 10320-8.
110. Yen, J.H., et al., *Citrus flavonoid 5-demethylnobiletin suppresses scavenger receptor expression in THP-1 cells and alters lipid homeostasis in HepG2 liver cells.* Mol Nutr Food Res, 2011. **55**(5): p. 733-48.
111. Health., P.s.R.o.C.M.o., *Chinese Pharmacopoeia, 8th ed., Chemical Industry Press: Beijing, China, 2005.*
112. Xu, J., et al., *Quantitative determination and pharmacokinetic study of casticin in rat plasma by liquid chromatography-mass spectrometry.* J Pharm Biomed Anal, 2012. **61**: p. 242-6.
113. Ling, Y., et al., *Metabolism studies of casticin in rats using HPLC-ESI-MS(n).* Biomed Chromatogr, 2012. **26**(12): p. 1502-8.
114. Lee, H., et al., *Casticin, an active compound isolated from Vitex Fructus, ameliorates the cigarette smoke-induced acute lung inflammatory response in a murine model.* Int Immunopharmacol, 2015. **28**(2): p. 1097-101.
115. Chen, D., et al., *Induction of apoptosis by casticin in cervical cancer cells through reactive oxygen species-mediated mitochondrial signaling pathways.* Oncol Rep, 2011. **26**(5): p. 1287-94.
116. Zeng, F., et al., *Induction of apoptosis by casticin in cervical cancer cells: reactive oxygen species-dependent sustained activation of Jun N-terminal kinase.* Acta Biochim Biophys Sin (Shanghai), 2012. **44**(5): p. 442-9.
117. Zhang, B., et al., *Vitexicarpin acts as a novel angiogenesis inhibitor and its target network.* Evid Based Complement Alternat Med, 2013. **2013**: p. 278405.
118. Haidara, K., et al., *The flavonoid Casticin has multiple mechanisms of tumor cytotoxicity action.* Cancer Lett, 2006. **242**(2): p. 180-90.
119. Mitchell, P., *Chemiosmotic coupling in oxidative and photosynthetic phosphorylation. 1966.* Biochim Biophys Acta, 2011. **1807**(12): p. 1507-38.
120. Rousset, S., et al., *The biology of mitochondrial uncoupling proteins.* Diabetes, 2004. **53 Suppl 1**: p. S130-5.
121. Childress, E.S., et al., *Small Molecule Mitochondrial Uncouplers and Their Therapeutic Potential.* Journal of Medicinal Chemistry, 2018. **61**(11): p. 4641-4655.

122. Busiello, R.A., S. Savarese, and A. Lombardi, *Mitochondrial uncoupling proteins and energy metabolism.* Front Physiol, 2015. **6**: p. 36.
123. Matsuno-Yagi, A. and Y. Hatefi, *Uncoupling of oxidative phosphorylation: different effects of lipophilic weak acids and electrogenic ionophores on the kinetics of ATP synthesis.* Biochemistry, 1989. **28**(10): p. 4367-74.
124. Terada, H., *Uncouplers of oxidative phosphorylation.* Environ Health Perspect, 1990. **87**: p. 213-8.
125. Norman, C., et al., *Salicylic acid is an uncoupler and inhibitor of mitochondrial electron transport.* Plant Physiology, 2004. **134**(1): p. 492-501.
126. Petrescu, I. and C. Tarba, *Uncoupling effects of diclofenac and aspirin in the perfused liver and isolated hepatic mitochondria of rat.* Biochim Biophys Acta, 1997. **1318**(3): p. 385-94.
127. Gibellini, L., et al., *Natural Compounds Modulating Mitochondrial Functions.* Evid Based Complement Alternat Med, 2015. **2015**: p. 527209.
128. Ortega, R. and N. Garcia, *The flavonoid quercetin induces changes in mitochondrial permeability by inhibiting adenine nucleotide translocase.* J Bioenerg Biomembr, 2009. **41**(1): p. 41-7.
129. Lim, H.W., H.Y. Lim, and K.P. Wong, *Uncoupling of oxidative phosphorylation by curcumin: Implication of its cellular mechanism of action.* Biochemical and Biophysical Research Communications, 2009. **389**(1): p. 187-192.
130. Azhar, Y., et al., *Phytochemicals as novel agents for the induction of browning in white adipose tissue.* Nutrition & Metabolism, 2016. **13**.
131. Bessadottir, M., et al., *Proton-shuttling lichen compound usnic acid affects mitochondrial and lysosomal function in cancer cells.* PLoS One, 2012. **7**(12): p. e51296.
132. Goldgof, M., et al., *The Chemical Uncoupler 2,4-Dinitrophenol (DNP) Protects against Diet-induced Obesity and Improves Energy Homeostasis in Mice at Thermoneutrality.* Journal of Biological Chemistry, 2014. **289**(28): p. 19341-19350.
133. Perry, R.J., et al., *Reversal of hypertriglyceridemia, fatty liver disease, and insulin resistance by a liver-targeted mitochondrial uncoupler.* Cell Metab, 2013. **18**(5): p. 740-8.
134. Turrens, J.F., *Mitochondrial formation of reactive oxygen species.* J Physiol, 2003. **552**(Pt 2): p. 335-44.
135. Caldeira da Silva, C.C., et al., *Mild mitochondrial uncoupling in mice affects energy metabolism, redox balance and longevity.* Aging Cell, 2008. **7**(4): p. 552-60.
136. Geisler, J.G., et al., *DNP, mitochondrial uncoupling, and neuroprotection: A little dab'll do ya.* Alzheimers Dement, 2017. **13**(5): p. 582-591.
137. Alasadi, A., et al., *Effect of mitochondrial uncouplers niclosamide ethanolamine (NEN) and oxyclozanide on hepatic metastasis of colon cancer.* Cell Death Dis, 2018. **9**(2): p. 215.
138. Klaus, S., et al., *Augmenting energy expenditure by mitochondrial uncoupling: a role of AMP-activated protein kinase.* Genes and Nutrition, 2012. **7**(3): p. 369-386.
139. Keipert, S., et al., *Skeletal muscle uncoupling-induced longevity in mice is linked to increased substrate metabolism and induction of the endogenous antioxidant defense system.* American Journal of Physiology-Endocrinology and Metabolism, 2013. **304**(5): p. E495-E506.
140. Tao, H., et al., *Niclosamide ethanolamine-induced mild mitochondrial uncoupling improves diabetic symptoms in mice.* Nat Med, 2014. **20**(11): p. 1263-9.
141. Andrews, P., J. Thyssen, and D. Lorke, *The biology and toxicology of molluscicides, Bayluscide.* Pharmacol Ther, 1982. **19**(2): p. 245-95.
142. *National Diabetes Statistics Report: Estimates of Diabetes and Its Burden in the United States, 2014*. 2014, US Centers for Disease Control and Prevention: Atlanta, GA.

143. Kahn, B.B. and J.S. Flier, *Obesity and insulin resistance.* J Clin Invest, 2000. **106**(4): p. 473-81.
144. Qaseem, A., et al., *Oral pharmacologic treatment of type 2 diabetes mellitus: a clinical practice guideline from the American College of Physicians.* Ann Intern Med, 2012. **156**(3): p. 218-31.
145. Nathan, D.M., et al., *Medical management of hyperglycemia in type 2 diabetes: a consensus algorithm for the initiation and adjustment of therapy: a consensus statement of the American Diabetes Association and the European Association for the Study of Diabetes.* Diabetes Care, 2009. **32**(1): p. 193-203.
146. Muoio, D.M. and C.B. Newgard, *Obesity-related derangements in metabolic regulation.* Annu Rev Biochem, 2006. **75**: p. 367-401.
147. Henry, R.R., P. Wallace, and J.M. Olefsky, *Effects of weight loss on mechanisms of hyperglycemia in obese non-insulin-dependent diabetes mellitus.* Diabetes, 1986. **35**(9): p. 990-8.
148. Perseghin, G., et al., *Increased glucose transport-phosphorylation and muscle glycogen synthesis after exercise training in insulin-resistant subjects.* N Engl J Med, 1996. **335**(18): p. 1357-62.
149. Shulman, G.I., *Cellular mechanisms of insulin resistance.* Journal of Clinical Investigation, 2000. **106**(2): p. 171-176.
150. Lu, Y., et al., *Citrange fruit extracts alleviate obesity-associated metabolic disorder in high-fat diet-induced obese C57BL/6 mouse.* Int J Mol Sci, 2013. **14**(12): p. 23736-50.
151. Park, H.J., et al., *Citrus unshiu peel extract ameliorates hyperglycemia and hepatic steatosis by altering inflammation and hepatic glucose- and lipid-regulating enzymes in db/db mice.* J Nutr Biochem, 2013. **24**(2): p. 419-27.
152. Ding, X., et al., *Citrus ichangensis Peel Extract Exhibits Anti-Metabolic Disorder Effects by the Inhibition of PPARgamma and LXR Signaling in High-Fat Diet-Induced C57BL/6 Mouse.* Evid Based Complement Alternat Med, 2012. **2012**: p. 678592.
153. *People's Republic of China Ministry of Health, Chinese Pharmacopoeia, Chemical Industry Press, Beijing, China.* 2010.
154. Galarraga, M., et al., *Adiposoft: automated software for the analysis of white adipose tissue cellularity in histological sections.* Journal of Lipid Research, 2012. **53**(12): p. 2791-2796.
155. Wang, C.Y. and J.K. Liao, *A Mouse Model of Diet-Induced Obesity and Insulin Resistance.* Mtor: Methods and Protocols, 2012. **821**: p. 421-433.
156. Fergusson, G., et al., *Defective insulin secretory response to intravenous glucose in C57Bl/6J compared to C57Bl/6N mice.* Mol Metab, 2014. **3**(9): p. 848-54.
157. Scherer, P.E., *Adipose tissue: from lipid storage compartment to endocrine organ.* Diabetes, 2006. **55**(6): p. 1537-45.
158. Daval, M., F. Foufelle, and P. Ferre, *Functions of AMP-activated protein kinase in adipose tissue.* J Physiol, 2006. **574**(Pt 1): p. 55-62.
159. Lara-Castro, C. and W.T. Garvey, *Intracellular lipid accumulation in liver and muscle and the insulin resistance syndrome.* Endocrinol Metab Clin North Am, 2008. **37**(4): p. 841-56.
160. Nagle, C.A., E.L. Klett, and R.A. Coleman, *Hepatic triacylglycerol accumulation and insulin resistance.* J Lipid Res, 2009. **50 Suppl**: p. S74-9.
161. Kahn, S.E., R.L. Hull, and K.M. Utzschneider, *Mechanisms linking obesity to insulin resistance and type 2 diabetes.* Nature, 2006. **444**(7121): p. 840-6.
162. Verges, B., *Abnormal hepatic apolipoprotein B metabolism in type 2 diabetes.* Atherosclerosis, 2010. **211**(2): p. 353-60.
163. Boren, J., et al., *Ectopic lipid storage and insulin resistance: a harmful relationship.* J Intern Med, 2013. **274**(1): p. 25-40.

164. Rippe, J.M., S. Crossley, and R. Ringer, *Obesity as a chronic disease: modern medical and lifestyle management.* J Am Diet Assoc, 1998. **98**(10 Suppl 2): p. S9-15.
165. Adams, K.F., et al., *Overweight, obesity, and mortality in a large prospective cohort of persons 50 to 71 years old.* N Engl J Med, 2006. **355**(8): p. 763-78.
166. Ng, M., et al., *Global, regional, and national prevalence of overweight and obesity in children and adults during 1980-2013: a systematic analysis for the Global Burden of Disease Study 2013.* Lancet, 2014. **384**(9945): p. 766-81.
167. Feve, B., *Adipogenesis: cellular and molecular aspects.* Best Pract Res Clin Endocrinol Metab, 2005. **19**(4): p. 483-99.
168. Camp, H.S., D. Ren, and T. Leff, *Adipogenesis and fat-cell function in obesity and diabetes.* Trends Mol Med, 2002. **8**(9): p. 442-7.
169. Spalding, K.L., et al., *Dynamics of fat cell turnover in humans.* Nature, 2008. **453**(7196): p. 783-7.
170. Green, H. and O. Kehinde, *An established preadipose cell line and its differentiation in culture. II. Factors affecting the adipose conversion.* Cell, 1975. **5**(1): p. 19-27.
171. Tang, Q.Q., T.C. Otto, and M.D. Lane, *Mitotic clonal expansion: a synchronous process required for adipogenesis.* Proc Natl Acad Sci U S A, 2003. **100**(1): p. 44-9.
172. Farmer, S.R., *Transcriptional control of adipocyte formation.* Cell Metab, 2006. **4**(4): p. 263-73.
173. Siersbaek, R., R. Nielsen, and S. Mandrup, *PPARgamma in adipocyte differentiation and metabolism--novel insights from genome-wide studies.* FEBS Lett, 2010. **584**(15): p. 3242-9.
174. Hardie, D.G., *AMPK: A Target for Drugs and Natural Products With Effects on Both Diabetes and Cancer.* Diabetes, 2013. **62**(7): p. 2164-2172.
175. Giri, S., et al., *AICAR inhibits adipocyte differentiation in 3T3L1 and restores metabolic alterations in diet-induced obesity mice model.* Nutr Metab (Lond), 2006. **3**: p. 31.
176. Commission, C.P., *Pharmacopoeia of the People's Republic of China*. 2010, Beijing, China: Chemical Industry Press.
177. Li, S., C.Y. Lo, and C.T. Ho, *Hydroxylated polymethoxyflavones and methylated flavonoids in sweet orange (Citrus sinensis) peel.* J Agric Food Chem, 2006. **54**(12): p. 4176-85.
178. Guo, J., et al., *Prevention of Obesity and Type 2 Diabetes with Aged Citrus Peel (Chenpi) Extract.* J Agric Food Chem, 2016. **64**(10): p. 2053-61.
179. Kurowska, E.M. and J.A. Manthey, *Hypolipidemic effects and absorption of citrus polymethoxylated flavones in hamsters with diet-induced hypercholesterolemia.* J Agric Food Chem, 2004. **52**(10): p. 2879-86.
180. Manthey, J.A., et al., *Pharmacokinetic study of nobiletin and tangeretin in rat serum by high-performance liquid chromatography-electrospray ionization-mass spectrometry.* J Agric Food Chem, 2011. **59**(1): p. 145-51.
181. Gesta, S., Y.H. Tseng, and C.R. Kahn, *Developmental origin of fat: tracking obesity to its source.* Cell, 2007. **131**(2): p. 242-56.
182. Lee, Y.K., et al., *Curcumin exerts antidifferentiation effect through AMPKalpha-PPAR-gamma in 3T3-L1 adipocytes and antiproliferatory effect through AMPKalpha-COX-2 in cancer cells.* J Agric Food Chem, 2009. **57**(1): p. 305-10.
183. Motoshima, H., et al., *AMPK and cell proliferation - AMPK as a therapeutic target for atherosclerosis and cancer.* Journal of Physiology-London, 2006. **574**(1): p. 63-71.
184. Hruby, A. and F.B. Hu, *The Epidemiology of Obesity: A Big Picture.* Pharmacoeconomics, 2015. **33**(7): p. 673-89.
185. Shulman, G.I., *Cellular mechanisms of insulin resistance.* J Clin Invest, 2000. **106**(2): p. 171-6.

186. Jo, J., et al., *Hypertrophy and/or Hyperplasia: Dynamics of Adipose Tissue Growth.* PLoS Comput Biol, 2009. **5**(3): p. e1000324.
187. Ruiz-Ojeda, F.J., et al., *Cell Models and Their Application for Studying Adipogenic Differentiation in Relation to Obesity: A Review.* International Journal of Molecular Sciences, 2016. **17**(7).
188. Spiegelman, B.M. and J.S. Flier, *Adipogenesis and obesity: rounding out the big picture.* Cell, 1996. **87**(3): p. 377-89.
189. Lowe, C.E., S. O'Rahilly, and J.J. Rochford, *Adipogenesis at a glance (vol 124, pg 2681, 2011).* Journal of Cell Science, 2011. **124**(21): p. 3726-3726.
190. Chan, E.W.C., S.K. Wong, and H.T. Chan, *Casticin from Vitex species: a short review on its anticancer and anti-inflammatory properties.* J Integr Med, 2018. **16**(3): p. 147-152.
191. Guo, J.J., et al., *Aged citrus peel (chenpi) extract reduces lipogenesis in differentiating 3T3-L1 adipocytes.* Journal of Functional Foods, 2017. **34**: p. 297-303.
192. Tung, Y.C., et al., *5-Demethylnobiletin and 5-Acetoxy-6,7,8,3',4'-pentamethoxyflavone Suppress Lipid Accumulation by Activating the LKB1-AMPK Pathway in 3T3-L1 Preadipocytes and High Fat Diet-Fed C57BL/6 Mice.* J Agric Food Chem, 2016. **64**(16): p. 3196-205.
193. Patel, Y.M. and M.D. Lane, *Mitotic clonal expansion during preadipocyte differentiation: calpain-mediated turnover of p27.* J Biol Chem, 2000. **275**(23): p. 17653-60.
194. Shiming Li, M.-H.P., Chih-Yu Lo, Di Tan, Yu Wang, Fereidoon Shahidi, Chi-Tang Ho, *Chemistry and health effects of polymethoxyflavones and hydroxylated polymethoxyflavones.* Journal of Functional Foods, 2009. **1**(1): p. 2-12.
195. Kobayakawa, J., et al., *G2-M arrest and antimitotic activity mediated by casticin, a flavonoid isolated from Viticis Fructus (Vitex rotundifolia Linne fil.).* Cancer Lett, 2004. **208**(1): p. 59-64.
196. Shen, J.K., et al., *Casticin induces leukemic cell death through apoptosis and mitotic catastrophe.* Ann Hematol, 2009. **88**(8): p. 743-52.
197. Kawaii, S., et al., *Antiproliferative activity of flavonoids on several cancer cell lines.* Biosci Biotechnol Biochem, 1999. **63**(5): p. 896-9.
198. Ko, W.G., et al., *Polymethoxyflavonoids from Vitex rotundifolia inhibit proliferation by inducing apoptosis in human myeloid leukemia cells.* Food Chem Toxicol, 2000. **38**(10): p. 861-5.
199. Zhou, L., et al., *Casticin attenuates liver fibrosis and hepatic stellate cell activation by blocking TGF-beta/Smad signaling pathway.* Oncotarget, 2017. **8**(34): p. 56267-56280.
200. Banini, B.A. and A.J. Sanyal, *Nonalcoholic Fatty Liver Disease: Epidemiology, Pathogenesis, Natural History, Diagnosis, and Current Treatment Options.* Clin Med Insights Ther, 2016. **8**: p. 75-84.
201. Prevention, U.C.f.D.C.a., *National diabetes statistics report: estimates of diabetes and its burden in the United States, 2014.* 2014.
202. Ogden, C.L., et al., *Obesity and socioeconomic status in adults: United States, 2005-2008.* NCHS Data Brief, 2010(50): p. 1-8.
203. *National Institute of Diabetes and Digestive and Kidney Diseases (NIDDK). Insulin Resistance and Prediabetes.* NIH Publication No. 14–4893, 2014.
204. Seidell, J.C., *Obesity, insulin resistance and diabetes--a worldwide epidemic.* Br J Nutr, 2000. **83 Suppl 1**: p. S5-8.
205. Nathan, D.M., et al., *Medical Management of Hyperglycemia in Type 2 Diabetes: A Consensus Algorithm for the Initiation and Adjustment of Therapy A consensus statement of the American Diabetes Association and the European Association for the Study of Diabetes.* Diabetes Care, 2009. **32**(1): p. 193-203.

206. Randle, P.J., *Regulatory interactions between lipids and carbohydrates: The glucose fatty acid cycle after 35 years.* Diabetes-Metabolism Reviews, 1998. **14**(4): p. 263-283.
207. Samuel, V.T., K.F. Petersen, and G.I. Shulman, *Lipid-induced insulin resistance: unravelling the mechanism.* Lancet, 2010. **375**(9733): p. 2267-77.
208. Nedergaard, J., D. Ricquier, and L.P. Kozak, *Uncoupling proteins: current status and therapeutic prospects.* EMBO Rep, 2005. **6**(10): p. 917-21.
209. Tseng, Y.H., A.M. Cypess, and C.R. Kahn, *Cellular bioenergetics as a target for obesity therapy.* Nat Rev Drug Discov, 2010. **9**(6): p. 465-82.
210. Kopecky, J., et al., *Mitochondrial uncoupling and lipid metabolism in adipocytes.* Biochem Soc Trans, 2001. **29**(6): p. 791-7.
211. Harper, M.E., K. Green, and M.D. Brand, *The efficiency of cellular energy transduction and its implications for obesity.* Annu Rev Nutr, 2008. **28**: p. 13-33.
212. Ishigaki, Y., et al., *Dissipating excess energy stored in the liver is a potential treatment strategy for diabetes associated with obesity.* Diabetes, 2005. **54**(2): p. 322-32.
213. Organization, W.H.O.F.a.A., *Data sheet on pesticides No. 63 Niclosamide WHO/VBC/DS/88.63.* 1988.
214. Al-Gareeb, A.I., K.D. Aljubory, and H.M. Alkuraishy, *Niclosamide as an anti-obesity drug: an experimental study.* Eat Weight Disord, 2017.
215. Hollingworth, R.M., *in Handbook of Pesticide Toxicology Vol. 2, 2nd edn. (ed. Krieger, R.) 1225–1247 (Academic Press, San Diego, California, 2001).* in *in Handbook of Pesticide Toxicology*, R. Krieger, Editor. 2001: Academic Press, San Diego, California, 2001. p. 1225-1247.
216. Savjani, K.T., A.K. Gajjar, and J.K. Savjani, *Drug solubility: importance and enhancement techniques.* ISRN Pharm, 2012. **2012**: p. 1-10.
217. P. Andrews, J.T.a.D.L., *The biology and toxicology of molluscicides, bayluscide.* Pharmacology & Therapeutics, 1983. **19**(2): p. 245-295.
218. Assoc, A.D., *Standards of Medical Care in Diabetes-2014.* Diabetes Care, 2014. **37(Suppl. 1)**(3): p. S14-S80.
219. Marengo, A., R.I. Jouness, and E. Bugianesi, *Progression and Natural History of Nonalcoholic Fatty Liver Disease in Adults.* Clin Liver Dis, 2016. **20**(2): p. 313-24.
220. Younossi, Z.M., et al., *The economic and clinical burden of nonalcoholic fatty liver disease in the United States and Europe.* Hepatology, 2016. **64**(5): p. 1577-1586.
221. Pais, R., et al., *NAFLD and liver transplantation: Current burden and expected challenges.* J Hepatol, 2016. **65**(6): p. 1245-1257.
222. Parikh, N.D., et al., *Projected increase in obesity and non-alcoholic steatohepatitis-related liver transplantation waitlist additions in the United States.* Hepatology, 2017.
223. Day, C.P. and O.F. James, *Steatohepatitis: a tale of two "hits"?* Gastroenterology, 1998. **114**(4): p. 842-5.
224. Day, C.P., *From fat to inflammation.* Gastroenterology, 2006. **130**(1): p. 207-10.
225. Dowman, J.K., J.W. Tomlinson, and P.N. Newsome, *Pathogenesis of non-alcoholic fatty liver disease.* QJM, 2010. **103**(2): p. 71-83.
226. Cusi, K., *Role of insulin resistance and lipotoxicity in non-alcoholic steatohepatitis.* Clin Liver Dis, 2009. **13**(4): p. 545-63.
227. Kirpich, I.A., L.S. Marsano, and C.J. McClain, *Gut-liver axis, nutrition, and non-alcoholic fatty liver disease.* Clin Biochem, 2015. **48**(13-14): p. 923-30.
228. Yilmaz, Y., *Review article: is non-alcoholic fatty liver disease a spectrum, or are steatosis and non-alcoholic steatohepatitis distinct conditions?* Aliment Pharmacol Ther, 2012. **36**(9): p. 815-23.
229. Neuschwander-Tetri, B.A., *Nontriglyceride hepatic lipotoxicity: the new paradigm for the pathogenesis of NASH.* Curr Gastroenterol Rep, 2010. **12**(1): p. 49-56.

230. Ibrahim, S.H., R. Kohli, and G.J. Gores, *Mechanisms of lipotoxicity in NAFLD and clinical implications.* J Pediatr Gastroenterol Nutr, 2011. **53**(2): p. 131-40.
231. Kolios, G., V. Valatas, and E. Kouroumalis, *Role of Kupffer cells in the pathogenesis of liver disease.* World J Gastroenterol, 2006. **12**(46): p. 7413-20.
232. Rivera, C.A., et al., *Toll-like receptor-4 signaling and Kupffer cells play pivotal roles in the pathogenesis of non-alcoholic steatohepatitis.* J Hepatol, 2007. **47**(4): p. 571-9.
233. Bechmann, L.P., et al., *The interaction of hepatic lipid and glucose metabolism in liver diseases.* J Hepatol, 2012. **56**(4): p. 952-64.
234. Arrese, M., et al., *Innate Immunity and Inflammation in NAFLD/NASH.* Dig Dis Sci, 2016. **61**(5): p. 1294-303.
235. Crespo, J., et al., *Gene expression of tumor necrosis factor alpha and TNF-receptors, p55 and p75, in nonalcoholic steatohepatitis patients.* Hepatology, 2001. **34**(6): p. 1158-63.
236. Mederacke, I., et al., *Fate tracing reveals hepatic stellate cells as dominant contributors to liver fibrosis independent of its aetiology.* Nature Communications, 2013. **4**.
237. Friedman, S.L., et al., *Therapy for fibrotic diseases: nearing the starting line.* Sci Transl Med, 2013. **5**(167): p. 167sr1.
238. Geerts, A., *History, heterogeneity, developmental biology, and functions of quiescent hepatic stellate cells.* Semin Liver Dis, 2001. **21**(3): p. 311-35.
239. Tsuchida, T. and S.L. Friedman, *Mechanisms of hepatic stellate cell activation.* Nat Rev Gastroenterol Hepatol, 2017. **14**(7): p. 397-411.
240. Friedman, S.L., *Hepatic stellate cells: protean, multifunctional, and enigmatic cells of the liver.* Physiol Rev, 2008. **88**(1): p. 125-72.
241. Higashi, T., S.L. Friedman, and Y. Hoshida, *Hepatic stellate cells as key target in liver fibrosis.* Adv Drug Deliv Rev, 2017.
242. Henderson, N.C., et al., *Targeting of alpha(v) integrin identifies a core molecular pathway that regulates fibrosis in several organs.* Nature Medicine, 2013. **19**(12): p. 1617-1624.
243. Tao, H.L., et al., *Niclosamide ethanolamine-induced mild mitochondrial uncoupling improves diabetic symptoms in mice.* Nature Medicine, 2014. **20**(11): p. 1263-1269.
244. Charlton, M., et al., *Fast food diet mouse: novel small animal model of NASH with ballooning, progressive fibrosis, and high physiological fidelity to the human condition.* Am J Physiol Gastrointest Liver Physiol, 2011. **301**(5): p. G825-34.
245. Ichimura, M., et al., *High-fat and high-cholesterol diet rapidly induces non-alcoholic steatohepatitis with advanced fibrosis in Sprague-Dawley rats.* Hepatol Res, 2015. **45**(4): p. 458-69.
246. Rao, A., et al., *Inhibition of ileal bile acid uptake protects against nonalcoholic fatty liver disease in high-fat diet-fed mice.* Science Translational Medicine, 2016. **8**(357).
247. Wang, X.B., et al., *Hepatocyte TAZ/WWTR1 Promotes Inflammation and Fibrosis in Nonalcoholic Steatohepatitis.* Cell Metabolism, 2016. **24**(6): p. 848-862.
248. Matsuzawa, N., et al., *Lipid-induced oxidative stress causes steatohepatitis in mice fed an atherogenic diet.* Hepatology, 2007. **46**(5): p. 1392-403.
249. Yeh, M.M. and E.M. Brunt, *Pathology of nonalcoholic fatty liver disease.* Am J Clin Pathol, 2007. **128**(5): p. 837-47.
250. Alisi, A., et al., *The Role of Tissue Macrophage-Mediated Inflammation on NAFLD Pathogenesis and Its Clinical Implications.* Mediators Inflamm, 2017. **2017**: p. 8162421.
251. Baeck, C., et al., *Pharmacological inhibition of the chemokine CCL2 (MCP-1) diminishes liver macrophage infiltration and steatohepatitis in chronic hepatic injury.* Gut, 2012. **61**(3): p. 416-26.
252. Gerber, M.A. and S.N. Thung, *Histology of the liver.* Am J Surg Pathol, 1987. **11**(9): p. 709-22.

253. Reid, L.M., et al., *Extracellular matrix gradients in the space of Disse: relevance to liver biology.* Hepatology, 1992. **15**(6): p. 1198-203.
254. Bataller, R. and D.A. Brenner, *Liver fibrosis.* Journal of Clinical Investigation, 2005. **115**(4): p. 1100-1100.
255. Palacios, R.S., et al., *Activation of hepatic stellate cells is associated with cytokine expression in thioacetamide-induced hepatic fibrosis in mice.* Laboratory Investigation, 2008. **88**(11): p. 1192-1203.
256. Nitou, M., K. Ishikawa, and N. Shiojiri, *Immunohistochemical analysis of development of desmin-positive hepatic stellate cells in mouse liver.* J Anat, 2000. **197 Pt 4**: p. 635-46.
257. Chang, W., et al., *Isolation and culture of hepatic stellate cells from mouse liver.* Acta Biochim Biophys Sin (Shanghai), 2014. **46**(4): p. 291-8.
258. Boers, W., et al., *Transcriptional profiling reveals novel markers of liver fibrogenesis: gremlin and insulin-like growth factor-binding proteins.* J Biol Chem, 2006. **281**(24): p. 16289-95.
259. Soon, R.K., Jr. and H.F. Yee, Jr., *Stellate cell contraction: role, regulation, and potential therapeutic target.* Clin Liver Dis, 2008. **12**(4): p. 791-803, viii.
260. Piersma, B., R.A. Bank, and M. Boersema, *Signaling in Fibrosis: TGF-beta, WNT, and YAP/TAZ Converge.* Front Med (Lausanne), 2015. **2**: p. 59.
261. Nigdelioglu, R., et al., *Transforming Growth Factor (TGF)-beta Promotes de Novo Serine Synthesis for Collagen Production.* J Biol Chem, 2016. **291**(53): p. 27239-27251.
262. Lin, H., et al., *AMPK Inhibits the Stimulatory Effects of TGF-beta on Smad2/3 Activity, Cell Migration, and Epithelial-to-Mesenchymal Transition.* Mol Pharmacol, 2015. **88**(6): p. 1062-71.
263. Goldstein, J.L., et al., *Role of lysosomal acid lipase in the metabolism of plasma low density lipoprotein. Observations in cultured fibroblasts from a patient with cholesteryl ester storage disease.* J Biol Chem, 1975. **250**(21): p. 8487-95.
264. Grabowski GA, C.L., Du H, *Lysosomal Acid Lipase Deficiencies: The Wolman Disease/Cholesteryl Ester Storage Disease Spectrum. In: The Online Metabolic & Molecular Bases of Inherited Disease.* , B. Valle, Vogelstein, Kinzler, Antonarakis, Ballabio, Editor. 2012: Colombus, OH: McGraw-Hill. p. 1-9.
265. Fouchier, S.W. and J.C. Defesche, *Lysosomal acid lipase A and the hypercholesterolaemic phenotype.* Curr Opin Lipidol, 2013. **24**(4): p. 332-8.
266. Reiner, Z., et al., *Lysosomal acid lipase deficiency--an under-recognized cause of dyslipidaemia and liver dysfunction.* Atherosclerosis, 2014. **235**(1): p. 21-30.
267. Pullinger, C.R., et al., *Identification and metabolic profiling of patients with lysosomal acid lipase deficiency.* J Clin Lipidol, 2015. **9**(5): p. 716-26 e1.
268. Reynolds, T., *Cholesteryl ester storage disease: a rare and possibly treatable cause of premature vascular disease and cirrhosis.* J Clin Pathol, 2013. **66**(11): p. 918-23.
269. Paton, D.M., *Sebelipase alfa: enzymatic replacement treatment for lysosomal acid lipase deficiency.* Drugs Today (Barc), 2016. **52**(5): p. 287-93.
270. Porto, A.F., *Lysosomal acid lipase deficiency: diagnosis and treatment of Wolman and Cholesteryl Ester Storage Diseases.* Pediatr Endocrinol Rev, 2014. **12 Suppl 1**: p. 125-32.
271. Ricquier, D., *Respiration uncoupling and metabolism in the control of energy expenditure.* Proc Nutr Soc, 2005. **64**(1): p. 47-52.
272. Du, H., et al., *Targeted disruption of the mouse lysosomal acid lipase gene: long-term survival with massive cholesteryl ester and triglyceride storage.* Hum Mol Genet, 1998. **7**(9): p. 1347-54.
273. Du, H., et al., *Lysosomal acid lipase-deficient mice: depletion of white and brown fat, severe hepatosplenomegaly, and shortened life span.* J Lipid Res, 2001. **42**(4): p. 489-500.

274. Aqul, A., et al., *Hepatic entrapment of esterified cholesterol drives continual expansion of whole body sterol pool in lysosomal acid lipase-deficient mice.* Am J Physiol Gastrointest Liver Physiol, 2014. **307**(8): p. G836-47.
275. Han, S.K., et al., *OASIS 2: online application for survival analysis 2 with features for the analysis of maximal lifespan and healthspan in aging research.* Oncotarget, 2016. **7**(35): p. 56147-56152.
276. Perry, R.J., et al., *Controlled-release mitochondrial protonophore reverses diabetes and steatohepatitis in rats.* Science, 2015. **347**(6227): p. 1253-6.
277. Begriche, K., et al., *Mitochondrial adaptations and dysfunctions in nonalcoholic fatty liver disease.* Hepatology, 2013. **58**(4): p. 1497-507.
278. Du, H., et al., *Enzyme therapy for lysosomal acid lipase deficiency in the mouse.* Hum Mol Genet, 2001. **10**(16): p. 1639-48.
279. Du, H., et al., *The role of mannosylated enzyme and the mannose receptor in enzyme replacement therapy.* Am J Hum Genet, 2005. **77**(6): p. 1061-74.
280. Sun, Y., et al., *Reversal of advanced disease in lysosomal acid lipase deficient mice: a model for lysosomal acid lipase deficiency disease.* Mol Genet Metab, 2014. **112**(3): p. 229-41.
281. Du, H., et al., *Wolman disease/cholesteryl ester storage disease: efficacy of plant-produced human lysosomal acid lipase in mice.* J Lipid Res, 2008. **49**(8): p. 1646-57.
282. Lopez, A.M., et al., *PRD125, a potent and selective inhibitor of sterol O-acyltransferase 2 markedly reduces hepatic cholesteryl ester accumulation and improves liver function in lysosomal acid lipase-deficient mice.* J Pharmacol Exp Ther, 2015. **355**(2): p. 159-67.
283. Chuang, J.C., et al., *Ezetimibe markedly attenuates hepatic cholesterol accumulation and improves liver function in the lysosomal acid lipase-deficient mouse, a model for cholesteryl ester storage disease.* Biochem Biophys Res Commun, 2014. **443**(3): p. 1073-7.
284. Hecht, G. and C. Gloxhuber, *Tolerance to 2',5-dichloro-4-nitrosalicylanilide ethanolamine salt.* Parasitol. 13, 1–8, 1962.
285. Hollingworth, R.M., in *Handbook of Pesticide Toxicology*, R. Krieger, Editor. 2001, Academic Press: San Diego, California.

Appendices

ACC	Acetyl-CoA Carboxylase
AMPK	AMP-activated kinase
ALT	Alanine transaminase
ApoB	Apolipoprotein B
AST	Aspartate transaminase
CCl_4	carbon tetrachloride
CE	Cholesterol ester
C/EBPα	CCAAT-enhancer binding protein alpha
CPT	Continuous phase transition
DGAT	Diglyceride acyltransferase
DMSO	Dimethyl sulphoxide
DTT	Dithiothreitol
ECL	Chemiluminescent
EDTA	Ethylenediaminetetraacetic acid
FAS	Fatty acid synthase
FVB	Friend leukemia virus strain B
HDL	High density lipoprotein
H&E	Hematoxylin-eosin
HFD	High-fat diet
HSC	Hepatic stellate cell
KC	Kupffer cell
IL-1β	Interleukin-1 beta
LAL	Lysosomal acid lipase
LAL-D	Lysosomal acid lipase deficiency
LDL	Low density lipoprotein
MCP	Monocyte chemoattractant protein
MEM	Medium Essential Medium
NAFLD	Nonalcoholic fatty liver disease
NASH	Nonalcoholic steatohepatisis
NEFA	Nonesterified fatty acid
NEN	Niclosamide ethanolamine
NPP	Niclosamide piperazine
p-AMPK	Phospho-AMP-activated kinase
PBS	Phosphate-buffered saline
PDGF	Platelet-derived growth factor
PMFs	Polymethoxyflavones
PPARγ	Proliferator-activated receptor gamma
PVDF	Polyvinylidene difluoride

p70S6K	Phospho-ribosomal protein S6 kinase
RAN	RAs-related nuclear protein
SDS-PAGE	Sodium dodecyl sulphate polyacrylamide gel electrophoresis
SREBP	Sterol regulatory element-binding protein
T2D	Type 2 diabetes
TC	Total cholesterol
TG	Triglycerides
TGFβ	Transforming growth factor beta
TMRE	Tetramethylrhodamine ethyl ester
TNFα	Tumor necrosis factor alpha
UCP	Uncoupling protein
WAT	White adipose tissue
VLDL	Very low density lipoprotein
5-OH PMFs	5-demethylated polymethoxyflavones